

Gravitational Wave Data Analysis: Introduction to data analysis techniques Search for continuous waves

Alicia M Sintes

Dept. Física & IAC3 - Universitat de les Illes Balears &
Institut d'Estudis Espacials de Catalunya (IEEC).

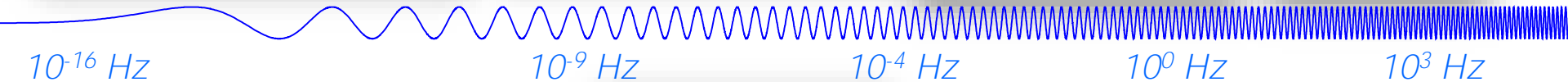
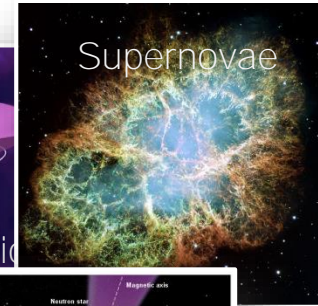
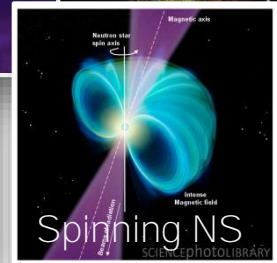
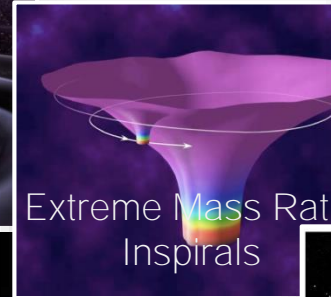
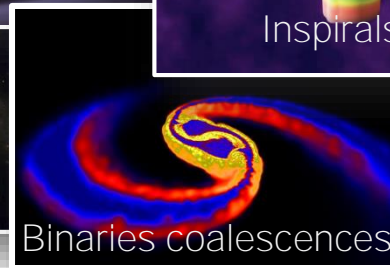
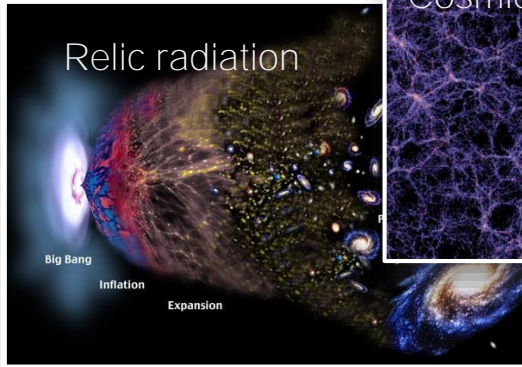
For the LIGO Scientific Collaboration and Virgo Collaboration



Outline

- Introduction
 - The Dawn of a New Era in Astronomy
 - The problem of data analysis in GW
- Search for continuous gravitational waves:
 - Neutron stars as sources of gravitational waves
 - Search strategies in the LVC

GWs that could be plausibly directly detected range from 10^{-9} Hz up to 10^{11} Hz.



10^{-16} Hz

10^{-9} Hz

10^{-4} Hz

10^0 Hz

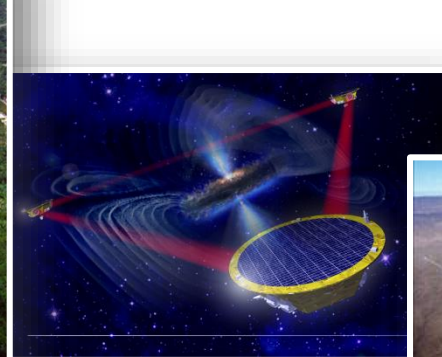
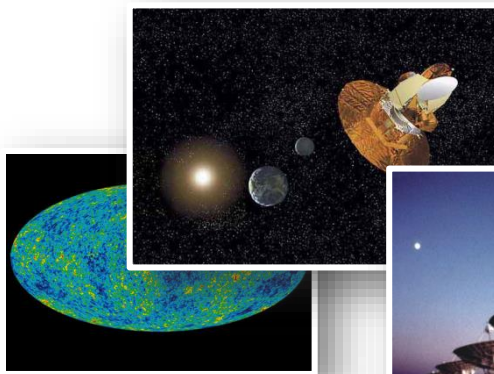
10^3 Hz

Inflation Probe

Pulsar timing

Space detectors

Ground interferometers



Gravitational wave detectors will study sources characterised by extreme physical conditions: strong non-linear gravity and relativistic motions, very high densities, temperatures and magnetic fields.

Some of the key scientific questions to which answers will be sought:

fundamental physics:

- What are the properties of gravitational waves?
- Is General Relativity still valid under strong-gravity conditions?
- Are nature's black holes the black holes of General Relativity?
- How does matter behave under extremes of density and pressure?

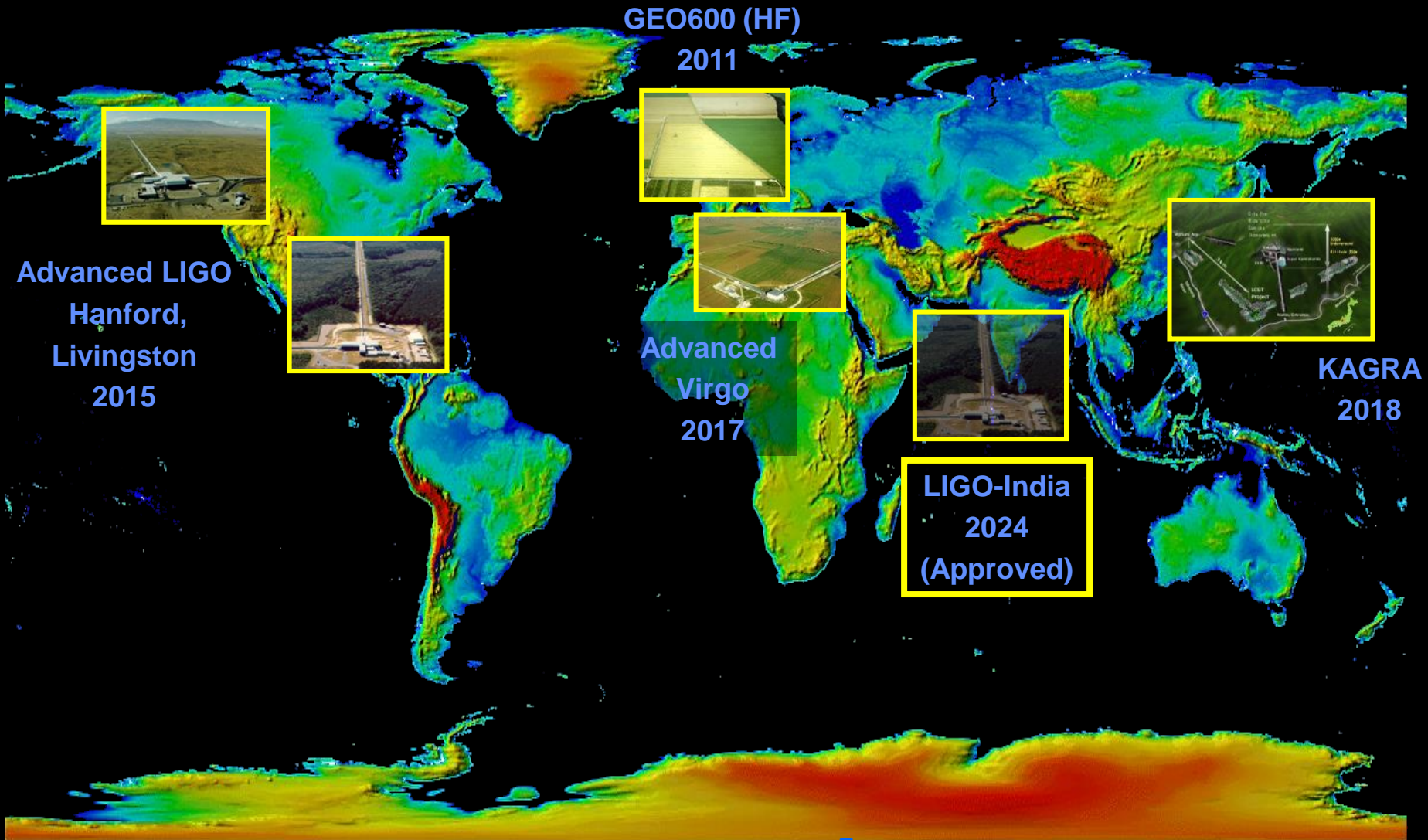
cosmology:

- What is the history of the accelerating expansion of the Universe?
- Were there phase transitions in the early Universe?

astrophysics:

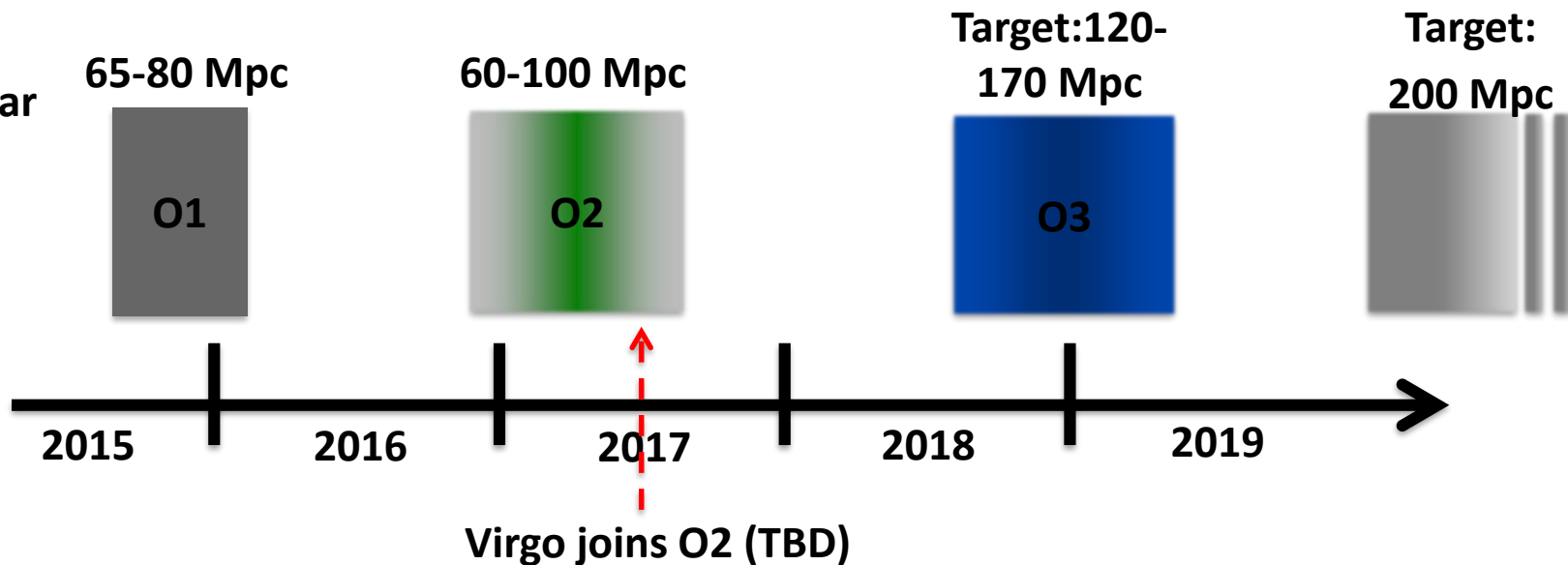
- How abundant are stellar-mass black holes?
- What is the mechanism that generates gamma-ray bursts?
- What are the conditions in the dense central cores of galactic nuclei dominated by massive black holes?
- Where and when do massive black holes form, and what role do they play in the formation of galaxies?
- What happens when a massive star collapses?
- How do compact binary stars form and evolve, and what has been their effect on star formation rates?

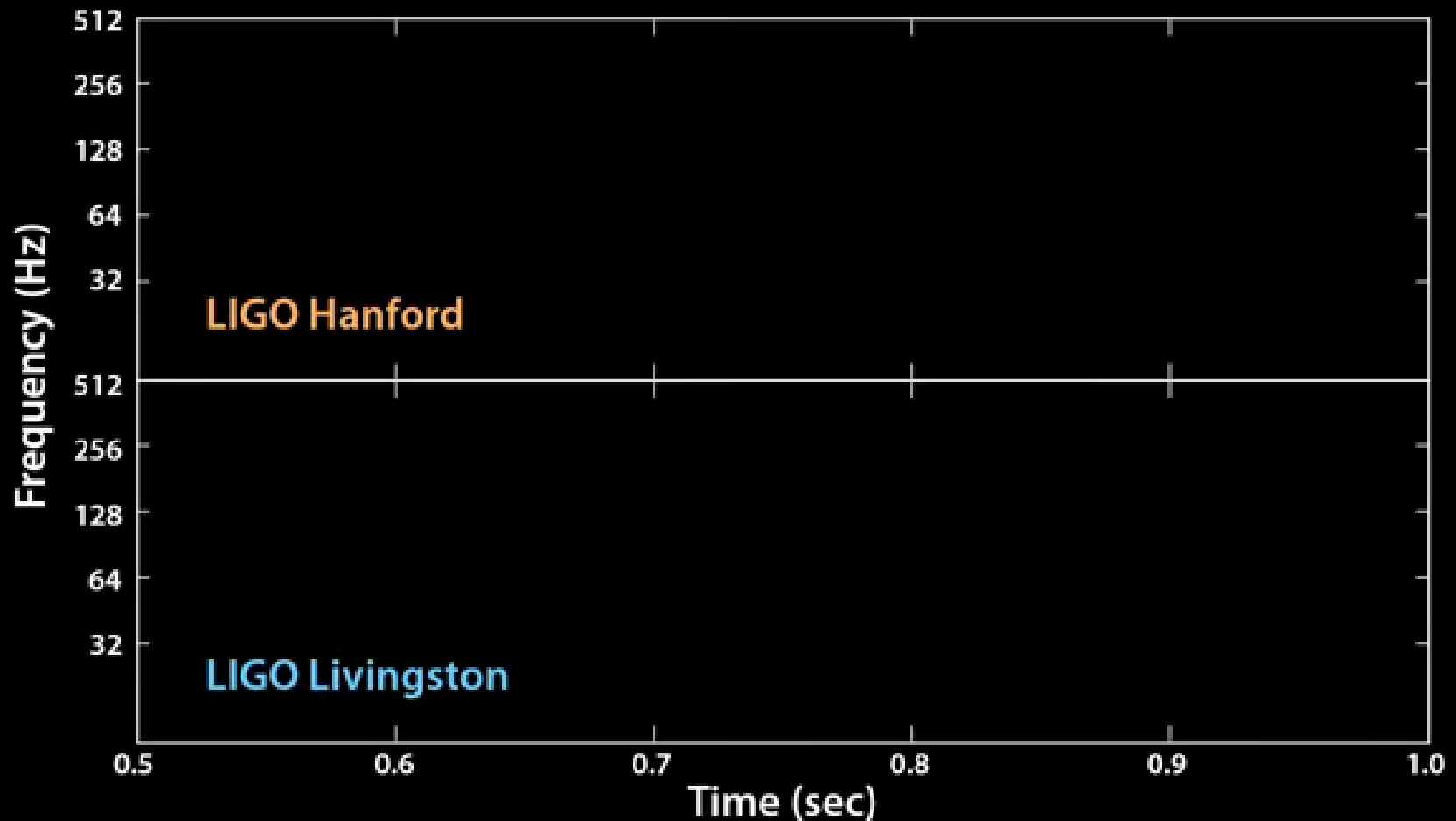
The advanced GW detector network



Plausible Observing Run Timeline (still under development within the LIGO and Virgo Collaborations)

Binary
Neutron Star
ranges





- GW150914 was detected first by L1 and 7ms later by H1.
- The frequency increased from 35 Hz to 150 Hz in two tenths of a second.
- In less than 3 minutes the CWB code (Coherent Wave Burst) recorded the event.
- LVC, Phys. Rev. Lett. 116, 061102 – Published 11 February 2016



Observation of Gravitational Waves from a Binary Black Hole Merger

B. P. Abbott *et al.**

(LIGO Scientific Collaboration and Virgo Collaboration)

(Received 21 January 2016; published 12 February 2016)

week ending
2 JUNE 2017



PHYSICAL REVIEW LETTERS



GW170104: Observation of a 50-Solar-Mass Binary Black Hole Coalescence at Redshift 0.2

B. P. Abbott *et al.**

(LIGO Scientific and Virgo Collaboration)
(Received 9 May 2017; published 1 June 2017)



PRL 118, 221101 (2017)

PHYSICAL REVIEW LETTERS

week ending
17 JUNE 2016

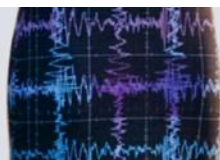


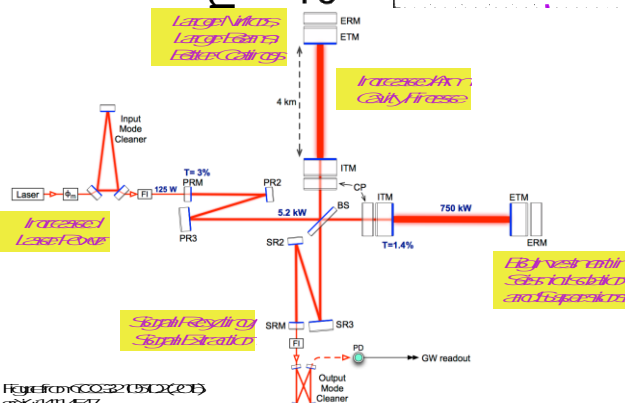
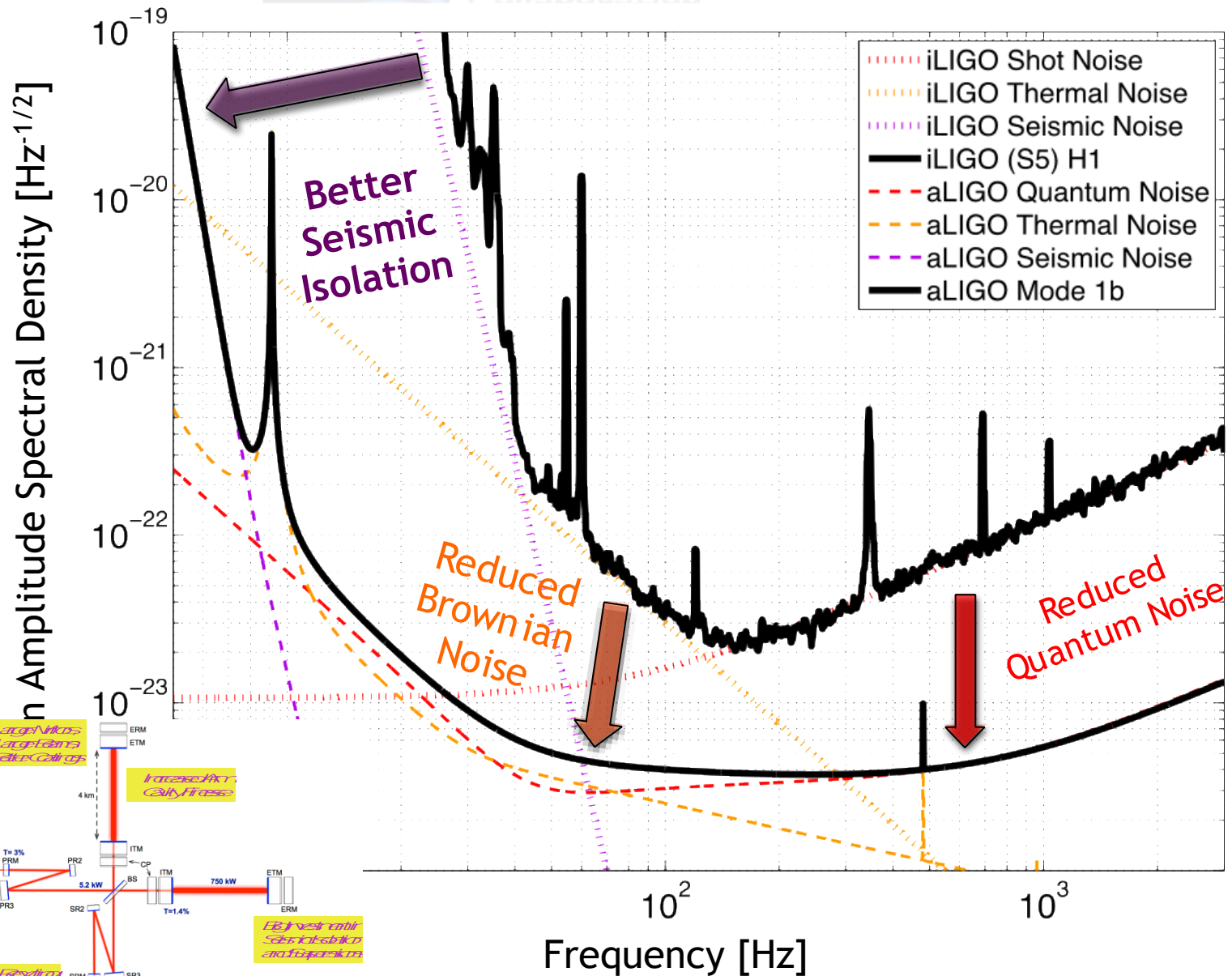
GW151226: Observation of Gravitational Waves from a 22-Solar-Mass Binary Black Hole Coalescence

B. P. Abbott *et al.**

(LIGO Scientific Collaboration and Virgo Collaboration)

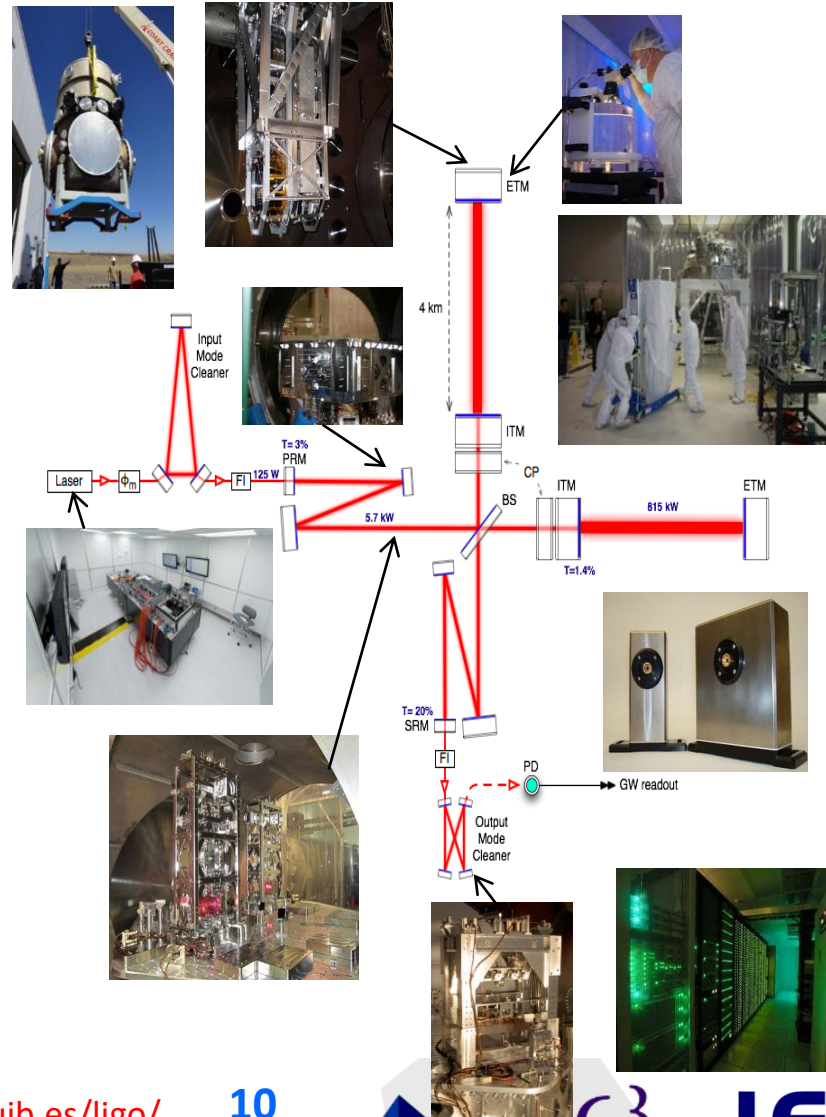
(Received 31 May 2016; published 15 June 2016)





Advanced LIGO: How to obtain a factor of x10 sensitivity improvement?

Parameter	Initial LIGO	Advanced LIGO
Input Laser Power	10 W (10 kW arm)	180 W (>700 kW arm)
Mirror Mass	10 kg	40 kg
Interferometer Topology	Power-recycled Fabry-Perot arm cavity Michelson	Dual-recycled Fabry-Perot arm cavity Michelson (stable recycling cavities)
GW Readout Method	RF heterodyne	DC homodyne
Optimal Strain Sensitivity	$3 \times 10^{-23} / \text{rHz}$	Tunable, better than $5 \times 10^{-24} / \text{rHz}$ in broadband
Seismic Isolation Performance	$f_{low} \sim 50 \text{ Hz}$	$f_{low} \sim 13 \text{ Hz}$
Mirror Suspensions	Single Pendulum	Quadruple pendulum



Challenges & Payoffs

Many major challenges in the new era of gravitational wave astronomy

Commissioning detectors;
achieving desired sensitivity

Building and installing
advanced detector hardware

Understanding the detectors
and the data they produce

Searching the data for
gravitational wave signals

Using GW observations in
astronomy, cosmology, relativity



GW Detectors

Sensitivity / Duty cycle / Glitchiness

Calibration / $h(t)$ reconstruction / Data quality

Initial detectors upper limits legacy

Computing

Sources

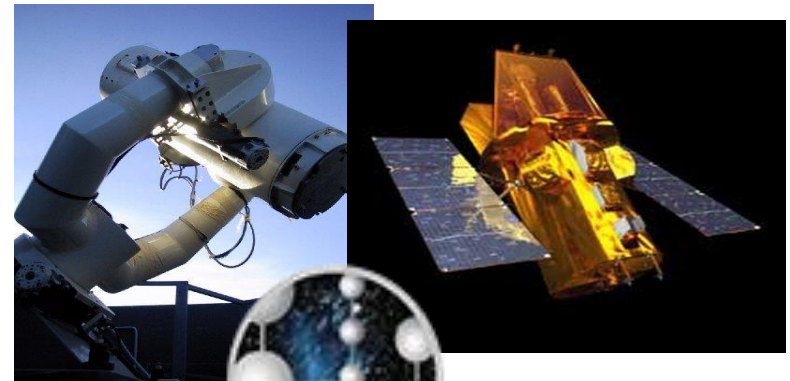
Data Analysis

Connecting with other messengers

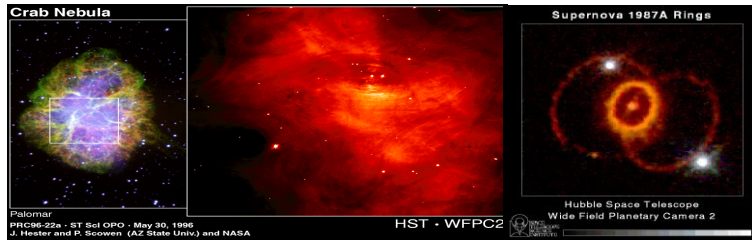
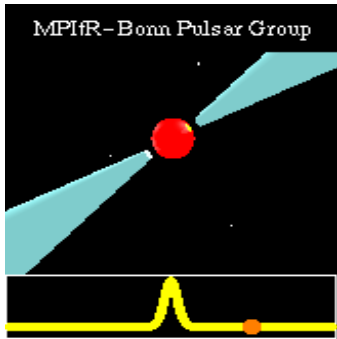
Waveform predictions

Astrophysics

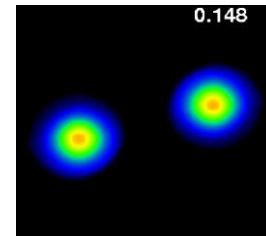
Fundamental Physics



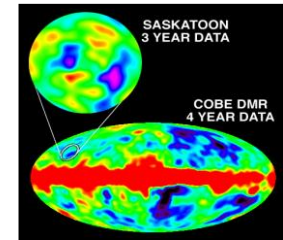
GW sources and methods



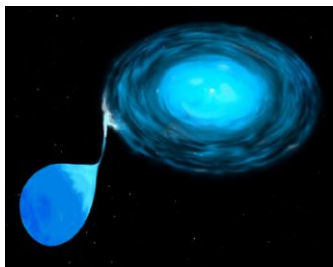
Supernovae, BH/NS formation



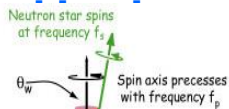
BH and NS Binaries



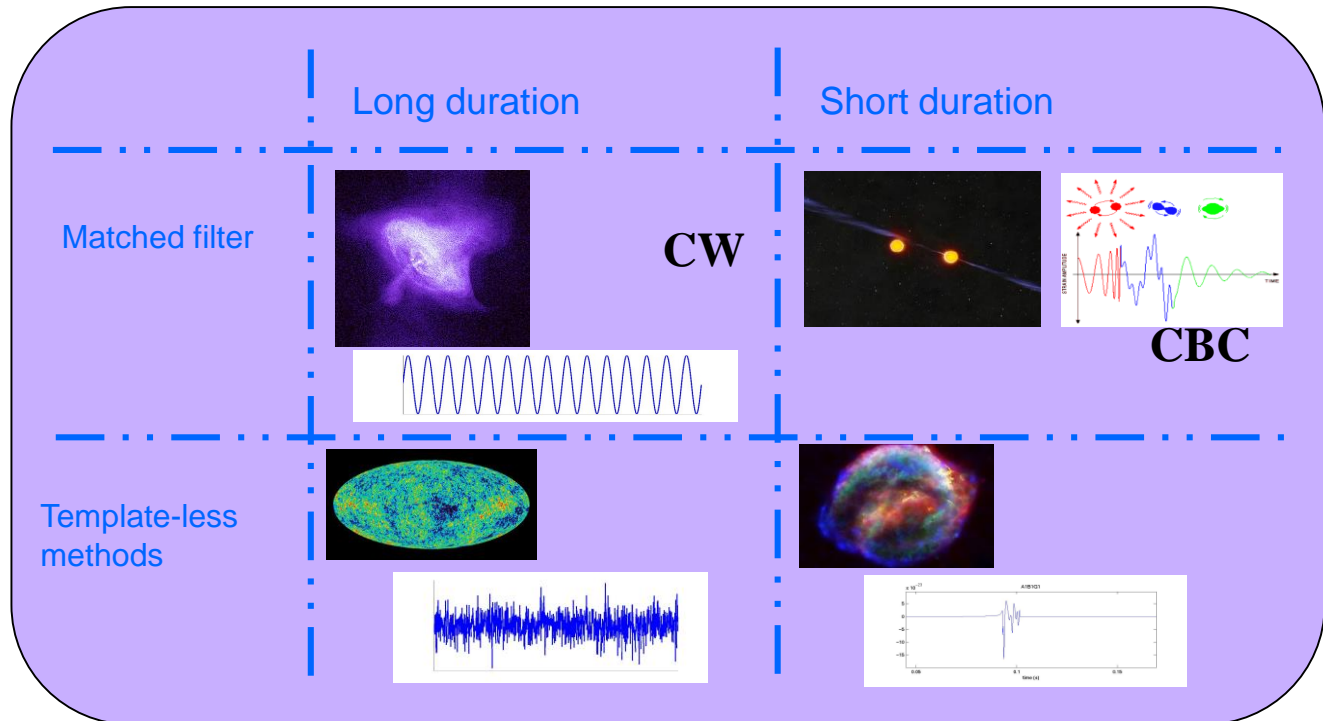
Stochastic background



Spinning NS in X-ray

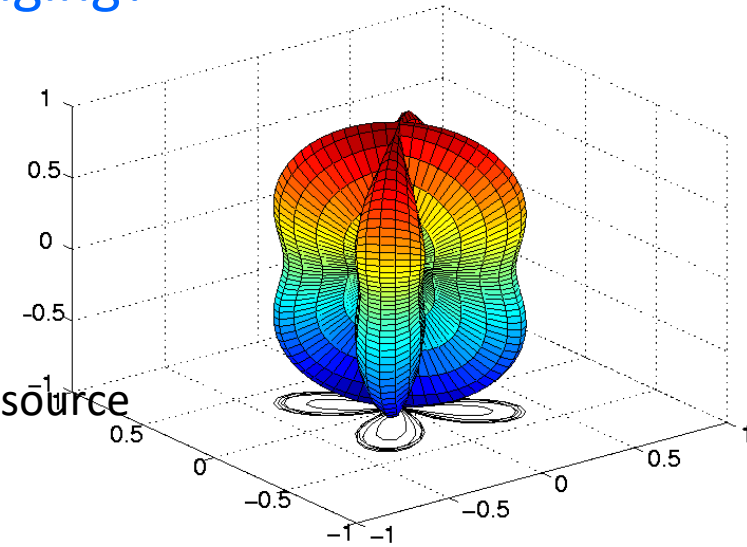


Wobbling NS



Why GW data analysis is challenging?

- All sky sensitivity
 - Quadrupolar antenna pattern
 - multiple detectors to determine direction to source
- Wide frequency band sensitivity
- Large data rates
 - Hundreds of instrumental and environmental channels
 - up to 10 MB per second from each detector
- Low event rates
- Large number of parameters and templates to search over



Antenna Pattern of a Laser Interferometer

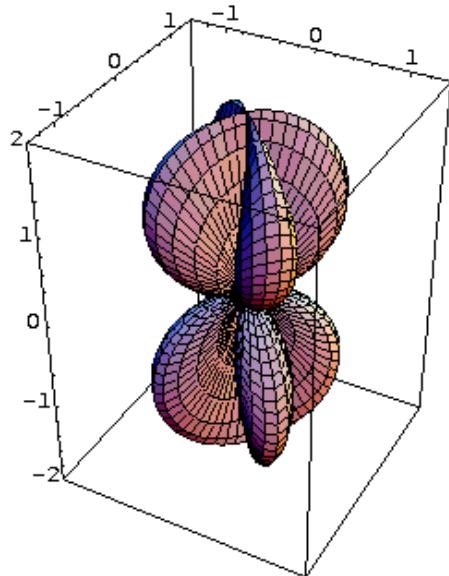
The strain $x(t)$ measured by a detector is mainly dominated by noise $n(t)$, such that even in the presence of a signal $h(t)$ we have

$$x(t) = n(t) + h(t)$$

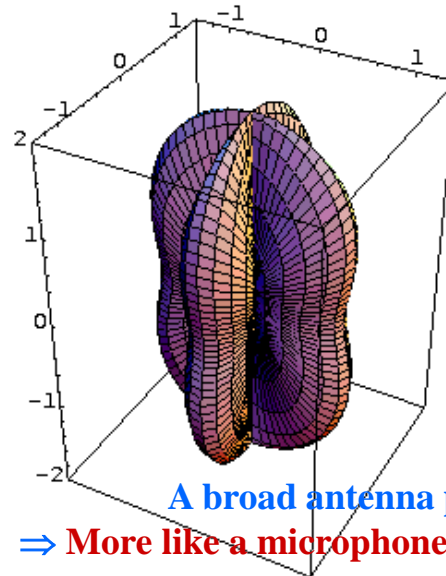
$$h(t) = F_+(t; \mathbf{y}) h_+(t) + F_\times(t; \mathbf{y}) h_\times(t)$$

F_+ and F_\times are the strain antenna patterns. They depend on the orientation of the detector and source and on the polarization of the waves.

“×” polarization



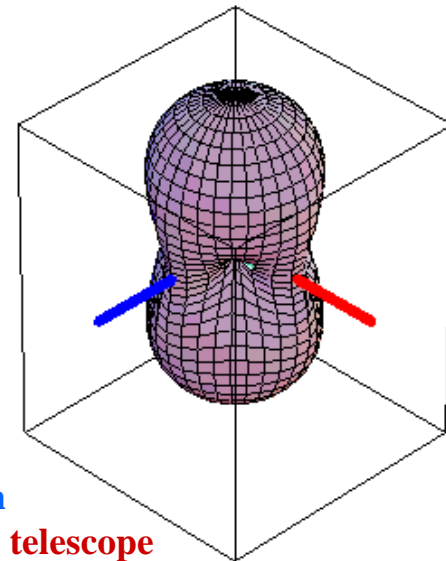
“+” polarization



A broad antenna pattern

⇒ More like a microphone than a telescope

RMS sensitivity



Using the GW Detector Network

A signal arriving at Earth is generally seen by all GW detectors operating at the time (assuming comparable sensitivities)

Antenna responses and relative times of arrival depend on sky position

Can in principle operate 24/7 monitoring whole sky; in practice, 60-90% up

All raw data is archived – enables many after-the-fact searches

Analyzing the data together allows us to:

Be more confident in events seen by multiple detectors

Infer the sky position

Separate the + and \times polarization components

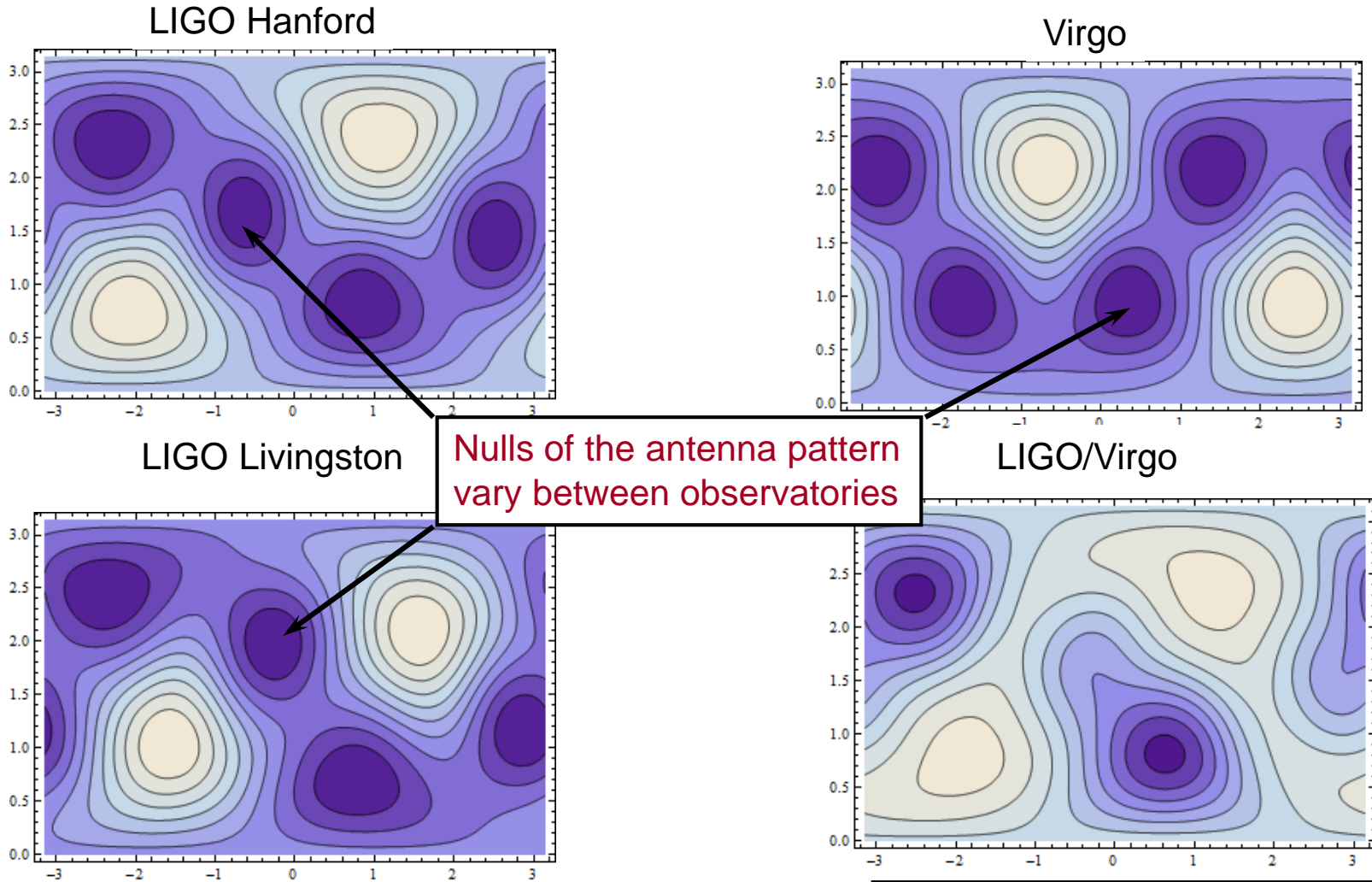
->GW detection is a cooperative endeavor

LIGO + GEO 600 + users = LIGO Scientific Collaboration (LSC)

LSC and Virgo Collaboration share all data, analyze and publish together

Benefits of a global network

- Improved sky coverage



Average response to signals with random linear polarization in Earth fixed coordinates

Less likely that event occurs in a null of the detector network

Benefits of a global network

- Improved duty cycle
 - Less likely that event occurs when no detectors are looking
- Increased signal to noise ratio
 - Coherently sum signals from multiple detectors
- Improved detection confidence
 - Multi-detector coincidence greatly reduces false rate
 - Coherent consistency tests can differentiate between gravitational-wave signals and instrumental anomalies
- Permits improved directional searches
 - Gamma ray burst progenitors
 - Supernovae
- Improved source reconstruction
 - “Inverse problem” requires 3 non-aligned detectors
 - Provides sky position and both polarizations of waveform
 - Permits comparison with theory
- Shared best practices
 - Learn from each other’s approaches

Gravitational-Wave Data

Data = Instantaneous estimate of strain for each moment in time

i.e. demodulated channel sensitive to arm length difference

That's not the whole story – there is the calibration issue

Digitized discrete **time series recorded in computer files**

$$(t_j, x_j)$$

LIGO and GEO **sampling rate**: 16384 Hz $\equiv f_s$

VIRGO sampling rate: 20000 Hz

Synchronized with GPS time signal

Common “frame” file format (*.gwf)

Many auxiliary channels recorded too

Total data volume: a few megabytes per second per interferometer

Relevance of the Sampling Rate

Is 16384 Hz a high enough sampling rate ?

The Sampling Theorem:

Discretely sampled data with sampling rate f_s can completely represent a continuous signal which only has frequency content below the **Nyquist frequency**, $f_s / 2$

GW signals of interest to ground-based detectors typically stay below a few kHz

e.g. binary neutron star inspiral reaches ISCO at ~ 1 to 1.5 kHz

Neutron star f -modes: ~ 3 kHz

Black hole quasinormal modes: ~ 1 kHz for $10 M_\odot$

Some core collapse supernova signals could go up to several kHz

What if the signal extends above Nyquist frequency?

Higher frequencies are “aliased” down to lower frequencies

Possible Properties of Noise

Stationary : statistical properties are independent of time

Ergodic process: time averages are equivalent to ensemble averages

Gaussian : A random variable follows Gaussian distribution

For a single random variable,
$$p(x) = \frac{1}{\sqrt{2\pi\sigma_x^2}} \exp\left[-\frac{1}{2} \frac{(x - \mu_x)^2}{\sigma_x^2}\right]$$

More generally, a set of random variables (e.g. a time series) is Gaussian if the joint probability distribution is governed by a covariance matrix

$$C_{xij} := \langle x_i x_j \rangle - \langle x_i \rangle \langle x_j \rangle$$

such that

$$p(x_1, x_2, \dots, x_N) = \frac{1}{(2\pi)^{N/2} \sqrt{\det C_x}} \exp\left[-\frac{1}{2} \sum_{i,j=0}^{N-1} C_{xij}^{-1} (x_i - \mu_{xi})(x_j - \mu_{xj})\right]$$

White : Signal power is uniformly distributed over frequency

⇒ Data samples are uncorrelated

Color : Signal does not have equal power in any band of a given bandwidth.

Frequency-domain representation of a Time-Series

Fourier transform

$$\tilde{x}(f) = \int_{-\infty}^{\infty} dt x(t) e^{-i2\pi ft}$$

$$\Rightarrow x(t) = \int_{-\infty}^{\infty} df \tilde{x}(f) e^{i2\pi ft}$$

A linear function, complex in general

Defined for all positive *and negative* frequencies

Frequency-Domain Representation of a *Discrete, Finite* Time Series

Time series x_j with N samples at times $t_j = t_0 + j \Delta t$

Discrete Fourier transform

$$\tilde{x}_k := \sum_{j=0}^{N-1} x_j e^{-i2\pi jk/N} \quad \delta_{jk} = \frac{1}{N} \sum_{\ell=0}^{N-1} e^{i2\pi(j-k)\ell/N}$$

$$\Rightarrow x_j = \frac{1}{N} \sum_{k=-N/2}^{N/2-1} \tilde{x}_k e^{i2\pi jk/N}$$

Frequency spacing is **inversely** proportional to N

Efficient way to calculate complete discrete Fourier Transform:

Fast Fourier Transform (FFT)

- The DFT and inverse DFT assume the signal is periodic with period $N\Delta t$.
- The relation between \tilde{x}_k and $\tilde{x}(f)$ is

$$\tilde{x}(f_k) \approx \Delta t \tilde{x}_k \quad (20)$$

where

$$f_k := k\Delta f = \frac{k}{N\Delta t}, \quad k = -N/2, -N/2 + 1, \dots, N/2 - 1 \quad (21)$$

- If the x_j are real, then $\tilde{x}_{-k} = \tilde{x}_k^*$.
- The DFT is usually implemented using the Fast Fourier Transform (FFT) algorithm—a very efficient ($N \log_2 N$) method of calculating FFTs.
- The FFT is so efficient that e.g., a convolution in the time domain is actually done by first DFT'ing the functions to the frequency domain, multiplying them together, and then IDFT'ing the result back to the time domain. The DFT, IDFT, and multiplication operations are computationally less expensive than a straightforward implementation of the convolution in the time domain.

Power Spectral Density

Parseval's theorem:

$$\int_{-\infty}^{\infty} dt |x(t)|^2 = \int_{-\infty}^{\infty} df |\tilde{x}(f)|^2$$

⇒ Total energy in the data can be calculated in either time domain or frequency domain

$|\tilde{x}(f)|^2$ can be interpreted as energy spectral density

When noise (or signal) has infinite extent in time domain, can still define the **power spectral density (PSD)**

$$\lim_{T \rightarrow \infty} \frac{1}{T} |\tilde{x}_T(f)|^2$$

Watch out for one-sided vs. two-sided PSDs

Estimating the PSD

Generally we need to determine the PSD empirically, using a finite amount of data

Simplest approach: FFT the data, calculate square of magnitude of each frequency component – this is a **periodogram**

For stationary noise, one can show that the frequency components are statistically independent

This estimate is unbiased (has the correct mean), but has a large variance – so average several periodograms

Alternately, smooth periodogram; give up frequency resolution either way

Generally apply a “window” to the data to avoid **spectral leakage**

Leakage arises from the assumption that the data is periodic!

Tapered window forces data to go to zero at ends of time interval

Welch's method of estimating a PSD averages periodograms calculated from windowed data

Estimating the PSD

- The simplest approach is to estimate $P_x(f)$ using

$$\hat{P}_x(f) = \frac{1}{T} |\tilde{x}_T(f)|^2 \quad (6)$$

where $\tilde{x}_T(f)$ is the finite duration Fourier transform of $x(t)$.

- The above estimator is called the *periodogram*.
- Being an estimator, the periodogram $\hat{P}_x(f)$ is itself a random variable and has a mean and variance (with respect to ensemble averages). The periodogram is *unbiased*:

$$\langle \hat{P}_x(f) \rangle = P_x(f) \quad (7)$$

but has a variance given by

$$\langle \hat{P}_x^2(f) \rangle - \langle \hat{P}_x(f) \rangle^2 = P_x^2(f) \quad (8)$$

The the uncertainty in the power spectrum estimate is as large as the estimate itself!

Estimating the PSD (cont.)

- To beat down the variance, one can break up the interval T into M smaller subintervals of duration $T_s = T/M$ and then average together the periodogram estimates for each of these subintervals. This approach reduces the variance by a factor of $1/M$ (the standard deviation by a factor of $1/\sqrt{M}$), although the frequency resolution will be worse by a factor of M (which is usually not a problem).
- One can even go a step further by windowing the data in the individual subintervals to reduce spectral leakage from lines that don't coincide with one of the discrete frequencies. For example, it is common to use Hann windows with 50% overlap to reduce the variance by *almost* a factor of $1/(2M)$. (*Almost*, since there is slight correlation between the data in the overlapping segments).
- This method of averaging together periodograms constructed from windowed data is called *Welch's method* of PSD estimation.

Finding the signal: the noise spectral density

We need first to represent the behaviour of the *input* noise $n(t)$ which is summed to the GW strain $h(t)$ to give what we call the detector output $x(t) = n(t) + h(t)$.

We suppose that the noise is stationary; then, the different Fourier components are uncorrelated and therefore:

$$\langle \tilde{n}^*(f) \tilde{n}(f') \rangle = \delta(f - f') \frac{1}{2} S_n(f)$$

$S_n(f)$ (Hz^{-1}) is the *single-sided noise spectral density* or *power spectrum* (PSD).

If we restrict the time interval to $[-T/2; T/2]$, and write $\Delta f = 1 / T$, we get:

$$\frac{1}{2} S_n(f) = \langle |\tilde{n}(f)|^2 \rangle \Delta f$$

It is often used the square root called *spectral amplitude* (ASD) and has the dimension of $\text{Hz}^{-1/2}$

Credits: M. Maggiore- Gravitational Waves

Matched filtering I

Normally we are in a situation where the signal is much weaker than the noise: we must be able to filter the signal in such a way we can dig into the noise

If we know the signal we are looking for, we can think to multiply the detector output $x(t)$ for the signal $h(t)$ (a filter) and integrate over an observation time T :

$$y = 1/T \int_0^T dt x(t)K(t) \quad \Longrightarrow \quad y = 1/T \int_0^T dt x(t)h(t)$$

$$y = \int_{-\infty}^{\infty} dt x(t)K(t) = \int_{-\infty}^{\infty} df \tilde{x}(f)\tilde{K}^*(f)$$

As the signal and the noise are uncorrelated, this should «amplify» the first with respect to the second.

We want to find the *optimum filter*, i.e. the filter function $K(t)$ that maximizes the signal-to-noise ratio SNR:

S/N = expected value of the filtered output y when the signal is present / *rms* value of y when the signal is absent.

Credits: M. Maggiore- Gravitational Waves

Matched filtering II

Taking $\langle n(t) \rangle = 0$ and making use of the noise spectral density definition, we can express SNR as:

$$\frac{S}{N} = \frac{\int_{-\infty}^{\infty} df \tilde{h}(f) \tilde{K}^*(f)}{\left[\int_{-\infty}^{\infty} df (1/2) S_n(f) |\tilde{K}(f)|^2 \right]^{1/2}}$$

Defining the scalar product between real functions: $(A|B) = \text{Re} \int_{-\infty}^{\infty} df \frac{\tilde{A}^*(f) \tilde{B}(f)}{(1/2) S_n(f)}$
we can re-write the signal-to-noise ratio as:

$$\frac{S}{N} = \frac{(u|h)}{(u|u)^{1/2}} \quad \text{with} \quad \tilde{u}(f) = \frac{1}{2} S_n(f) \tilde{K}(f)$$

Credits: M. Maggiore- Gravitational Waves

Matched filtering III

The unit vector $u/(u|u)^{1/2}$ which maximize the scalar product is then parallel to h , i.e. we need to choose:

$$\tilde{K}(f) = \text{const.} \frac{\tilde{h}(f)}{S_n(f)}$$

Thus we have that the optimal value of the SNR is:

$$\left(\frac{S}{N}\right)^2 = 4 \int_0^\infty df \frac{|\tilde{h}(f)|^2}{S_n(f)}$$

and the statistic we use:

$$\rho = y(\theta^\alpha) = \int_{-\infty}^{\infty} df \frac{\tilde{x}(f)\tilde{s}^*(f; \theta^\alpha)}{P_n(f)}$$

where s is here the normalized h signal wrt n .

Wiener filter is the optimal detection statistic if noise is Gaussian

Credits: M. Maggiore- Gravitational Waves

Maximum Likelihood estimator

To claim that an event coming out of the matched filtering is a detection we need to understand the statistical properties of ρ .

We compute the *likelihood function* Λ , i.e., in general, the probability of the data given the hypothesis: supposing that the noise is stationary and Gaussian, we can express the probability of a given noise realization n_0 as:

$$\Lambda(x; h) \equiv \frac{P(x|h)}{P(x|0)} \quad p(n_0) = \mathcal{N} \exp\{-(n_0|n_0)/2\}$$

Then the likelihood function for the observed output $s(t)$, given the hypothesis that there is a GW signal with parameters θ_t is obtained using: $n_0 = s - h(\theta_t)$:

$$P(s|\theta_t) = \mathcal{N} \exp\left\{(h_t|s) - \frac{1}{2}(h_t|h_t) - \frac{1}{2}(s|s)\right\} \quad \Longrightarrow \quad \log \Lambda(s|\theta_t) = (h_t|s) - \frac{1}{2}(h_t|h_t)$$

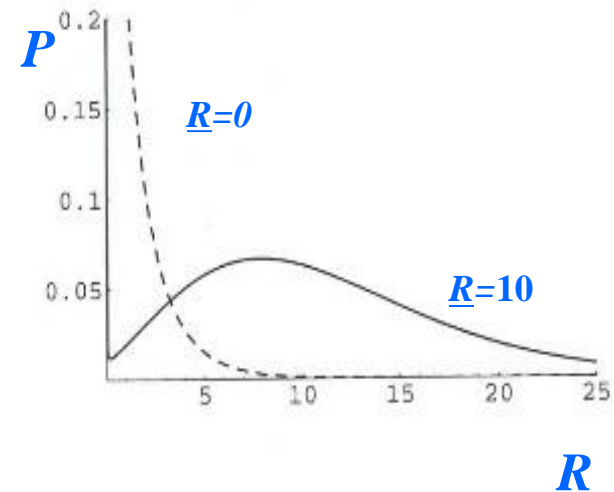
Credits: M. Maggiore- Gravitational Waves

Matched filtering statistics

To discriminate between events which are produced by noise and events which are produced by a real GW we need to know the probability distribution of the matched filtering statistics.

Instead of using the statistics of ρ , we refer to the probability distribution $P(R|\underline{R})$ of $R = \rho^2$, where \underline{R} is the value in presence of a GW signal:

$$\frac{1}{\sqrt{2\pi R}} e^{-(\bar{R}+R)/2} \cosh \left[\sqrt{R\bar{R}} \right] dR$$

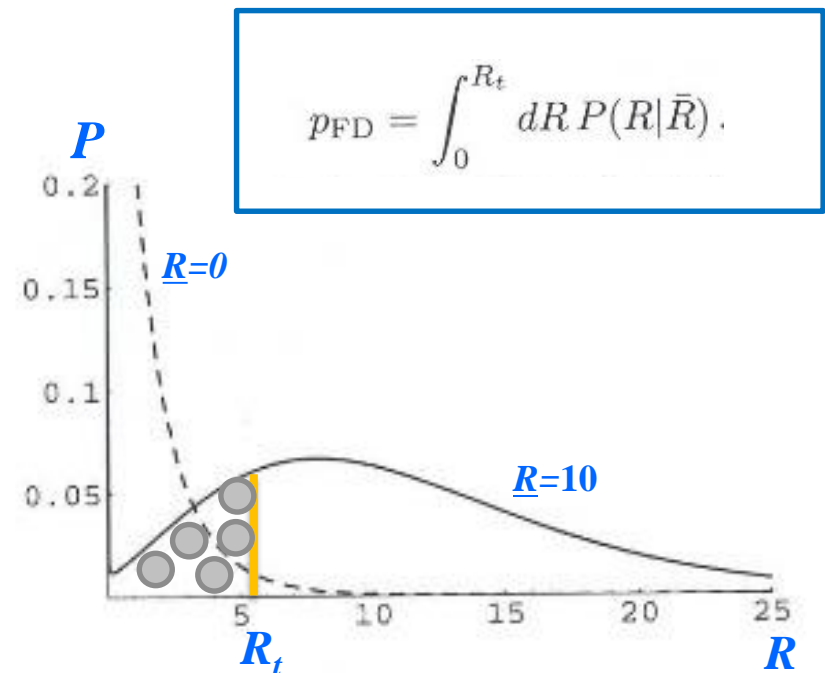
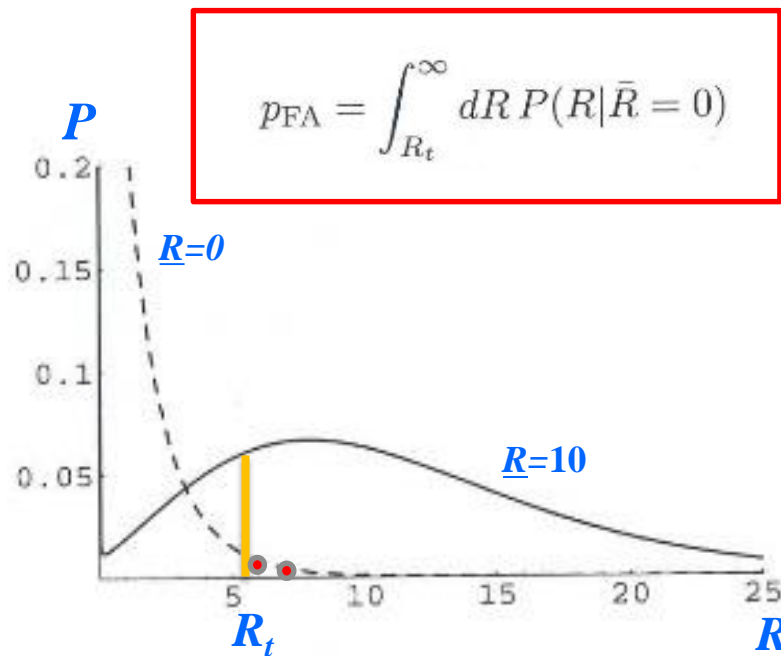


Credits: M. Maggiore- Gravitational Waves

Matched filtering statistics: p_{FA} and p_{FD}

We can set a threshold R_t which helps to discriminate in Gaussian noise between noise and GW events.

We can then define a False Alarm probability and a False Dismissal Probability:

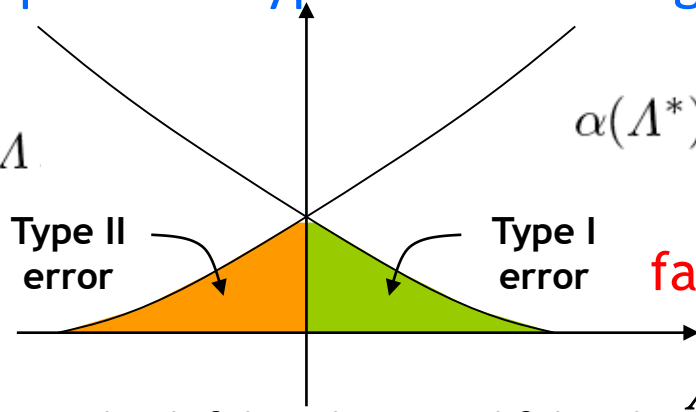


Frequentist hypothesis testing

$$\beta(\Lambda^*|h) \equiv \int_{-\infty}^{\Lambda^*} P(\Lambda|H_1) d\Lambda$$

$$\alpha(\Lambda^*) \equiv \int_{\Lambda^*}^{\infty} P(\Lambda|H_0) d\Lambda$$

False dismissal probability



false alarm probability

- We should strive to minimise both false alarm and false dismissal probabilities.
- According to the Neyman-Pearson lemma, this optimal test is the so-called likelihood ratio:

$$\Lambda(x; h) \equiv \frac{P(x|h)}{P(x|0)}$$

- For Gaussian noise, one finds

$$\ln \Lambda(x; h) = (x||h) - \frac{1}{2}(h||h)$$

$$(x||y) \xrightarrow{\Delta t \rightarrow 0} 4\Re \int_0^{\infty} \frac{\tilde{x}(f) \tilde{y}^*(f)}{S_n(f)} df$$

which is the well-known expression for the **matched-filtering amplitude**.

If some of the parameters of the signal $h(t; A, \lambda)$ are unknown, one has to find the maximum of $\ln \Lambda$ as a function of the unknown parameters

Amplitude maximization

We have to recall that we should search the maximum of Λ varying the signal parameters: in particular, we can analytically maximize over the amplitude A and the initial phase ϕ .

Assume that the signal has a certain form $s(t) = A \cos(\phi(t) + \phi_0)$, what is the associated likelihood?

It is immediate to show that the most probable amplitude is given by

$$A_{\text{MLE}} = \frac{\langle \bar{s}, \mathbf{x} \rangle}{\langle \bar{s}, \bar{s} \rangle}$$

where $\bar{s}(t) = \cos(\phi(t) + \phi_0)$. Hence

$$\max_A \Lambda(\mathbf{x}|s) = \exp\left(\frac{1}{2} \frac{\langle s, \mathbf{x} \rangle^2}{\langle s, s \rangle}\right);$$

in other words, one has to define the normalized *template*

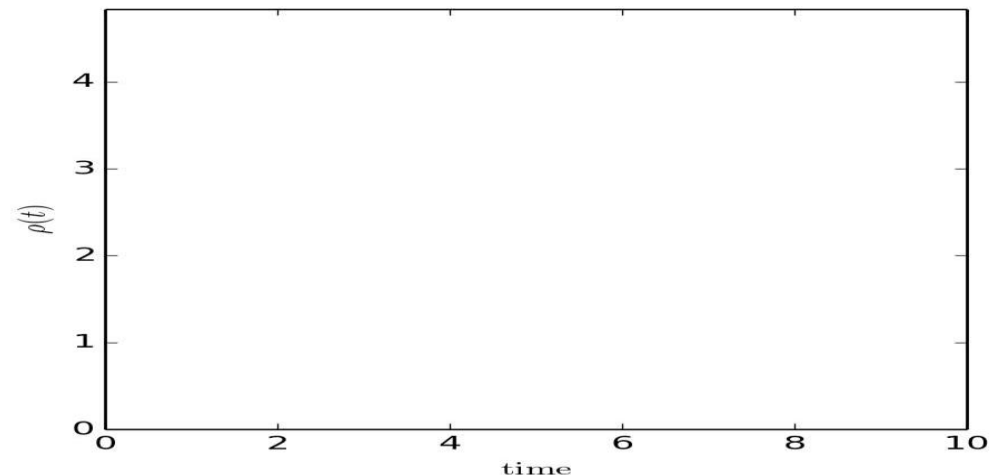
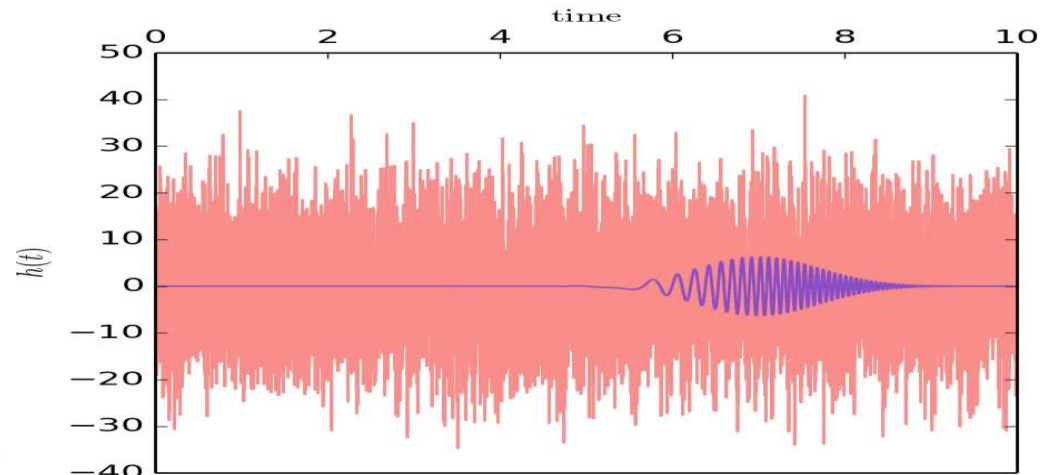
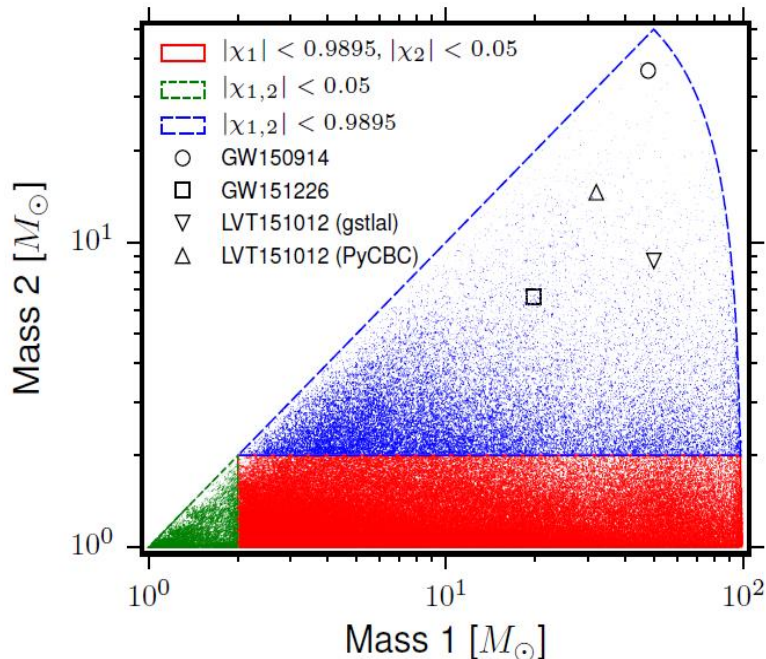
$$\mathbf{v} = \frac{s}{\sqrt{\langle s, s \rangle}}$$

and look for the maximum of the expression $|\langle \mathbf{v}, \mathbf{x} \rangle|$: this is the famous matched filtering procedure, invented by Wiener.

Finding a weak signal in noise

- “Matched filtering” lets us find a weak signal submerged in noise.
- For calculated signal waveforms, multiply the waveform by the data
- Find signal from cumulative signal/noise

PHYS. REV. X 6,041015 (2016)



Spanning the signal parameter space: we need a *bank* of templates!

To cover in an efficient way the physical parameter space (i.e. masses and spins, frequencies) of the signals with our modelled waveforms h , also called **templates** T , we construct a set of waveforms which assures that a signal can be found with a maximum loss in SNR of a fixed chosen value (i.e. 0.03)

A *mismatch* bewteen template waveforms T is defined as:

$$\mathcal{M}(T_j, T_k) = \frac{(T_j; T_k)}{\sqrt{(T_j; T_j) (T_k; T_k)}}$$

where maximization is done over time and φ .

The Fitting Factor is then defined as:

$$FF(h_s) = \max_{h \in \{h_b\}} \mathcal{M}(h_s, h)$$

Template placement

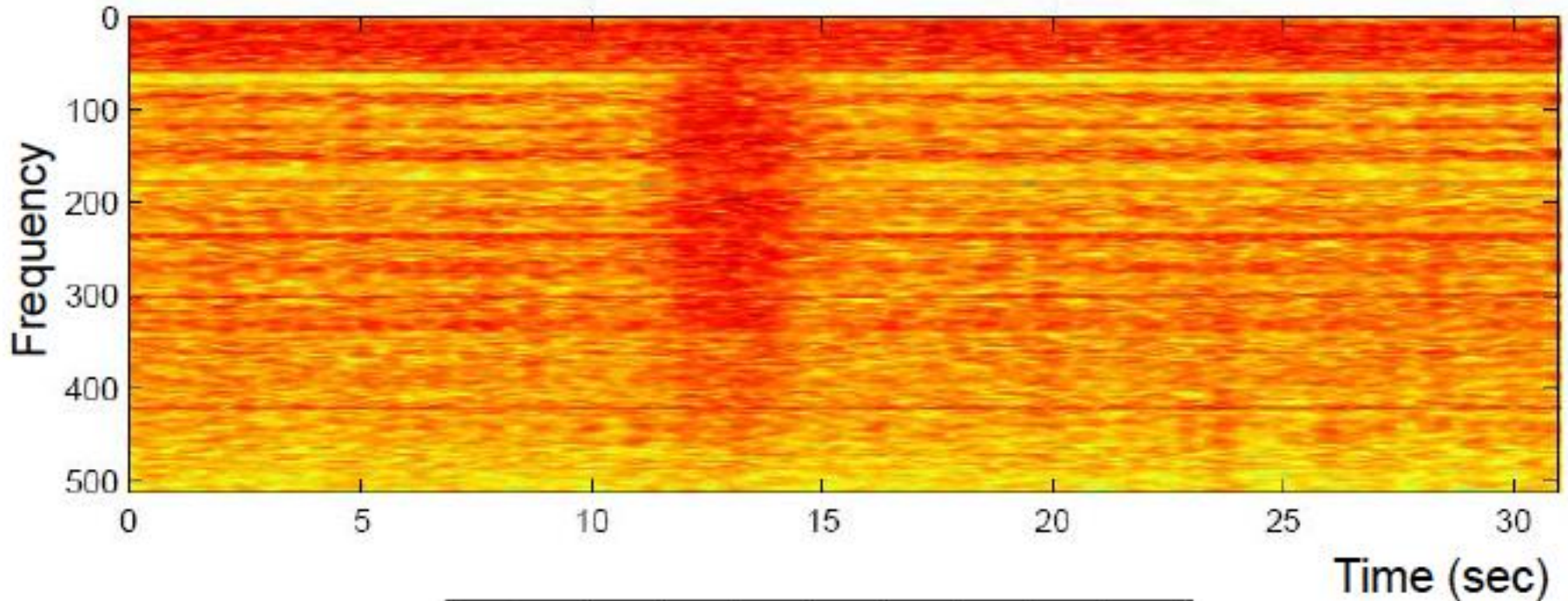
We can define a distance and construct a metric from the mismatch:

$$d(T(\xi_j), T(\xi_k)) = \sqrt{1 - \mathcal{M}(T(\xi_j), T(\xi_k))}$$

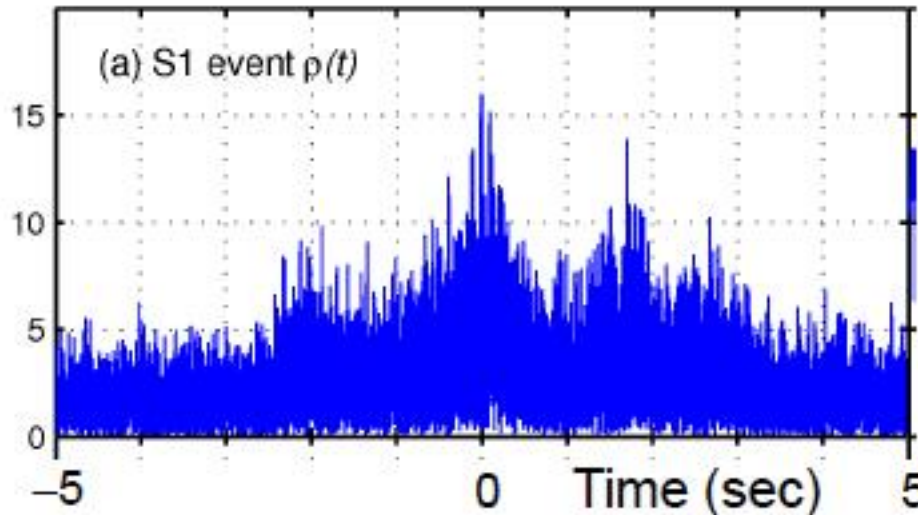
$$d^2(\xi, \xi + \delta) = 1 - \mathcal{M}(T(\xi), T(\xi + \delta)) = g_{jk}(\xi) \delta^j \delta^k$$

The metric tensor $g_{jk}(\xi) = -\frac{1}{2} \frac{\partial^2 \mathcal{M}(T(\xi), T(\xi + \delta))}{\partial \delta_j \partial \delta_k}$ can be found after maximization over t_c and φ .

Dealing with Non-Stationary Noise



Inspiral
filter output:



How do we know whether a signal in the data is a real GW?

Available tools:

- Consistency of the signal with a source model (if there is a model)
- Coincidence / consistency of signals in multiple GW detectors
- Absence of instrumental problems at the time of the signal
- Validation of instrument response and data analysis software
- Association with a known astrophysical object / event

Consistency with Source Model?

- Inspiral: (Matched filter already supposes a source model)
 - Chi-squared test
 - Sanity of filter output and/or chi-squared time series
- Cont.-wave:
 - Does it show the expected Doppler modulation?
 - Is it present all the time?
- Stochastic:
 - Does the signal have the expected spectrum?
 - Is it on all the time?
- Burst: Is it isolated in time?

Is it a real GW signal?

Coincidence / Consistency Tests:

- **Having multiple detectors is extremely valuable**
- **Signals should arrive at consistent times**
 - LIGO Hanford vs. Livingston: within ± 10 ms
 - LIGO vs. Virgo: within ± 27 ms
 - Also get sky position information from having multiple detectors
- **Signals should have consistent properties**
 - Same or similar templates, if a matched-filter search
 - Consistent frequencies, durations
 - Consistent amplitudes (allowing for different orientations)

Signal Consistency Tests

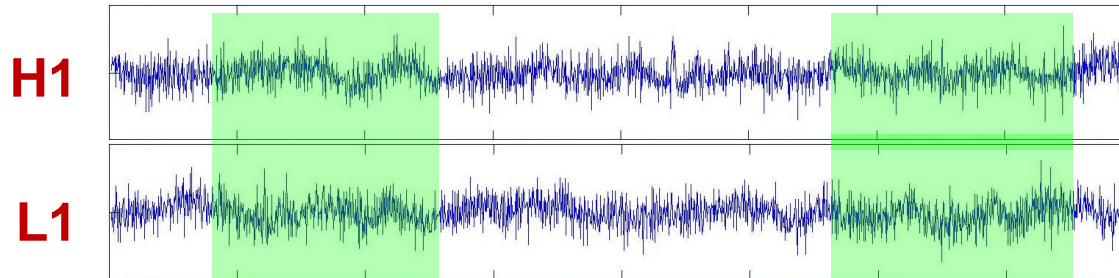
Crucial since a GW burst in a single detector may look just like an instrumental glitch !

Coincidence

Require signals in different detectors to have compatible times, frequencies, amplitudes and/or other waveform properties

Cross-correlation

Look for same signal buried in two data streams



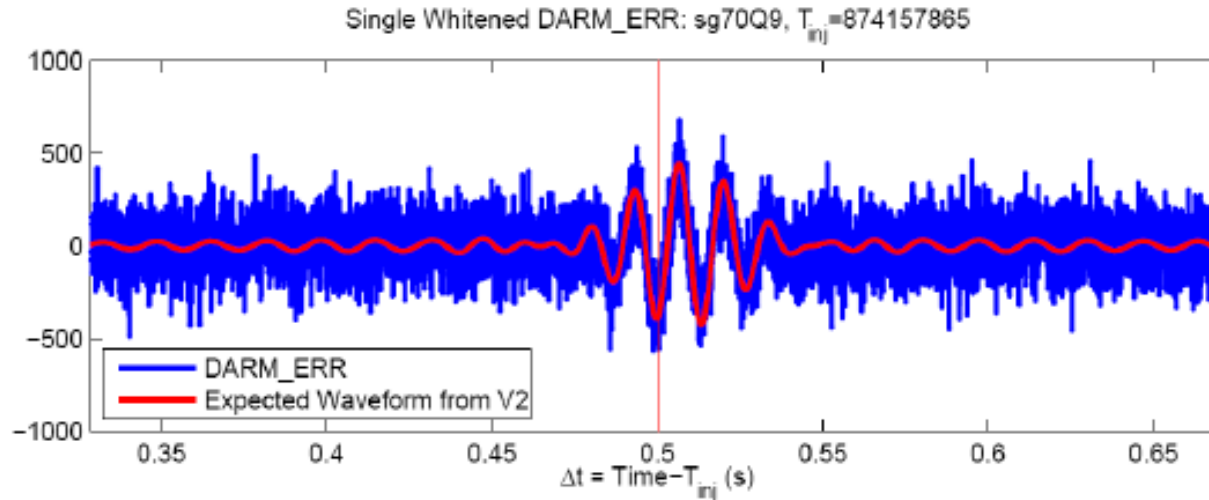
Checks for consistent *shape*, regardless of relative amplitude

Best to integrate over a time interval comparable to the target signal

Validating the Detector: Hardware Signal Injections

Shake the mirrors to mimic a GW signal

Can inject an arbitrary waveform



Also used to inject simulated pulsar signals continuously

Goals:

End-to-end test of interferometer and data analysis software

Checks calibration

Useful for veto “safety” checks

Significance: claiming a discovery

- If we measure a signal yield s sufficiently inconsistent with zero, we can claim a discovery
- **Statistical significance** = probability p to observe s or larger signal in the case of pure background fluctuation
- Often preferred to quote “ $n\sigma$ ” **significance**, where:

$$p = \int_{n\sigma}^{\infty} \frac{1}{\sqrt{2\pi}} e^{-x^2/2} dx = 1 - \frac{1}{2} \operatorname{erf} \left(\frac{n}{\sqrt{2}} \right)$$

- Usually, in literature:
 - If the significance is > 3 (“ 3σ ”) one claims “*evidence of*”
 - If the significance is > 5 (“ 5σ ”) one claims “*observation*” (discovery!)
 - probability of background fluctuation = 2.87×10^{-7}

When using upper limits

- Not always experiments lead to discoveries ☹️
- What conclusion can be drawn if no evidence of signal is observed?
- One possible definition of upper limit:
 - “largest value of the signal s for which the probability of a signal under fluctuation smaller or equal to what has been observed is less than a given level α (usually 10% or 5%)”
 - Upper limit @ x Confidence Level = s such that $\alpha(s) = 1 - x$
 - Similar to confidence interval with a central value, but the interval is fully asymmetric now
- Other approaches are possible:
 - Bayesian limits: extreme of an interval over which the poster probability of $[0, s]$ is $1 - \alpha$
 - It's a different definition!
 - Unified Feldman-Cousins frequentist limits

Spinning Neutron Stars

Relic of past collapse of a moderately massive star

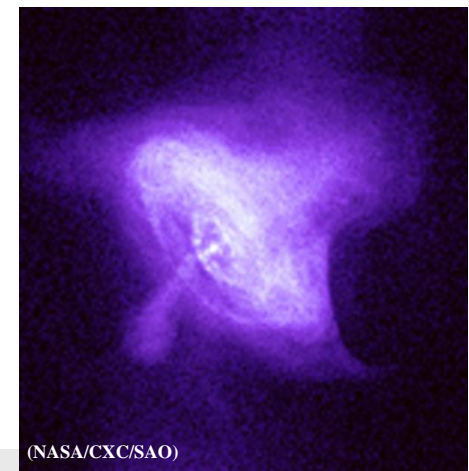
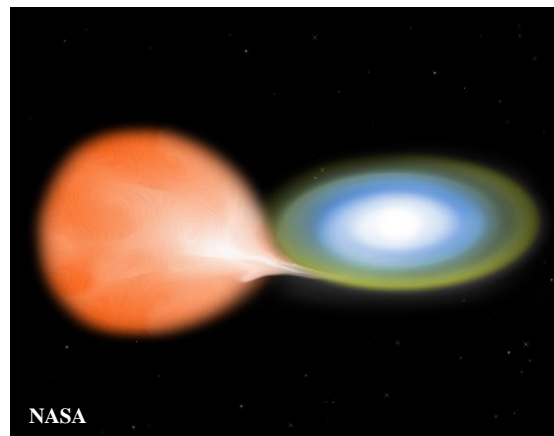
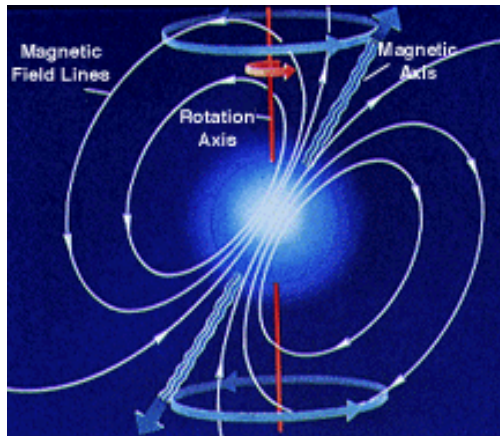
Remnant spin from progenitor, or from having been spun up by accretion

Generally magnetized, sometimes very strongly

A small fraction of neutron stars are seen as pulsars

If not axisymmetric, will emit gravitational waves

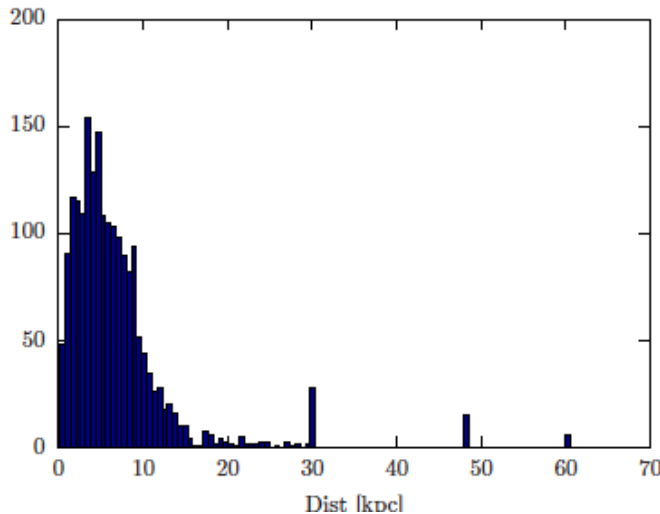
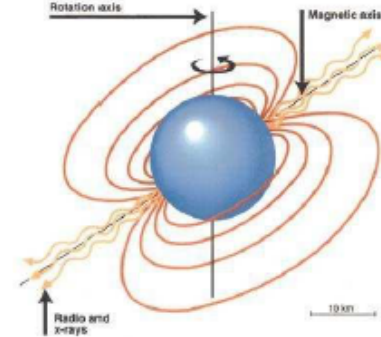
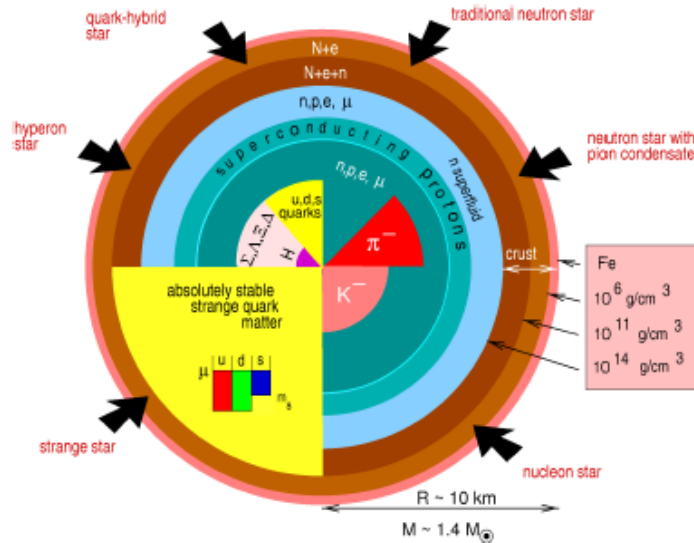
Example: ellipsoid with distinct transverse axes



No continuous gravitational waves (CW) detected... yet!

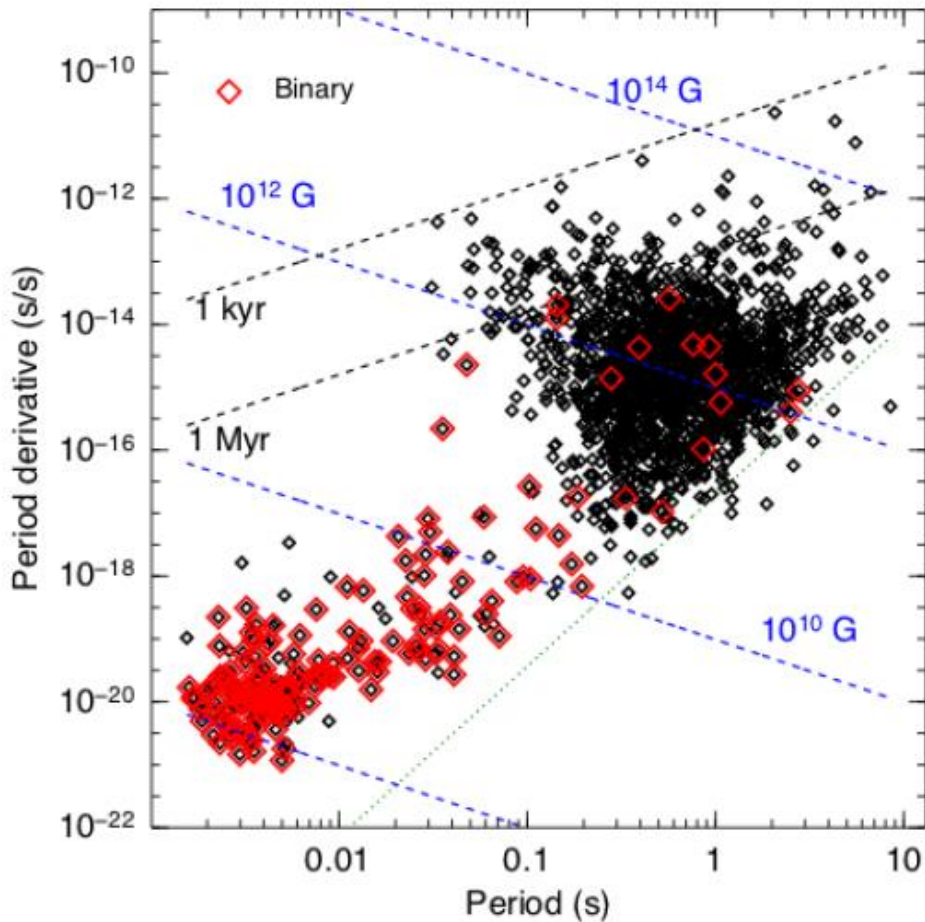
- Most searches begin *after* an observing run has ended, and all the data is in
- Still analysing LIGO O1 data
- Strict emission limits have already been set from initial detector era data on signals from known and unknown **neutron star** sources.

Neutron Stars and Pulsars



- $M \sim 1.4 M_{\odot}$, $R \sim 12$ km
- Rotation: $0.1 \text{ Hz} \lesssim \nu \lesssim 700 \text{ Hz}$
- EOS/composition uncertain
- Magnetic field $B \sim 10^9 - 10^{14} \text{ G}$
- ~ 2000 pulsars currently known (SKA: $\sim 20\,000$)
- ~ 300 in LIGO frequency band
- potentially many more ($\sim 10^8$) unknown NSs in galaxy

Pulsar population



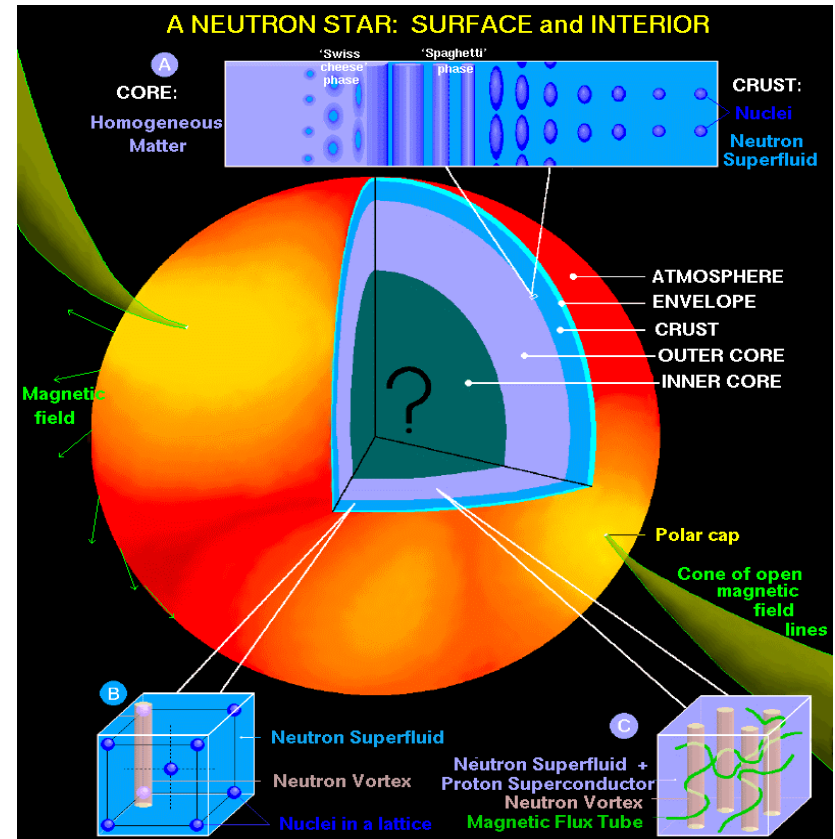
- Should be ~160 000 isolated and ~40 000 binary pulsars in the Galaxy
- Should be a total of $\sim 10^8+$ neutron stars in the Galaxy
- where are they all?

The P- \dot{P} Diagram is useful for following the lives of pulsars, playing a role similar to the Hertzsprung-Russell diagram for ordinary stars.

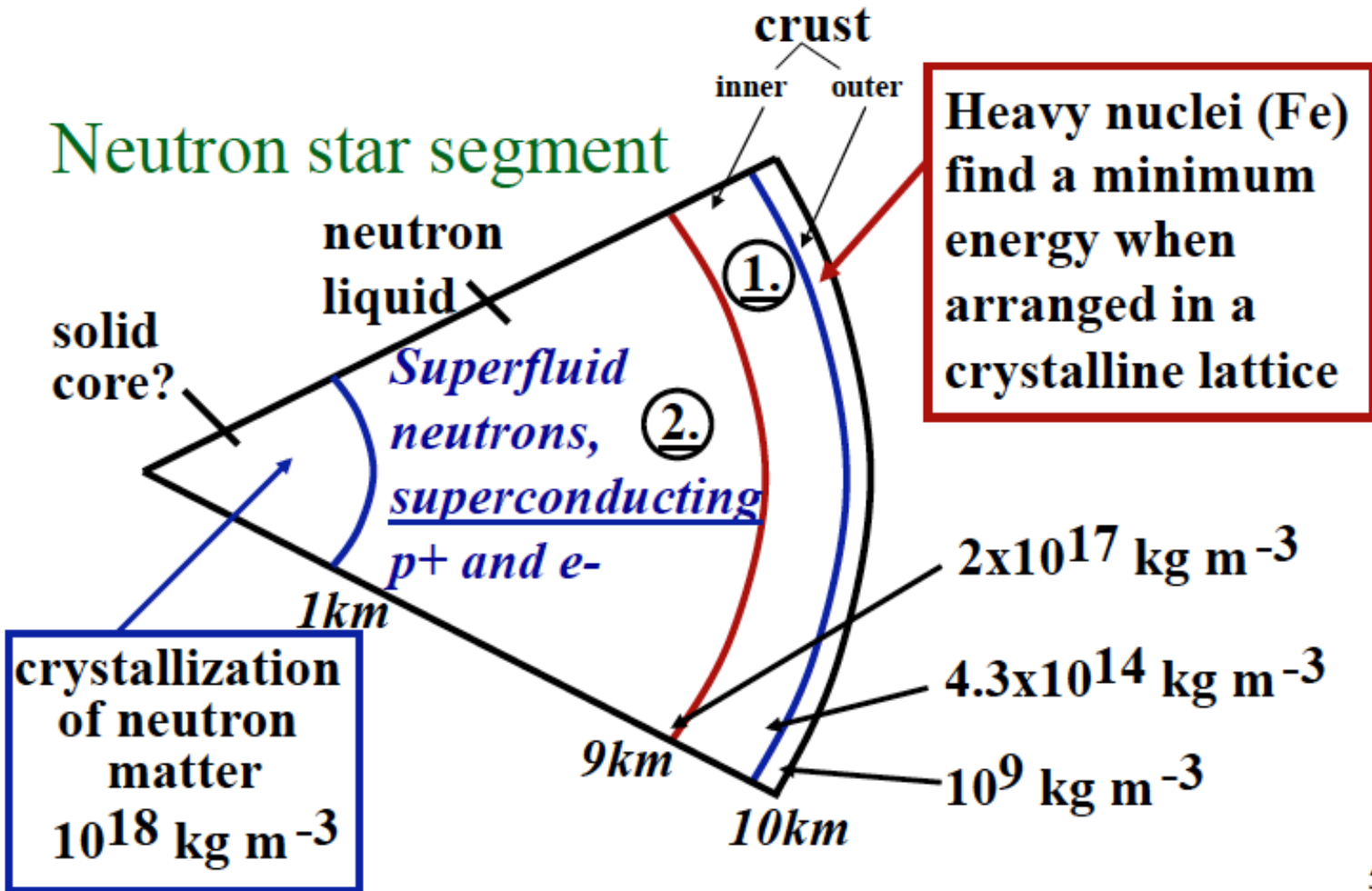
It encodes a tremendous amount of information about the pulsar population and its properties, as determined and estimated from two of the primary observables, P and \dot{P} . Using those parameters, one can estimate the pulsar age, magnetic field strength B, and spin-down power dE/dt .

Neutron Stars Sources

- Great interest in detecting radiation: physics of such stars is poorly understood.
 - After many years we still don't know what makes pulsars pulse.
 - Interior properties not understood: equation of state, superfluidity, superconductivity, solid core, source of magnetic field.
 - May not even be neutron stars: could be made of strange matter!



Neutron star structure



Regions of NS Interior

Main Components:

- (1) Crystalline solid crust
 - (2) Neutron liquid interior
- Boundary at $\rho = 2 \cdot 10^{17} \text{ kg/m}^3$ – density of nuclear matter

Outer Crust:

- Solid; matter similar to that found in white dwarfs
- Heavy nuclei (mostly Fe) forming a Coulomb lattice embedded in a relativistic degenerate gas of electrons.
- Lattice is minimum energy configuration for heavy nuclei.

Inner Crust (1):

- -Lattice of neutron-rich nuclei (electrons penetrate nuclei to combine with protons and form neutrons) with free degenerate neutrons and degenerate relativistic electron gas.
- For $\rho > 4.3 \cdot 10^{14} \text{ kg/m}^3$ – the neutron drip point, massive nuclei are unstable and release neutrons.
- Neutron fluid pressure increases with ρ

Regions of NS Interior (cont)

Neutron Fluid Interior (2):

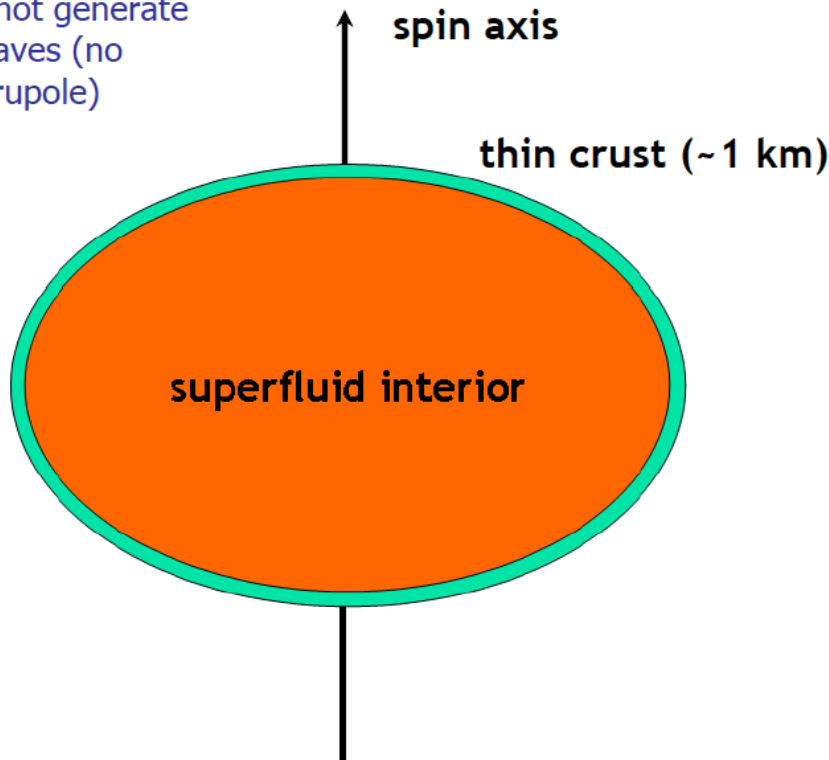
- For $1 \text{ km} < r < 9 \text{ km}$, ‘neutron fluid’ – superfluid of neutrons and Superconducting protons and electrons.
- Enables B field maintenance.
- Density is $2 \cdot 10^{17} < \rho < 1 \cdot 10^{18} \text{ kg/m}^3$.
- Near inner crust, some neutron fluid can penetrate into inner part of lattice and rotate at a different rate – glitches?

Core:

- Extends out to $\sim 1 \text{ km}$ and has a density of $1 \cdot 10^{18} \text{ kg/m}^3$.
- Its substance is not well known.
- Could be a neutron solid, quark matter or neutrons squeezed to form a pion concentrate.

Simple view of a neutron star

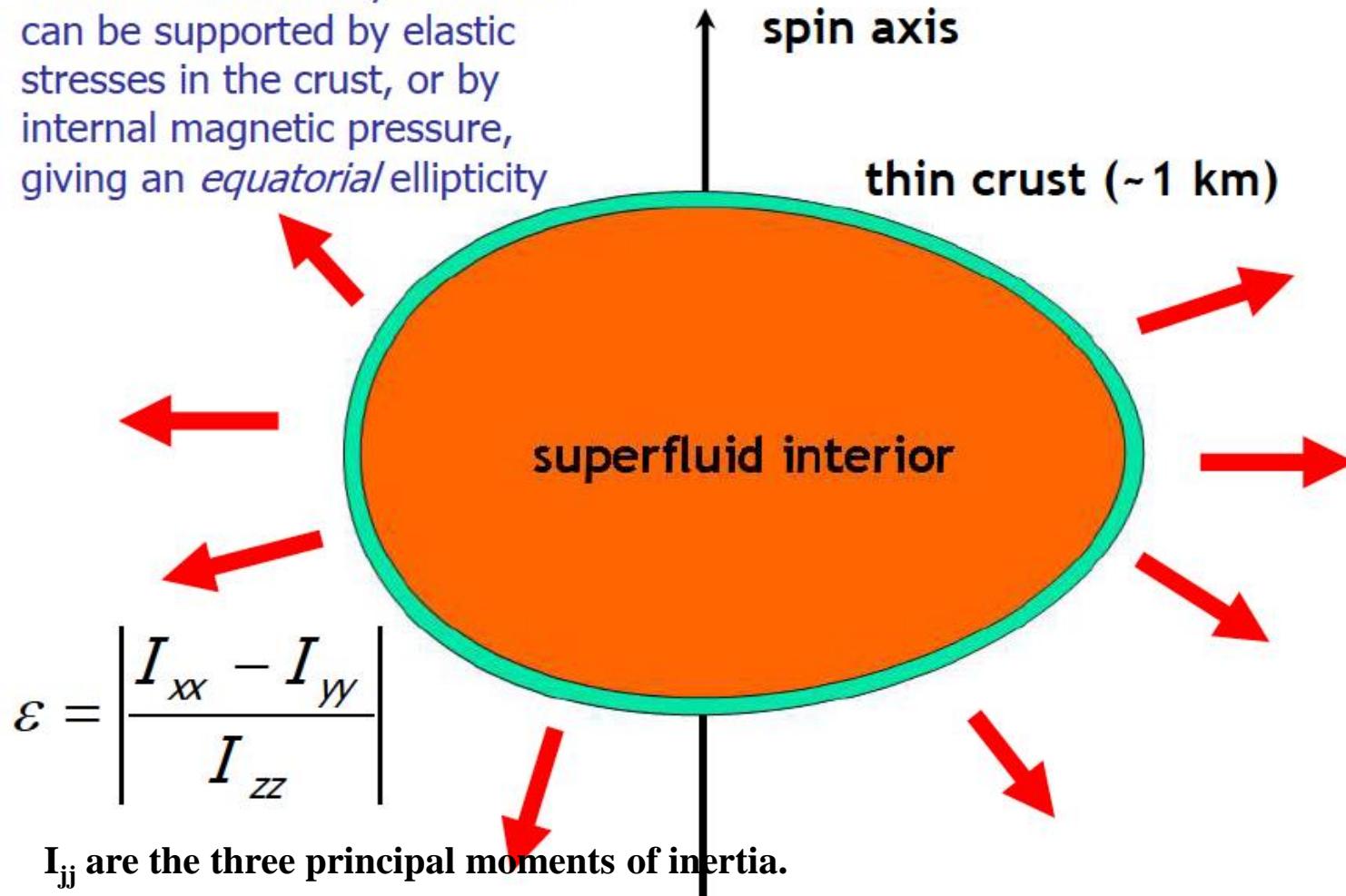
Axisymmetric centrifugal
oblateness cannot generate
gravitational waves (no
changing quadrupole)



Non-axisymmetric
distortions do not
exist in perfect fluid
stars, but in realistic
neutron stars such
deformations can be
supported either by
elastic stresses or by
magnetic fields.

Simple view of a neutron star

But neutron star asymmetries can be supported by elastic stresses in the crust, or by internal magnetic pressure, giving an *equatorial* ellipticity



Rigid crust epsilon?

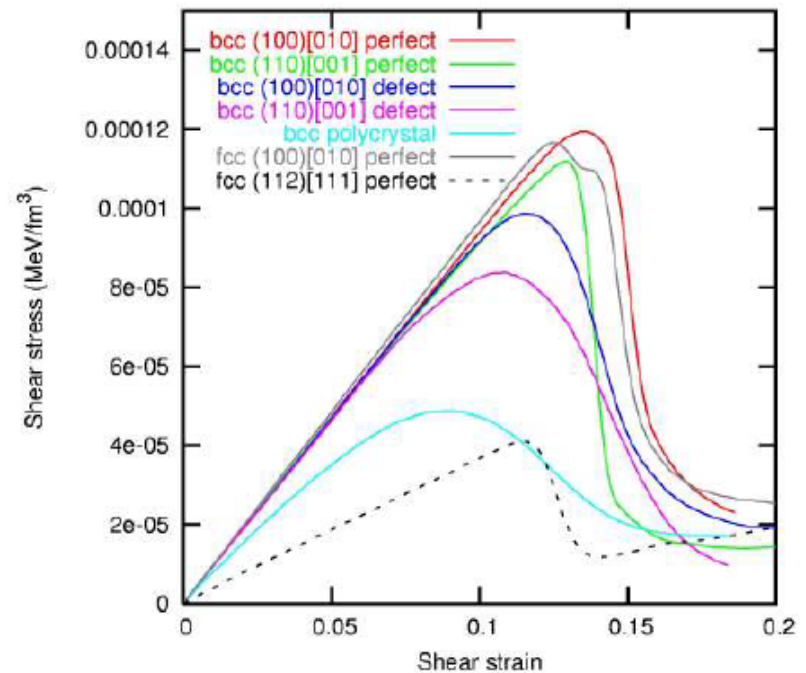
- For a neutron star, Ushomirsky, Cutler and Bildsten MNRAS 319, 902 (2000):

$$\epsilon_{\max} \approx 5 \times 10^{-7} \left(\frac{\sigma}{10^{-2}} \right)$$

Breaking strain, maybe 10^{-1}
(Horowitz & Kadau 2009)
but maybe a lot less!

- But for a quark star,
Owen, 2005, Phys. Rev. Lett.
95, 211101 (2005)

$$\epsilon_{\max} \approx 4 \times 10^{-4} \left(\frac{\sigma}{10^{-2}} \right)$$



Horowitz & Kadau

Phys. Rev. Lett. 102:191102,2009

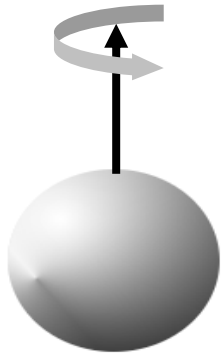
R-modes and other exotics

In addition to GWs from elastic crustal distortions, we can also expect them from:

- unstable oscillation in the fluid part of the neutron star -- Chandrasekhar-Friedman-Schutz (CFS) instabilities e.g. through r-modes
- free precession
- magnetic stresses
- accretion induced deformation
- ...

Emission mechanisms for continuous GW from spinning NS in the LIGO-VIRGO frequency band

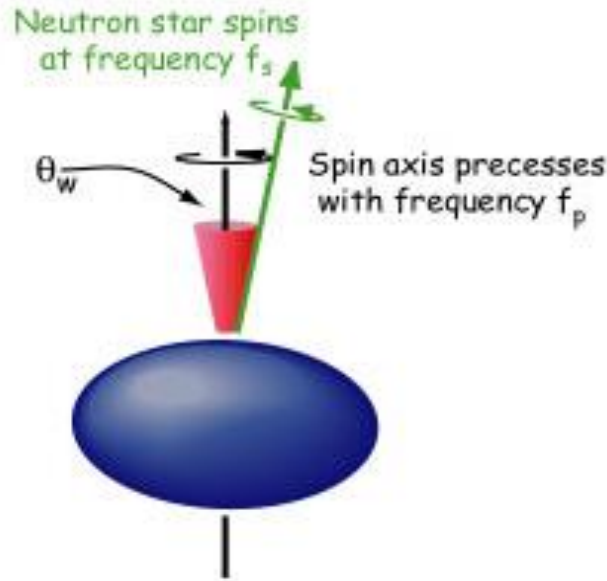
- Non-axisymmetric distortions
- Unstable oscillation modes in the fluid part of the star
- Free precession



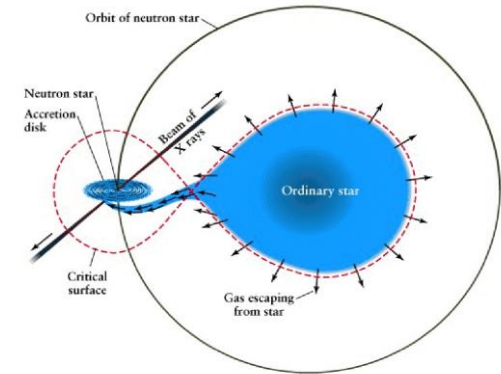
Bumpy Neutron Star



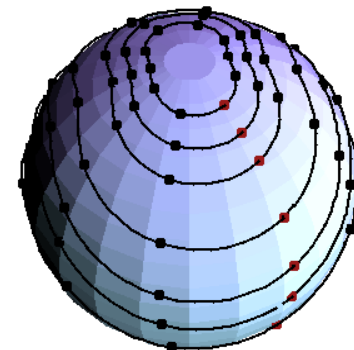
Magnetic mountains



Wobbling Neutron Star



Low Mass X-Ray Binaries



R-modes in accreting stars

Gravitational Waves from Spinning Neutron Stars

Review article: Reinhard Prix for the LIGO Scientific Collaboration, “The Search for Gravitational Waves from Spinning Neutron Stars”, Springer Lecture Notes Series.

GW energy emission rate from a spinning neutron star

$$R_s = 2GM/c^2$$

Schwarzschild radius

$$V = 2\pi R\nu$$

Rotational velocity at the surface

$$L_{\text{GW}} \sim \frac{c^5}{G} \epsilon^2 \left(\frac{R_s}{R}\right)^2 \left(\frac{V}{c}\right)^6$$

↑
10⁵²W

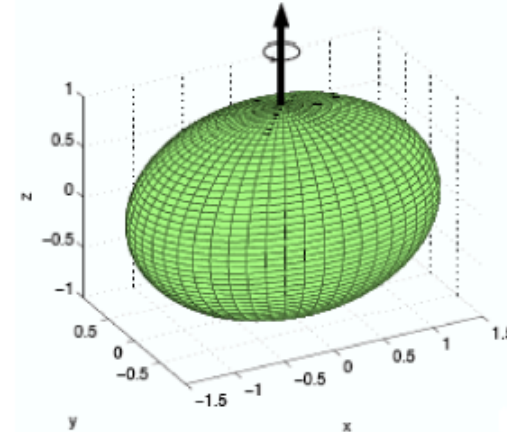
compact objects (i.e. with $R_s \sim R$) in rapid rotation ($V \sim c$), such as spinning neutron stars, can emit enormous GW luminosities even for small ϵ .

However, spacetime is a very “stiff” medium: large amounts of energy are carried by GWs of small amplitude.

$$h \sim 10^2 \frac{G}{c^4} \frac{\epsilon I_{zz} \nu^2}{d} \sim 3 \times 10^{-25} \left(\frac{\epsilon}{10^{-6}}\right) \left(\frac{I_{zz}}{10^{38} \text{ kg m}^2}\right) \left(\frac{\nu}{100 \text{ Hz}}\right)^2 \left(\frac{100 \text{ pc}}{d}\right)$$

Continuous GWs from Spinning Compact Objects

- rotation rate ν around z axis
- moment of inertia I_{ij}
- non-axisymmetry $\epsilon = \frac{I_{xx} - I_{yy}}{I_{zz}}$



☞ monochromatic signal at $f = 2\nu$, amplitude h_0 at distance d :

$$h_0 = \left(\frac{16\pi^2 G}{c^4} \right) \frac{(\epsilon I_{zz}) \nu^2}{d}$$

Strongly-deformed, closeby, fast-spinning neutron star:

$$h_0 = 10^{-25} \left(\frac{\epsilon}{10^{-6}} \frac{I_{zz}}{10^{38} \text{ kg m}^2} \right) \left(\frac{\nu}{50 \text{ Hz}} \right)^2 \left(\frac{100 \text{ pc}}{d} \right)$$

[Compare GW150914: $h_0 \sim 10^{-21}$ [LVC,PRL116,061102(2016)]]

Continuous GWs from Spinning Compact Objects

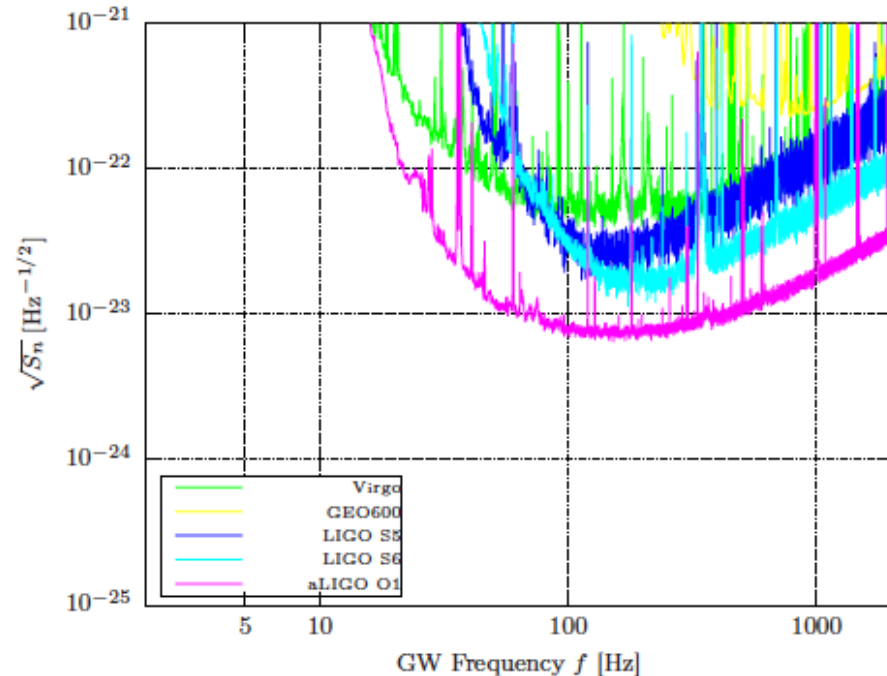
Matched filtering

Signal-to-Noise ratio

$$\text{SNR} \propto \frac{h_0}{\sqrt{S_n}} \sqrt{T}$$

aLIGO O1 strain noise:

$$\sqrt{S_n} \sim 10^{-23} \text{ Hz}^{-1/2}$$



- GW150914: $h_0 \sim 10^{-21}$, $T \sim 0.2\text{s}$ \Rightarrow SNR ~ 24
- spinning NS: $h_0 \lesssim 10^{-25}$ \Rightarrow need $T \gtrsim$ days – months

“Sensitivity Depth” needed in O1: $\mathcal{D} \equiv \frac{\sqrt{S_n}}{h_0} \gtrsim 100 \text{ Hz}^{-1/2}$

Continuous GWs from Spinning Compact Objects

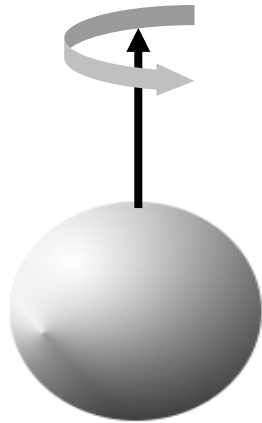
- Various physical mechanisms could operate in a neutron star to produce interesting levels of GW emission
- As the signal-strength is generally expected to be weak, long integrations times (several days to years) are required in order for the signal to be detectable in the noise.
- Therefore this GW emission has to last for a long time, which characterizes the class of ‘continuous-wave’ signals.

Large uncertainties!

Prior range: $\varepsilon \sim [10^{-12}; 10^{-4}]$ for $I_{zz} = 10^{38} \text{kgm}^2$

quadrupole moments $Q \sim I_{zz} \varepsilon \sim [10^{26}; 10^{34}] \text{kgm}^2$

Neutron stars might also be interesting sources of burst-like GW emission,
f-mode or p-mode oscillations excited by a glitch
crustal torsion modes



1) Non-axisymmetric distortions

A non-axisymmetric neutron star at distance a , rotating with frequency ν around the I_{zz} axis emits monochromatic GWs of frequency $f = 2\nu$ with an amplitude

$$h_0 = \frac{4\rho^2 G}{c^4} \frac{I_{zz} e f_{gw}^2}{d}$$

Bumpy Neutron Star

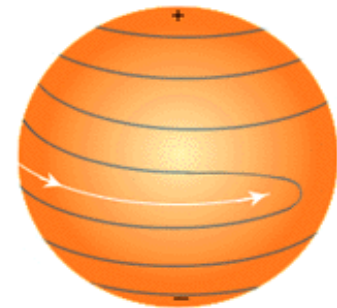
$$e = \frac{I_{xx} - I_{yy}}{I_{zz}}$$

The strain amplitude h_0 refers to a GW from an optimally oriented source with respect to the detector

The equatorial ellipticity is highly uncertain, $\varepsilon \sim 10^{-7}$. In the most speculative model can reach up to 10^{-4} .

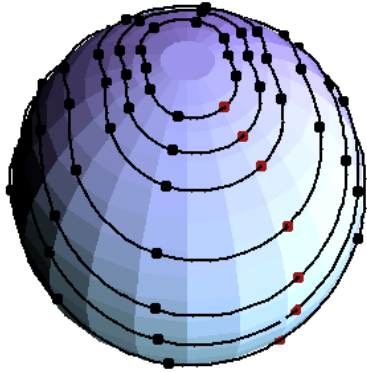
Accreting neutron stars in binary systems can also have large crust deformations

Strong internal magnetic fields could produce deformations of up to $\varepsilon \sim 10^{-6}$. These deformations would result in GW emission at $f = \nu$ and $f = 2\nu$.



Magnetic mountains

2) Non-axisymmetric instabilities

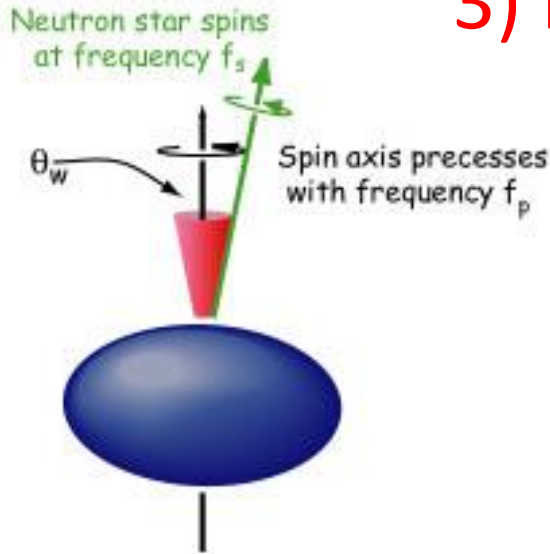


R-modes in accreting stars

At birth or during accretion, rapidly rotating NS can be subject to various non-axisymmetric instabilities, which would lead to GW emission,

The r-mode instability (toroidal modes with a Coriolis restoring force) has been proposed as a source of GWs (with frequency $f = 4\nu/3$) from newborn NS and from rapidly accreting NS.

3) Free precession



Similar emission would occur if the core and crust had non-aligned spins. This results in emission at (approximately) the rotation rate ν and twice the rotation rate, i.e. $f = \nu + \nu_{prec}$ and $f = 2\nu$.

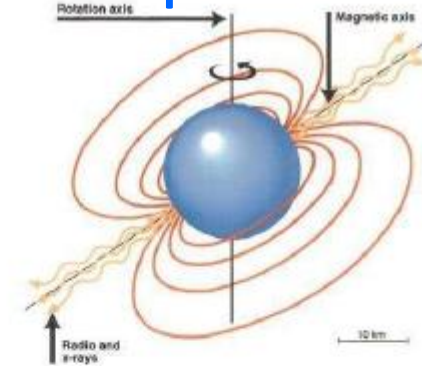
$$h_0 \sim 10^{-27} \left(\frac{\theta_w}{0.1} \right) \left(\frac{1 \text{ kpc}}{d} \right) \left(\frac{\nu}{500 \text{ Hz}} \right)^2$$

Wobbling Neutron Star

Spindown upper-limits for known pulsars.

Rotational energy lost: $\dot{E}_{\text{rot}} \propto I_{\text{ZZ}} \nu \dot{\nu}$

Energy emitted in GWs: $\dot{E}_{\text{GW}} \propto \nu^6 I_{\text{ZZ}}^2 \epsilon^2$



Spindown upper limit: Spindown fully due to GW emission

Assumed $I_{\text{ZZ}} = 10^{38} \text{ kg m}^2$ and known distance d :

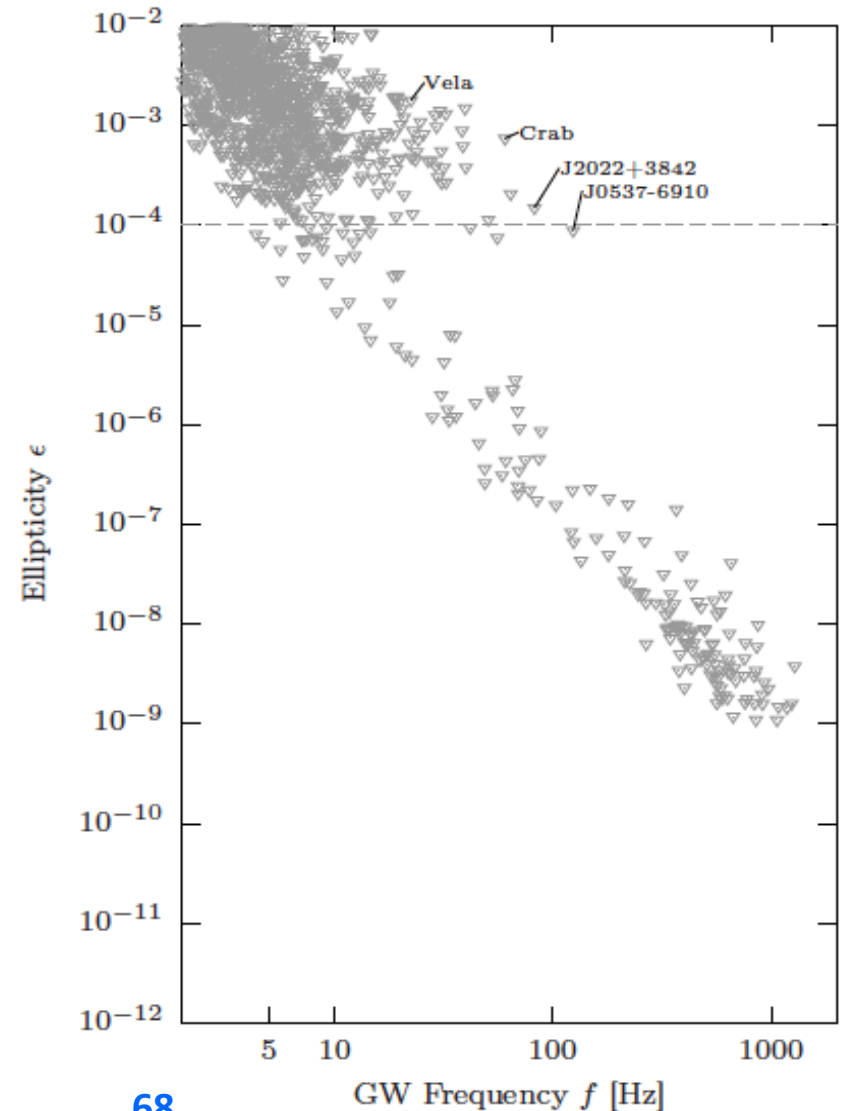
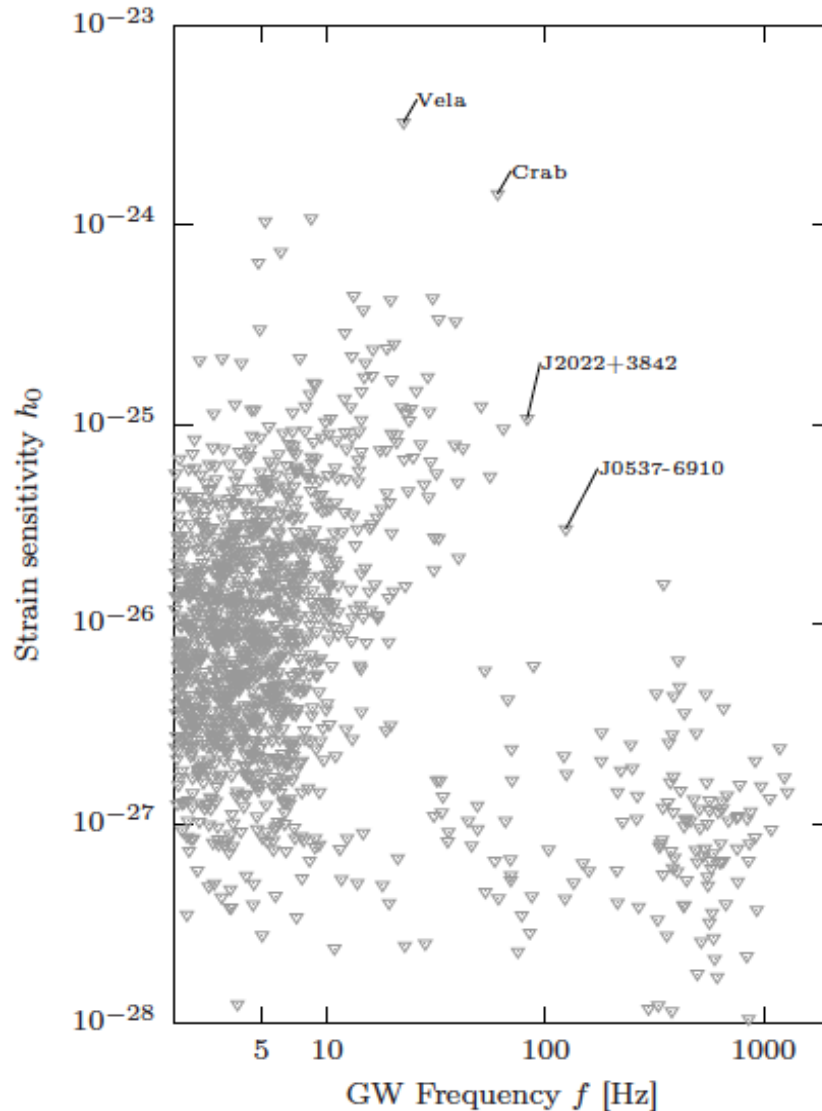
⇒ Upper limit on deformation ϵ :

$$\epsilon_{\text{sd}} \propto \sqrt{\frac{1}{I_{\text{ZZ}}} \frac{|\dot{\nu}|}{\nu^5}}$$

⇒ Upper limit on amplitude h_0 :

$$h_{\text{sd}} \propto \frac{1}{d} \sqrt{I_{\text{ZZ}} \frac{|\dot{\nu}|}{\nu}}$$

Spindown upper-limits for known pulsars.



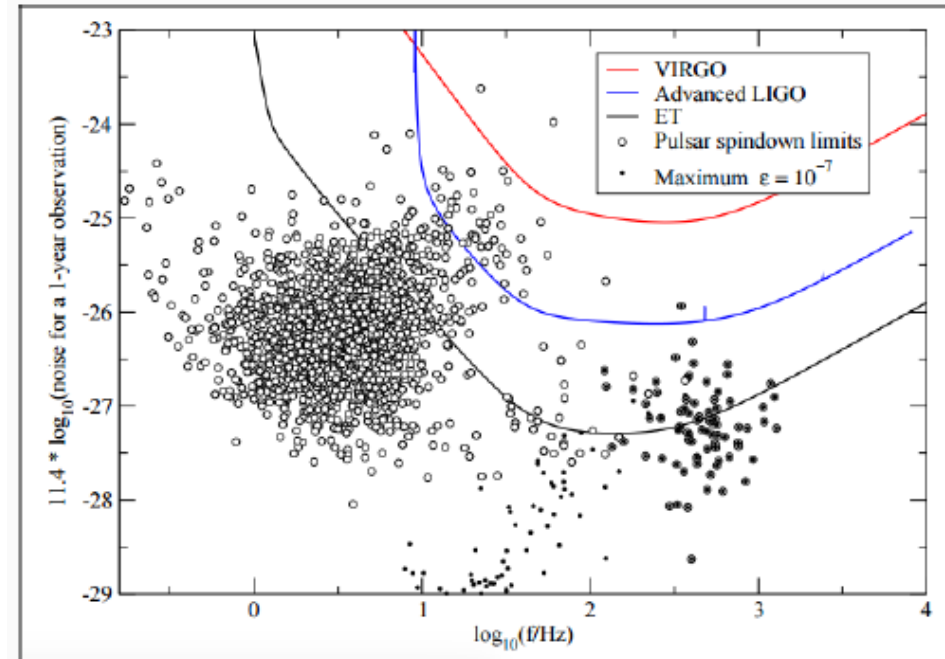
Theoretical maximum sustainable ellipticities provide upper limit, but whether these are realised in nature is unknown/unlikely.

Methods of producing/sustaining ellipticities are also highly uncertain:

- mountains locked-in to crust following formation
- strong internal magnetic fields

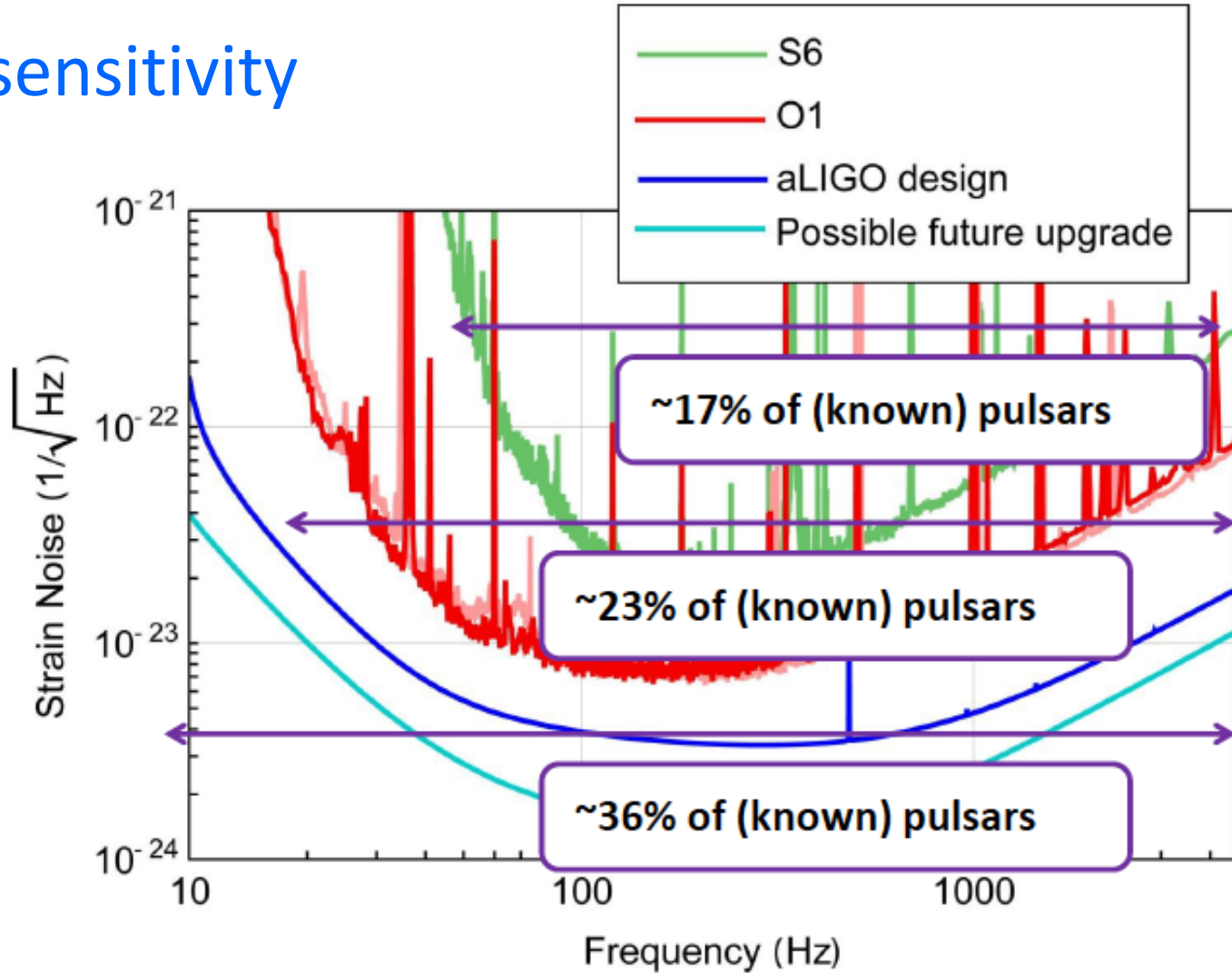
We have no idea how many signal detections to expect in first years of aLIGO/AdV.

Advocate for better modeling of neutron star deformation to enhance science case?



Credit: Andersson *et al*, GReGr, 43 (2011)
arXiv:0912.0384

aLIGO sensitivity



B.P. Abbott et al., *PRL* 116:131103 (2016)

What would we learn from a CW signal?

if accompanied by EM observation either from a known pulsar search or through follow-up of unknown sources

- $f_{\text{GW}} = 2f_{\text{rot}}$ star is probably a triaxial ellipsoid
- $f_{\text{GW}} \approx 2f_{\text{rot}}$ shows components producing EM and GW emission are not completely coupled (information on crust and core coupling of star?)
- $f_{\text{GW}} \approx f_{\text{rot}}$ precession play important role in emission
- $f_{\text{GW}} \approx (4/3) f_{\text{rot}}$ emission from r-modes is favoured (information on interior fluid motion of star)

What would we learn from a CW signal?

- if ellipticities are at the very high range we could potentially narrow down neutron star EOS
- multiple sources could yield information on ellipticity distributions to help constrain models of formation of deformations
 - are there different distributions for “normal” and millisecond pulsars?

But, we actually measure $h \propto I_{zz} \varepsilon / d$, where I_{zz} is the moment of inertia and d is the distance, so measuring ε requires this additional information

- Compare GW phase to EM pulse timing -- phase locking/drift?
- Test General Relativity with a long-lived source.

Theoretical implications

Interpretation of upper limits

- Constraints to the energy budget
- Can't constrain equations of state (stars could just be axially symmetric) unless we *know* there are mountains
- Can constrain internal magnetic strength/configuration

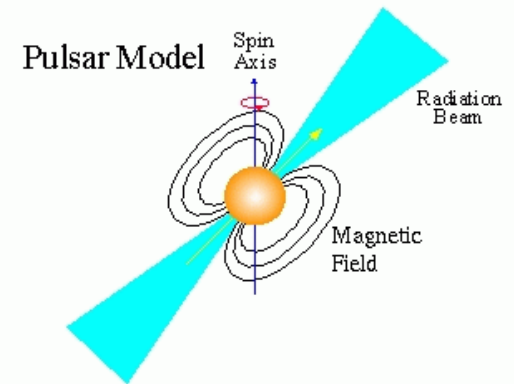
Interpretation of detections

- High ellipticity means some exotic equation of state (quarks)
- Somewhat high $\bar{\nu}$ means EOS or high internal B field: which?
- Frequency ratio reveals emission mechanism ($\bar{\nu}$ or r-mode); also rough guide to star's compactness if r-mode
- Steady r-mode signal means strange particles in core

The signal from a NS

- The 'periodic' GW signal from a neutron star:

$$h(t) = h_0 A(t) e^{F(t)}$$



- Nearly-monochromatic continuous signal
 - spin precession at $\sim f_{\text{rot}}$
 - excited oscillatory modes such as the r-mode at $4/3 * f_{\text{rot}}$
 - non-axisymmetric distortion of crystalline structure, at $2f_{\text{rot}}$

- (Signal-to-noise)² ~

$$\int_0^T \frac{h^2(t)}{S_h(f_{\text{gw}})} dt$$



Expected Signal on Earth (1)

Spin-down \Rightarrow phase evolution

the phase of the received signal depends on the initial phase, the frequency evolution of the signal and on the instantaneous relative velocity between source and detector.

$$\Phi(t) = \phi_0 + 2\pi \sum_{n=0}^{\infty} \frac{f_{(n)}}{(n+1)!} (T(t) - T(t_0))^{n+1}$$

$T(t)$ is the time of arrival of a signal at the Solar System Barycentre (SSB)

t is the time at the detector

Expected Signal on Earth (2)

Relative motion detector/source \Rightarrow frequency modulation

Doppler shift:
$$\frac{\Delta f}{f} = \frac{\mathbf{v} \cdot \mathbf{n}}{c}$$

Antenna sensitivity of the detector \Rightarrow amplitude modulation

$$h(t) = F_+(t; \psi) h_+(t) + F_\times(t; \psi) h_\times(t) \quad \begin{aligned} h_+ &= A_+ \cos \Phi(t) \\ h_\times &= A_\times \sin \Phi(t) \end{aligned}$$

$$\left. \begin{aligned} F_+(t, \psi) \\ F_\times(t, \psi) \end{aligned} \right\}$$

strain antenna patterns of the detector to plus and cross polarization, bounded between -1 and 1.

They depend on the orientation of detector and source and on the waves polarization.

Expected Signal on Earth (3)

For an isolated tri-axial *non-precessing* neutron star emitting at twice its rotational frequency:

$$A_+ = \frac{1}{2} h_0 (1 + \cos^2 \iota)$$

$$A_\times = h_0 \cos \iota$$

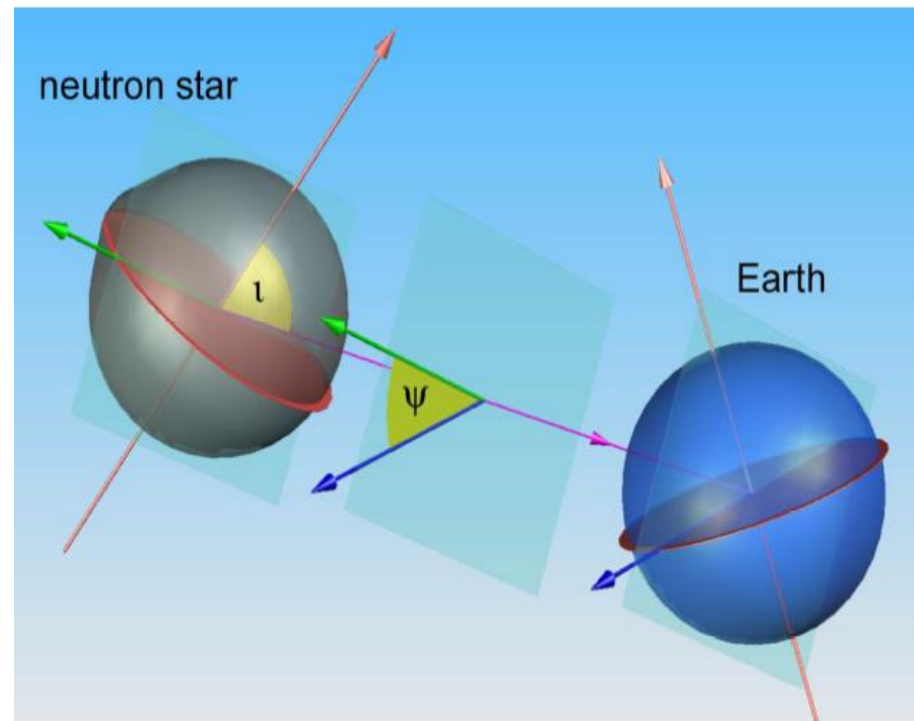
$$h(t) = F_+(t; \psi) h_0 \left(\frac{1 + \cos^2 \iota}{2} \right) \cos \Phi(t) - F_\times(t; \psi) h_0 \cos \iota \sin \Phi(t)$$

Signal parameters:

- ψ = polarization angle
- ι = inclination angle of source with respect to line of sight
- $\Phi(t) = \phi(t) + \phi_0$
- ϕ_0 = initial phase of pulsar
- h_0 = amplitude of the GW signal

$$h_0 = \frac{4\pi^2 G}{c^4} \frac{I_{zz} \varepsilon f_{gw}^2}{d} \quad \varepsilon = \frac{I_{xx} - I_{yy}}{I_{zz}}$$

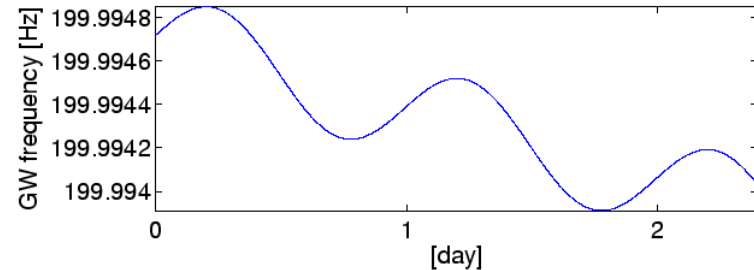
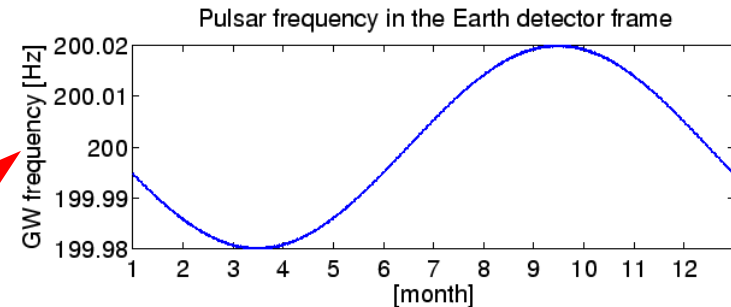
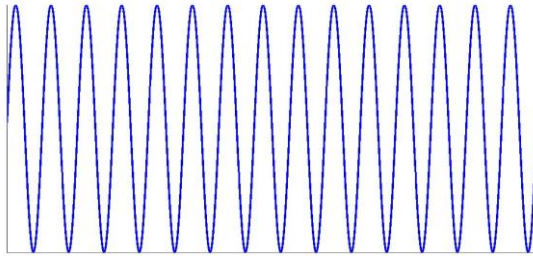
equatorial ellipticity



The Signal

• At the source

• At the detector



- Annual variation: up to $\sim 10^{-4}$
- Daily variation: up to $\sim 10^{-6}$

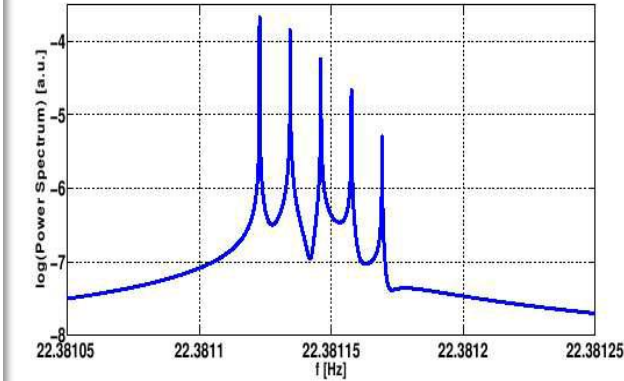
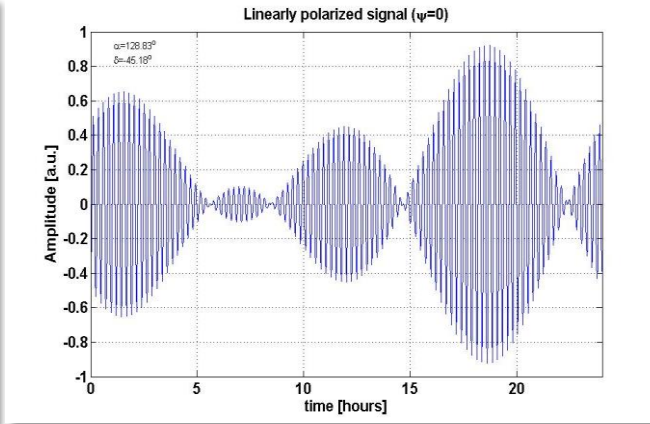
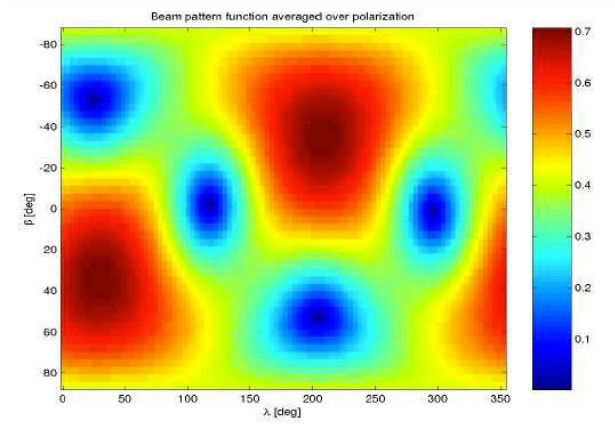
... more complications for GW signals from pulsars in binary systems

Additional Doppler shift due to orbital motion of neutron star

Varying gravitational red-shift if orbit is elliptical

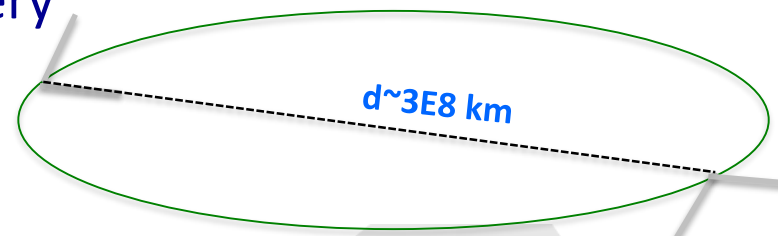
Shapiro time delay if GW passes near companion

Amplitude and phase modulation, due to the detector sidereal response



- Signal persistent nature allows to significantly increase the detection significance, and to pin down the NS parameters to extremely high accuracy even with a single detector

In practice, the detector makes a very large baseline network with itself



Type of searches

- We will see GWs from any neutron star that is
 - sufficiently lumpy
 - sufficiently close
 - spinning at a rate that will appear in our band
- A two-part attack:
 - target neutron stars we can see electromagnetically,
 - 👍 reduced parameter space, so good sensitivity
 - 👎 detections would usually need ‘new’ physics (quark stars etc...)
 - perform a general search for EM-dark neutron stars,
 - 👍 large population
 - 👎 our range (reach) is computationally-bound, even with E@H! We need several different search methods optimised for specific search tasks.

Continuous Waves Searches (1)

These searches have several parameters:

May be known, used in the search:

position
frequency,
frequency derivatives
orbital parameters

Not explicitly searched for:

initial phase
inclination angle
polarization
amplitude

Different algorithms have been developed, depending on what we know about the source: source parameters knowledge, waveform knowledge, isolated or binary system sources etc.

Neutron star populations

- Known radio, X-ray and γ -ray pulsars
 - Position & frequency evolution known (including derivatives, timing noise, glitches, orbit)
- Unknown neutron stars
 - Nothing known, search over position, frequency & its derivatives
- Accreting neutron stars in low-mass x-ray binaries
 - Position known, sometimes orbit & frequency
- Known, isolated, non-pulsing neutron stars
 - Position known, search over frequency & derivatives

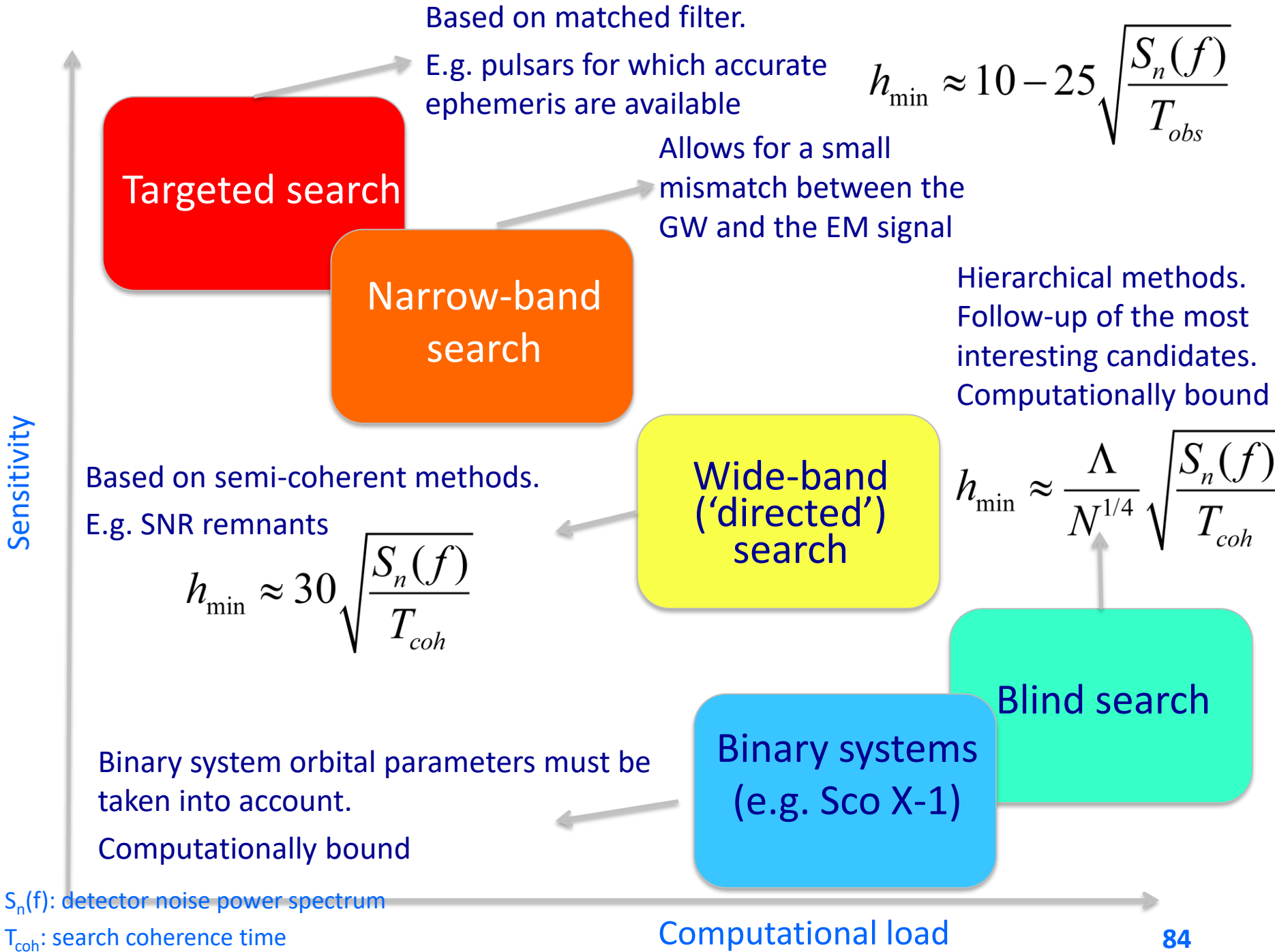
Neutron star searches

- As a consequence, searches are roughly divided in a few categories:
 - Targeted searches for signals from known pulsars
 - Blind searches of previously unknown objects
 - Directed searches (i.e. searches for targets with unknown rotation rate but with some knowledge of source, generally sky position,) :
 - supernova remnants (e.g. Cas A),
 - galactic center,
 - LMXBs (e.g. Sco X-1)

- The cornerstones of CW searches are:
 - sensitivity
 - robustness with respect to signal uncertainties and instrumental noise
 - computational load

- Methods:
 - Coherent methods (require accurate prediction of the phase evolution of the signal)
 - Semi-coherent methods (require prediction of the frequency evolution of the signal)

What drives the choice The computational expense of the search



If you know what you're looking for, it's easier to find it

- Coherent integration gains signal-to-noise as $T^{1/2}$
- Easy if you know sky position, frequency, derivatives, ...
- If you don't know these, integrate for each possible parameter value
- Cost may scale as up to T^7 , so T is computationally limited
- Incoherent combination of N coherent stretches gains as $N^{1/4}$
- Scaling and overall factor depend on parameter space searched - smaller is better!

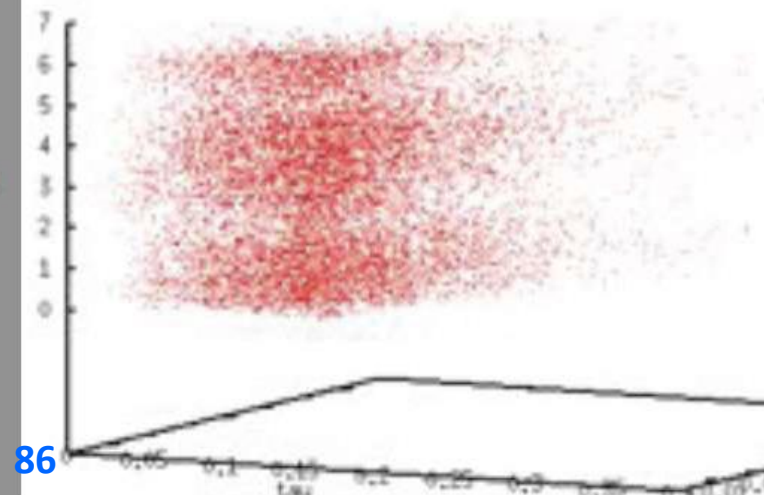
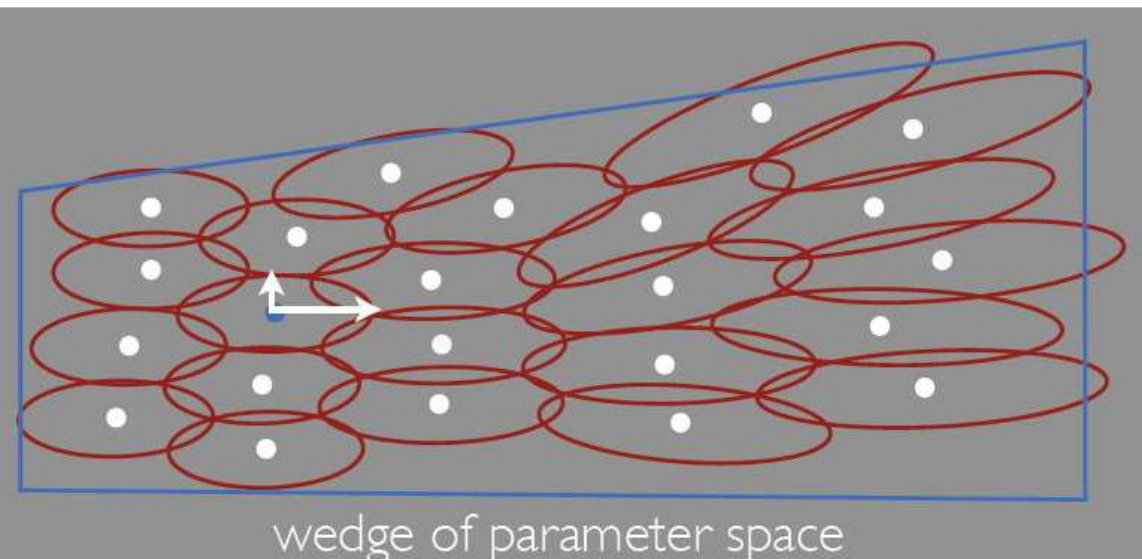
Gridding the parameter space

- Define a metric on parameter space to measure fractional-loss of statistic S from parameter-mismatch $\Delta\lambda = \{\Delta f, \Delta\dot{f}, \Delta\alpha, \Delta\delta\}$ (Owen, Phys. Rev. D 53, 6749, 1996):

$$ds^2 = -\Delta S/S = g_{ab} \Delta\lambda^a \Delta\lambda^b$$

- Use the metric to construct an
 - optimal grid, or without much loss in efficiency, a
 - random grid (Messenger, Prix, Papa, Phys. Rev. D79, 104017, 2009), or a
 - stochastic grid (Harry, Allen, Sathyaprakash, Phys. Rev. D80, 104014, 2009)

with a specified maximum loss of the detection statistic S



Sensitivity for semi-coherent CW searches scales as :

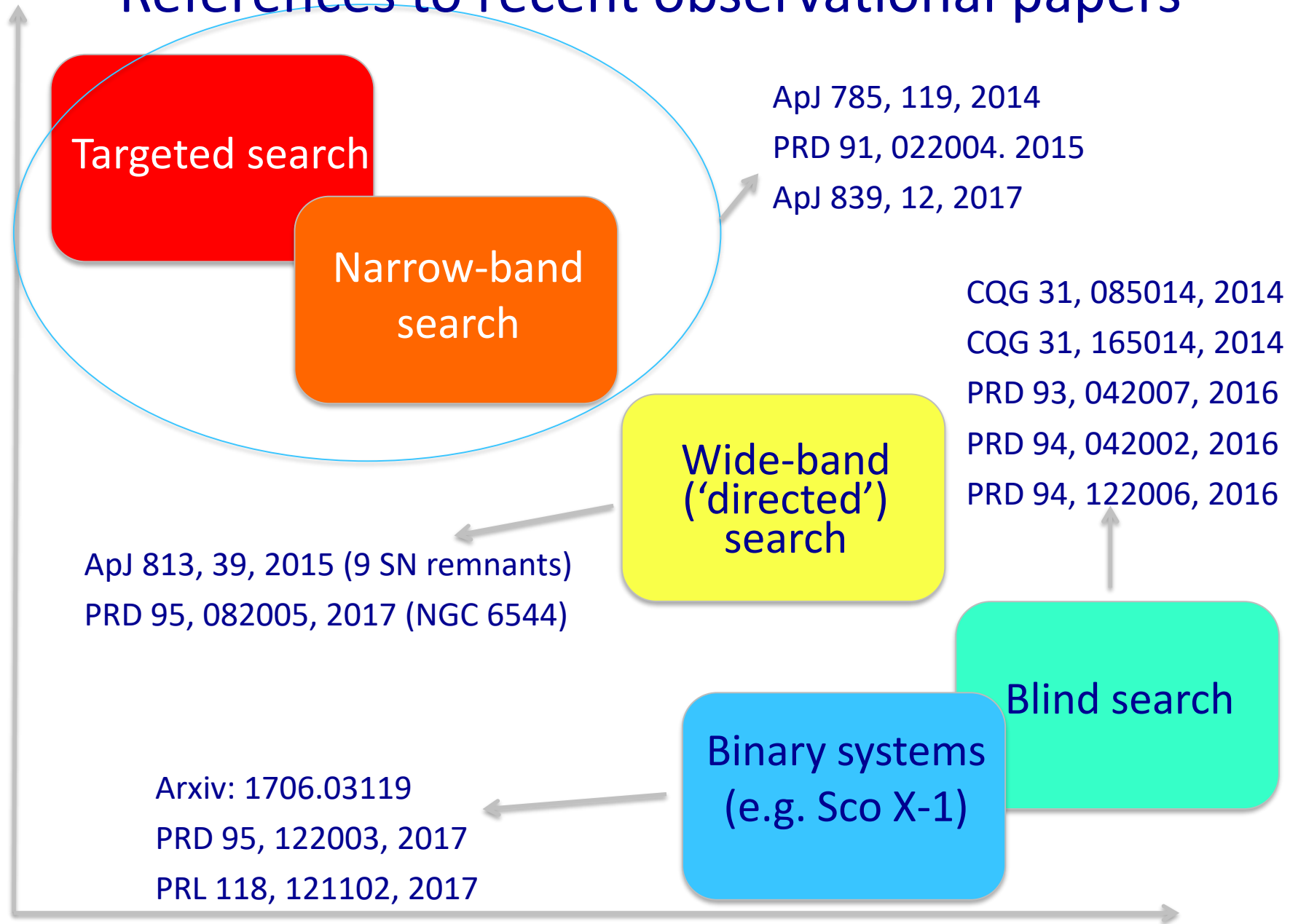
$$h \approx \frac{C}{N^{1/4}} \sqrt{\frac{S_n(f)}{T_{\text{coh}}}}$$

- where T_{coh} is the coherent time, N is the number of coherent data stretches, $S_n(f)$ is the power spectral density and C is a search dependent pre-factor.
- C is proportional to the number of templates used – longer coherent times and larger parameter spaces require more templates to ensure phase coherence. Also, computational cost (for all-sky searches) scales as T_{coh}^3 - T_{coh}^6
- Best way to improve search sensitivity is to improve $S_n(f)$

For all-sky and directed searches any candidate detections can be followed up using fully coherent methods to regain $T^{1/2}$ sensitivity increase

- provide better parameter estimation to constrain ellipticity
- for year long (or potentially less) integrations provides source sky position to arcsec precision, which greatly aids EM follow-up

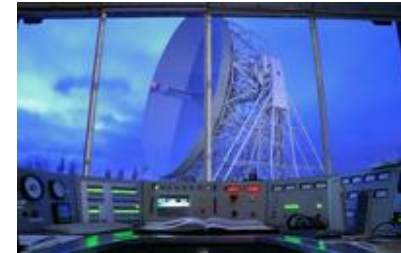
References to recent observational papers



EM observations

Sensitivity can be improved by narrowing the parameter space (fewer templates), so input from EM observations are vital:

- targeted searches rely on EM information to provide phase evolution templates, so need to make sure we have access to latest radio, X-ray, γ -ray (new surveys, LOFAR, SKA, Fermi, ASTROSAT)
- encourage deeper searches (Einstein@home) in existing data to find more sources.
- LMXB searches require huge template banks due to many source uncertainties, so narrowing these uncertainties (e.g. finding the rotation period of Sco X–1) would greatly increase sensitivity
- Directed searches could also be improved with more information, e.g. finding rotation periods of isolated X-ray sources, or neutron stars in supernova remnants



Jodrell Bank



Green Bank



Parkes Telescope

Advocate for pulsar surveys and X-ray timing with future radio and high energy observatories

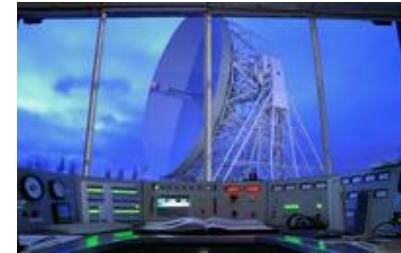
EM follow-up

For all-sky searches EM follow-up of detections enables greater physics return

- observations of pulsations gives rotational frequency and immediately narrows down the emission mechanism

But, pulsations may not be observed. We could require deeper imaging to look for faint X-ray source, or supernova remnant/pulsar wind nebula. How much telescope time would be required/could be obtained for these?

Follow-up of LMXBs may be most useful if it is coincident with further GW observations - can observe how GW and EM signals change over the same periods. This would require long term monitoring.



Jodrell Bank



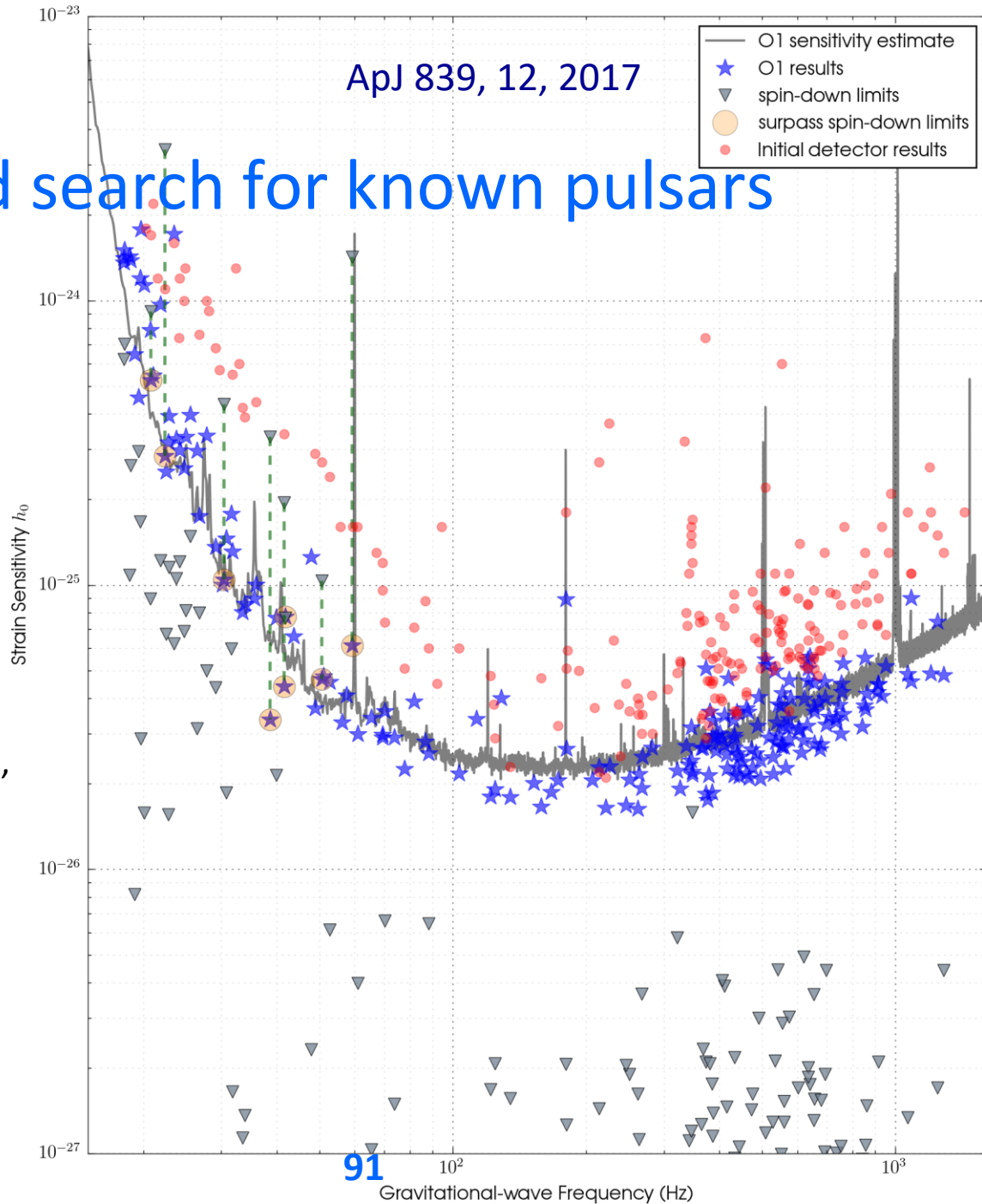
Green Bank

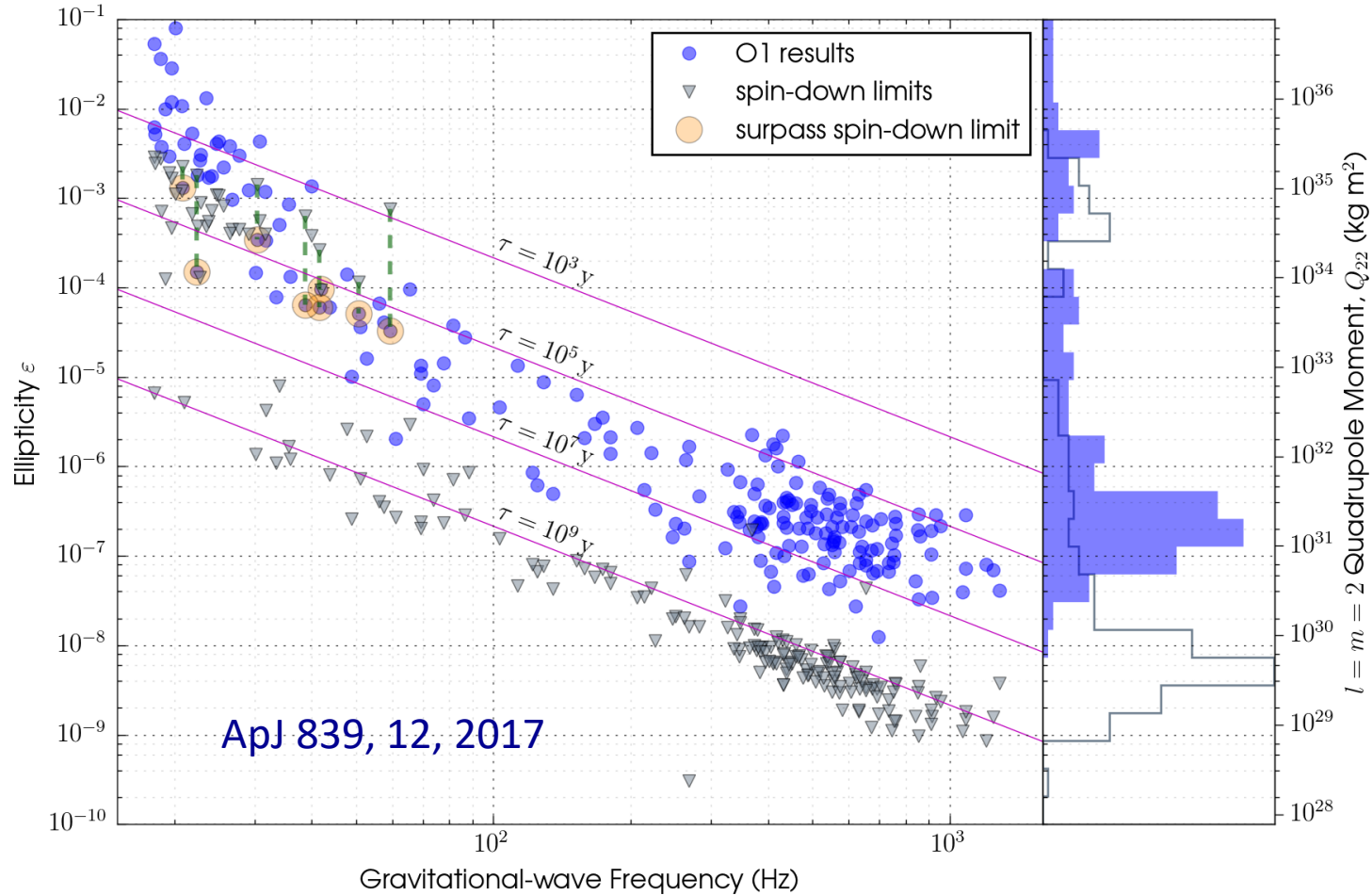


Parkes Telescope

O1 targeted search for known pulsars

- ✧ About 430 known pulsars in Advanced LIGO band (~20-2000 Hz)
- ✧ 200 known pulsars analyzed,
- ✧ 11 high-value targets using 3 pipelines: TD Bayesian, TD \mathcal{F}/\mathcal{G} -Stat and FD 5-vector method, rest with the TD Bayesian method.
- ✧ **ULs improved by a factor 2.5** w.r.t the Initial LIGO/Virgo results,
- ✧ spindown limit beaten for 8 pulsars, including Crab & Vela:
 - ✧ **Crab: less than $2 \times 10^{-3} \dot{E}_{rot}$ in GW, ~ 10 cm deformation**
 - ✧ **Vela: less than $10^{-2} \dot{E}_{rot}$ ellipticity $\rightarrow \sim 50$ cm**
- ✧ PSR J1918-0642: smallest UL
 $h_0 = 1.6 \times 10^{-26}$.





The ellipticity can roughly be converted to a "mountain" size using $25 \times (\epsilon/10^{-4}) \text{ cm}$
 The diagonal lines show the ellipticities that would be required if a star had a particular characteristic age and was losing energy purely through gravitational radiation.

Coherent detection methods

There are essentially two types of coherent searches that are performed

Frequency domain

Conceived as a module in a hierarchical search

- **Matched filtering techniques. Aimed at computing a detection statistic.**

These methods have been implemented in the frequency domain (although this is not necessary) and are very computationally efficient.

- **Best suited for large parameter space searches**
(when signal characteristics are uncertain)
- **Frequentist approach** used to cast upper limits.

Time domain

process signal to remove frequency variations due to Earth's motion around Sun and spindown

- **Standard Bayesian analysis**, as fast numerically but provides natural parameter estimation
- **Best suited to target known objects, even if phase evolution is complicated**
- Efficiently handles missing data
- Upper limits interpretation: **Bayesian approach**

F-statistics

$$h(t; \mathcal{A}, \boldsymbol{\lambda}) = \sum_{\mu=1}^4 \mathcal{A}^{\mu} h_{\mu}(t; \boldsymbol{\lambda})$$

$$h(t; \mathcal{A}, \boldsymbol{\lambda}) = F_{+}(t; \mathbf{n}, \psi) A_{+} \cos [\phi_0 + \phi(t; \boldsymbol{\lambda})] \\ + F_{\times}(t; \mathbf{n}, \psi) A_{\times} \sin [\phi_0 + \phi(t; \boldsymbol{\lambda})]$$

$$F_{+}(t; \mathbf{n}, \psi) = a(t; \mathbf{n}) \cos 2\psi + b(t; \mathbf{n}) \sin 2\psi$$

$$F_{\times}(t; \mathbf{n}, \psi) = b(t; \mathbf{n}) \cos 2\psi - a(t; \mathbf{n}) \sin 2\psi$$

$$h_1(t; \boldsymbol{\lambda}) = a(t; \mathbf{n}) \cos \phi(t; \boldsymbol{\lambda}), \quad h_2(t; \boldsymbol{\lambda}) = b(t; \mathbf{n}) \cos \phi(t; \boldsymbol{\lambda}),$$

$$h_3(t; \boldsymbol{\lambda}) = a(t; \mathbf{n}) \sin \phi(t; \boldsymbol{\lambda}), \quad h_4(t; \boldsymbol{\lambda}) = b(t; \mathbf{n}) \sin \phi(t; \boldsymbol{\lambda}),$$

$$\mathcal{A}^1 = A_{+} \cos \phi_0 \cos 2\psi - A_{\times} \sin \phi_0 \sin 2\psi,$$

$$\mathcal{A}^2 = A_{+} \cos \phi_0 \sin 2\psi + A_{\times} \sin \phi_0 \cos 2\psi,$$

$$\mathcal{A}^3 = -A_{+} \sin \phi_0 \cos 2\psi - A_{\times} \cos \phi_0 \sin 2\psi,$$

$$\mathcal{A}^4 = -A_{+} \sin \phi_0 \sin 2\psi + A_{\times} \cos \phi_0 \cos 2\psi.$$

We can express $h(t)$ in terms of amplitude A $\{A_{+}, A_{\times}, \psi, \phi_0\}$ and Doppler parameters $\boldsymbol{\lambda}$

F-Statistics

- Analytically maximize the likelihood over A

$$\ln \Lambda(x; h) = (x||h) - \frac{1}{2}(h||h)$$

$$\ln \Lambda(x; \mathcal{A}, \boldsymbol{\lambda}) = \mathcal{A}^\mu x_\mu - \frac{1}{2} \mathcal{A}^\mu \mathcal{A}^\nu \mathcal{M}_{\mu\nu}$$

$$x_\mu(\boldsymbol{\lambda}) \equiv (x||h_\mu), \quad \text{and} \quad \mathcal{M}_{\mu\nu}(\boldsymbol{\lambda}) \equiv (h_\mu||h_\nu).$$

We can now maximize $\ln \Lambda$ over \mathcal{A}^μ to obtain the maximum-likelihood estimators $\mathcal{A}_{\text{ML}}^\mu$ from the data $x(t)$, namely

$$\frac{\partial \ln \Lambda}{\partial \mathcal{A}^\mu} = 0 \quad \Longrightarrow \quad \mathcal{A}_{\text{ML}}^\mu = \mathcal{M}^{\mu\nu} x_\nu,$$

$$\text{where } \mathcal{M}^{\mu\alpha} \mathcal{M}_{\alpha\nu} = \delta_\nu^\mu$$

$$2\mathcal{F}(x; \boldsymbol{\lambda}) = x_\mu \mathcal{M}^{\mu\nu} x_\nu$$

Frequency domain method

- The outcome of a target search is a number F^* that represents the optimal detection statistic for this search.
- $2F^*$ is a random variable: For *Gaussian stationary noise*, follows a χ^2 distribution with 4 degrees of freedom with a non-centrality parameter $\lambda \propto (h|h)$. Fixing ι , ψ and ϕ_0 , for every h_0 , we can obtain a pdf curve: $p(2F|h_0)$
- The frequentist approach says the data will contain a signal with amplitude $\geq h_0$, with confidence C , if in repeated experiments, some fraction of trials C would yield a value of the detection statistics $\geq F^*$

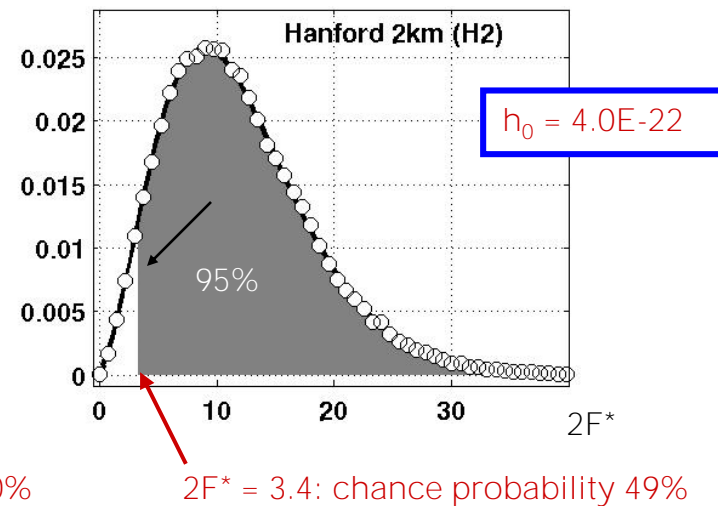
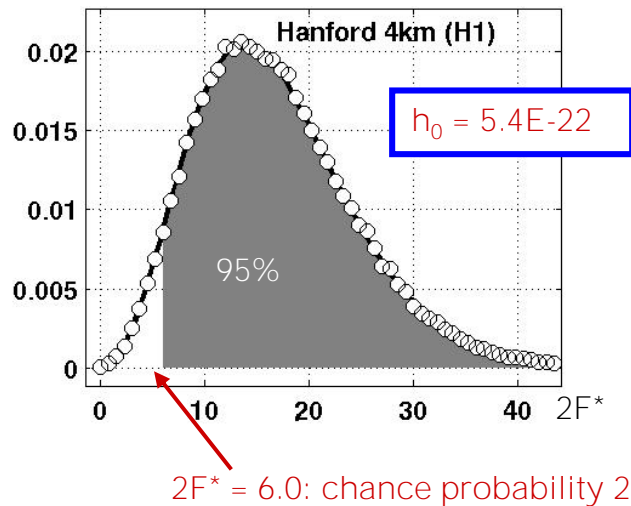
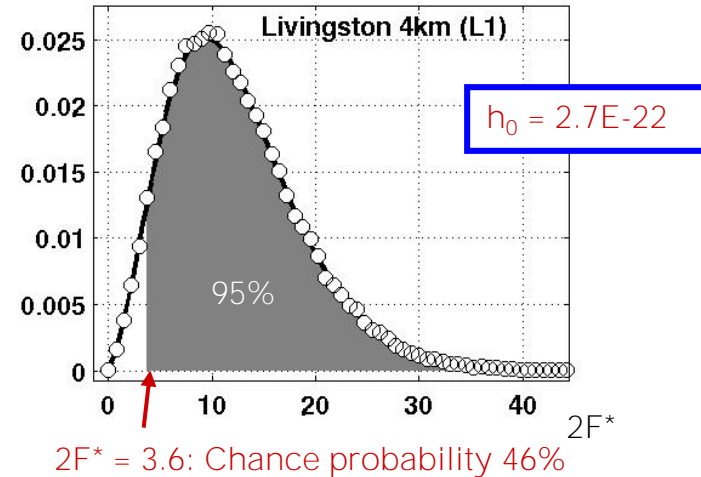
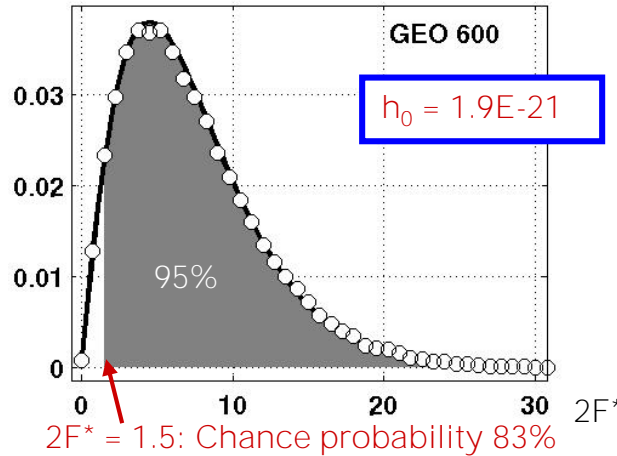
$$C(h_0) = \int_{2F^*}^{\infty} p(2F | h_0) d(2F)$$

- Use signal injection Monte Carlos to measure Probability Distribution Function (PDF) of F

Measured PDFs for the F statistic with fake injected *worst-case* signals at nearby frequencies

S1 Example

Note:
hundreds of
thousands of
injections
were needed
to get such
nice clean
statistics!



Time Domain Search for GWs from Known Pulsars

Sky position and spin frequency known accurately

Method: heterodyne time-domain data using the known spin phase of the pulsar

- Requires precise timing data from radio or X-ray observations
- Include binary systems in search when orbits known accurately
- Exclude pulsars with significant timing uncertainties
- Special treatment for the Crab and other pulsars with glitches, timing noise

Heterodyne, i.e. multiply by: $e^{-i\phi(t)}$ ← Known phase evolution of the signal: account for both spin-down rate and Doppler shift.

so that the expected demodulated signal is then:

$$y(t_k; \mathbf{a}) = \frac{1}{4} F_+(t_k; \psi) h_0 (1 + \cos^2 \iota) e^{i\phi_0} - \frac{i}{2} F_\times(t_k; \psi) h_0 (\cos \iota) e^{i\phi_0}$$

Here, $\mathbf{a} = \mathbf{a}(h_0, \psi, \iota, \phi_0)$, a vector of the signal parameters.

The only remaining time dependence is that of the antenna pattern

Search for Gravitational Waves from Known Pulsars

- Heterodyne IFO data at the instantaneous GW frequency ($2 \times$ radio rotation frequency)
 - Coarse stage (fixed frequency) 16384 \Rightarrow 4 samples/sec
 - Fine stage (Doppler & spin-down correction) \Rightarrow 1 samples/min $\Rightarrow B_k$
- Low-pass filter the data at each step. E.g., at 0.5Hz
- Down-sample from 16384Hz to 1/60Hz, or 1/minute $\Rightarrow B_k$
 - The data is down-sampled via averaging, yielding one value B_k of the complex time series, every 60s

$$y_k = \frac{1}{4} F_+(t_k; \psi) h_0 (1 + \cos^2 \iota) e^{i2\phi_0} - \frac{i}{2} F_\times(t_k; \psi) h_0 \cos \iota e^{i2\phi_0}$$

- Noise level is estimated from the variance of the data over each minute to account for non-stationarity $\Rightarrow \sigma_k$
- Additional parameters $a = a(h_0, \phi_0, \psi, \iota)$, are inferred from their Bayesian posterior probability distribution, assuming Gaussian noise


Time domain target search

- Standard Bayesian parameter fitting problem, using time-domain model for signal -- a function of the unknown source parameters h_0 , ι , ψ and ϕ_0

$$y(t; \mathbf{a}) = \frac{1}{4} h_0 F_+(t, \mathbf{y}) (1 + \cos^2 \iota) e^{2if_0} - \frac{1}{2} \iota h_0 F_-(t, \mathbf{y}) \cos \psi e^{2if_0}$$

- Additional parameters $\mathbf{a} = \mathbf{a}(h_0, \phi_0, \psi, \iota)$, are inferred from their Bayesian posterior probability distribution, assuming Gaussian noise
 - The data are broken up into M time segments over which the noise can be assumed stationary. Marginalize over noise floor.

$$p(\{B_k\} | \mathbf{a}) \propto \prod_j \left(\sum_{k=1+\sum_{i=1}^{j-1} m_i}^{\sum_{i=1}^j m_i} |B_k - y_k|^2 \right)^{-m_j}$$

 Number of data points in the j -th segment (5-30min to maximize analyzed data)

Time domain: Bayesian approach

- We take a **Bayesian approach**, and determine the **joint posterior distribution of the probability of our unknown parameters**, using uniform priors on $h_0, \cos \iota, \psi$ and ϕ_0 over their accessible values, i.e.

$$p(\mathbf{a} | \{B_k\}) \propto p(\mathbf{a}) \times p(\{B_k\} | \mathbf{a})$$

↑
↑
↑
posterior
prior
likelihood

- The **likelihood** $\propto \exp(-\chi^2/2)$, where

$$c^2(\mathbf{a}) = \prod_k \left| \frac{B_k - y(t; \mathbf{a})}{S_k} \right|^2$$
- To get the posterior PDF for h_0 , marginalizing with respect to the nuisance parameters $\cos \iota, \psi$ and ϕ_0 given the data \mathbf{B}_k

$$p(h_0 | \{B_k\}) \propto \int e^{-c^2/2} df_0 dy d\cos \iota$$

The Bayesian Approach

Bayesian statistics: quantifying the degree of certainty (or “degree of belief”) of a statement being true

posterior $p(\vec{a} | \{B_k\})$ \propto $p(\vec{a})$ $p(\{B_k\} | \vec{a})$ **likelihood**
prior

Assume uniform priors on all parameters

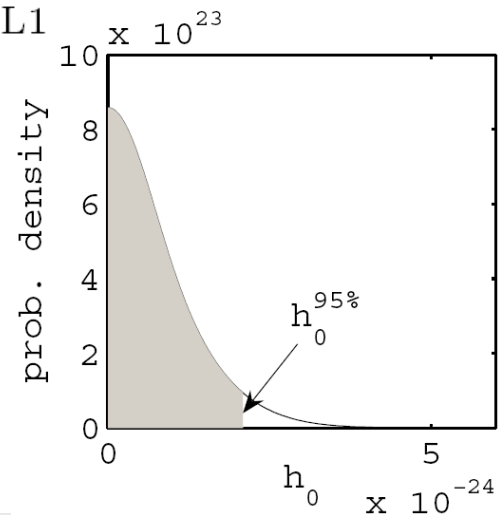
Combine posterior pdfs from different detectors

$$p(B_k | \mathbf{a})_{\text{Joint}} = p(B_k | \mathbf{a})_{\text{H1}} \cdot p(B_k | \mathbf{a})_{\text{H2}} \cdot p(B_k | \mathbf{a})_{\text{L1}}$$

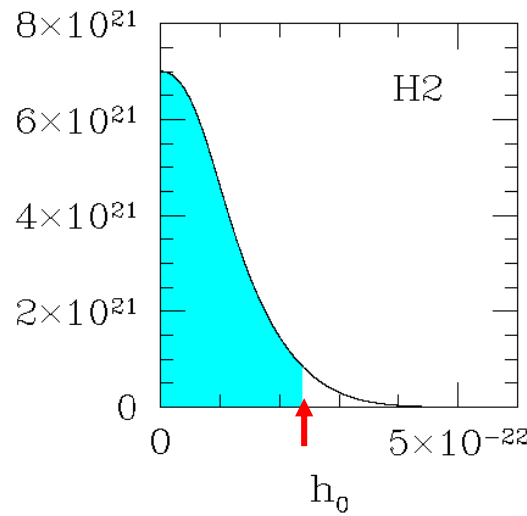
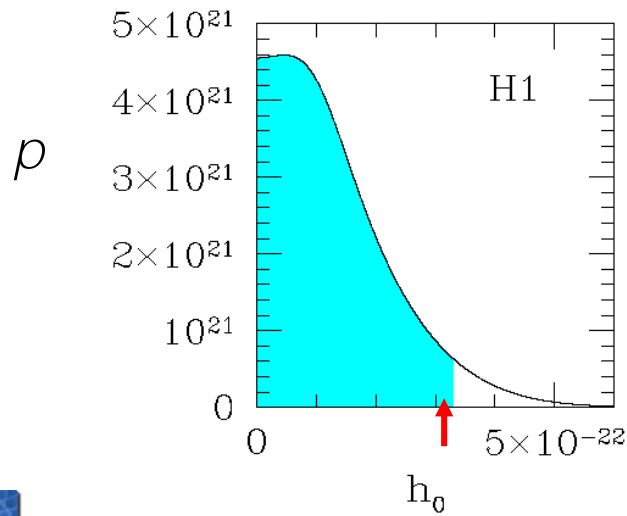
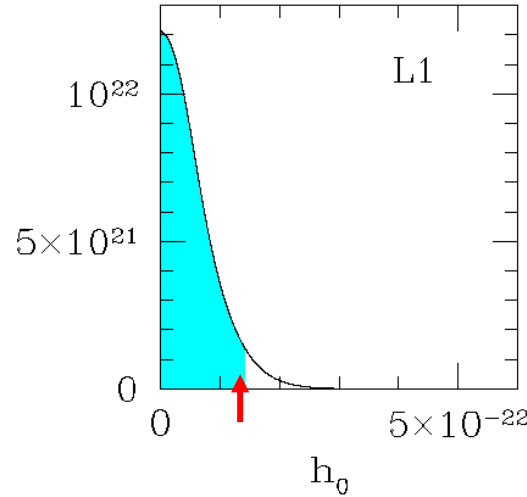
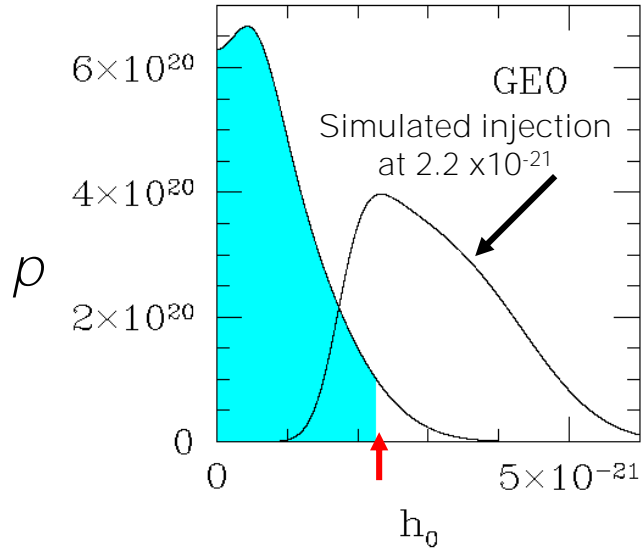
Marginalize the posterior over *nuisance* parameters (ϕ_0, ψ, ι)
 (i.e. integrate over possible values)

Set 95% upper limits on GW amplitude emitted by each pulsar solving:

$$0.95 = \int_0^{h_0^{95\%}} p(h_0 | \{B_k\}) dh_0$$



Posterior PDFs for CW time domain analyses



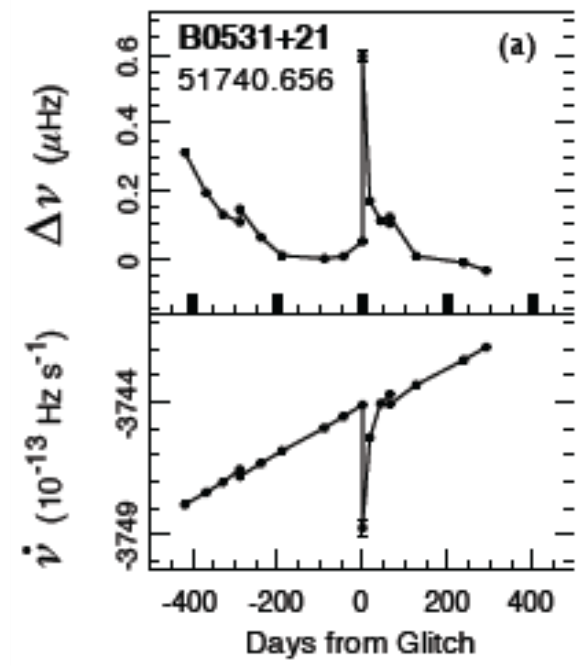
S1 Example
shaded area = 95% of total area

Pulsar glitches

Rotating neutron stars are, in general, very stable rotators but can be affected by two kinds of irregularity, especially in the case of young objects: glitches and timing noise.

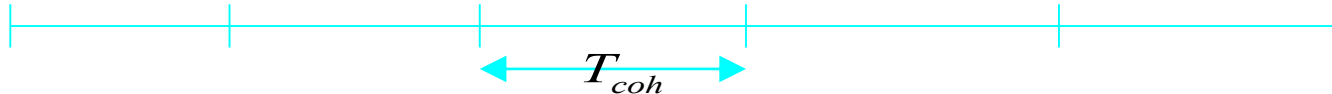
A glitch may produce a ‘jump’ in the phase of the GW signal: coherent analysis across the glitch time may not be possible.

Maybe due to a star-quake or to the interaction between the star crust and inner superfluid.



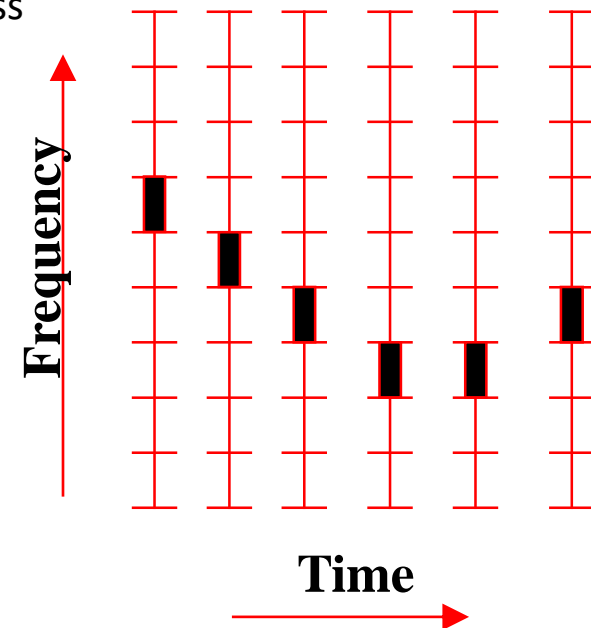
EM alerts on glitch occurrence for the most interesting targets are extremely important for CW analysis.

Semi-coherent power-sum methods



- The idea is to perform a search over the total observation time using an *incoherent* (sub-optimal) method.
- Three methods have been developed to search for cumulative excess power from a hypothetical periodic gravitational wave signal by examining successive spectral estimates:
 - Stack-slide (Radon transform)
 - Hough transform
 - Power-flux method

They are all based on breaking up the data into segments, FFT each, producing Short (30 min) Fourier Transforms (SFTs) from $h(t)$, as a coherent step (although other coherent integrations can be used if one increasing the length of the segments), and then track the frequency drifts due to Doppler modulations and df/dt as the incoherent step.



Differences among the semi-coherent methods

What is exactly summed

- **StackSlide** – Normalized power (power divided by estimated noise)
→ Averaging gives expectation of 1.0 in absence of signal
- **Hough** – Weighted binary counts (0/1 = normalized power below/above SNR), with weighting based on antenna pattern and detector noise
- **PowerFlux** – Average strain power with weighting based on antenna pattern and detector noise
→ Signal estimator is direct excess strain noise
(circular polarization and 4 linear polarization projections)

The Hough Transform

- Robust pattern detection technique.
- We use the Hough Transform to find the pattern produced by the Doppler modulation (due to the relative motion of the detector with respect to the source) and spin-down of a GW signal in the **time – frequency** plane of our data:

$$f(t) - \hat{f}(t) = \hat{f}(t) \frac{\vec{v}(t) \times \vec{n}}{c}$$

↑
↙ ↘

Detector
SSB

RF

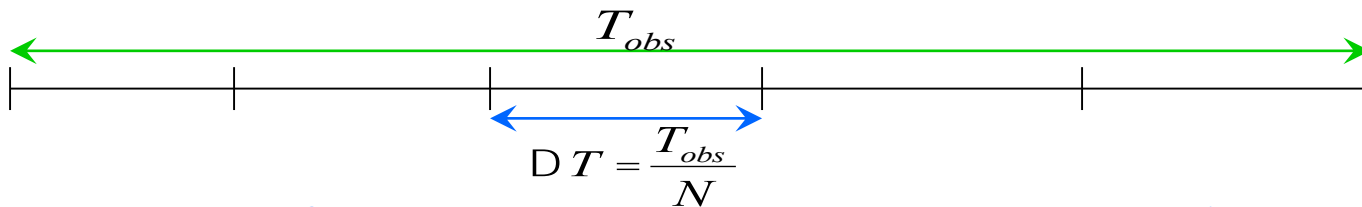
$$\hat{f}(t) = \hat{f}_0 + \dot{f}(t - t_0) + \dots$$

- For isolated NS the expected pattern depends on the parameters: $\{\alpha, \delta, f, \dot{f}, \dots\}$

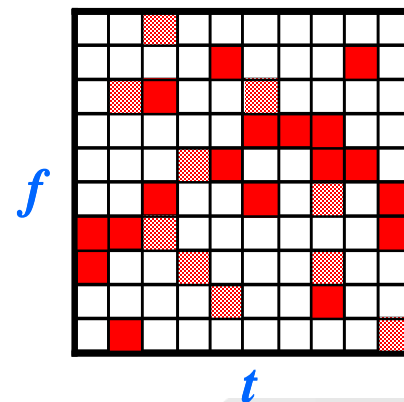
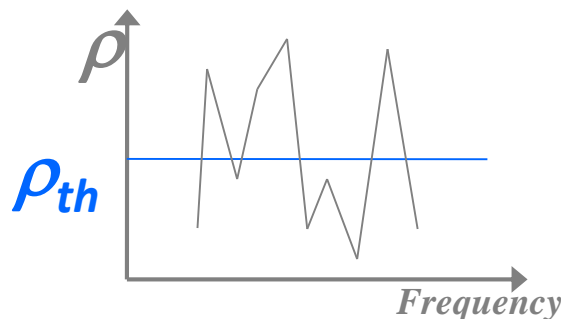
The Hough Transform

Procedure:

- 1 Break up data ($x(t)$ vs t) into segments

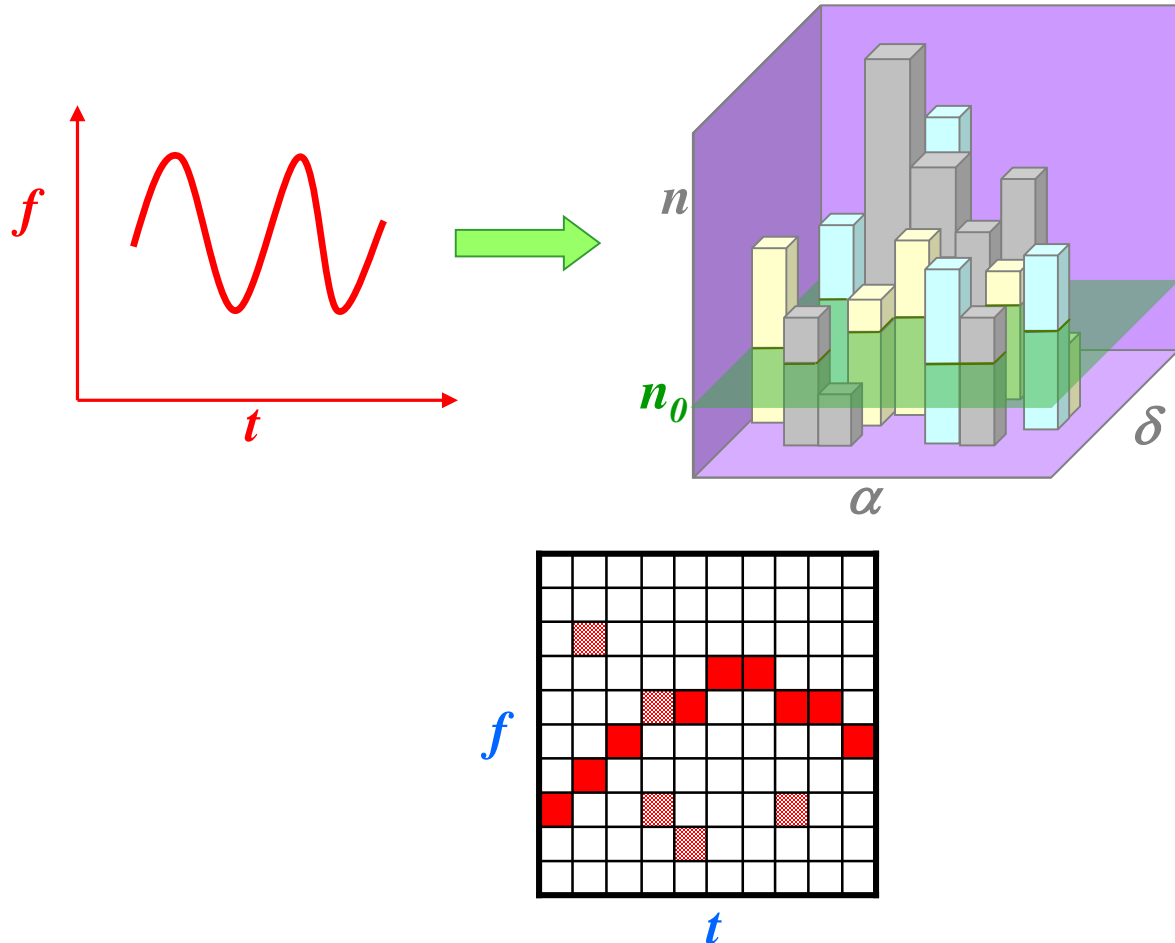


- 2 Take the FT of each segment and calculate the corresponding normalized power in each case (ρ_k)
- 3 Select just those that are over a certain threshold ρ_{th} .



The Hough Transform

Procedure:



Hough Transform Statistics

The probability for any pixel on the *time - frequency* plane of being selected is:

$$p = \begin{cases} \text{Signal absent} & q = e^{-\rho_{th}} \\ \text{Signal present} & \eta = e^{-\rho_{th}} \left\{ 1 + \frac{\rho_{th}}{2} I_k + O(I_k^2) \right\} \end{cases} \quad \text{SNR for a single SFT} \quad I_k = \frac{4 |\tilde{h}(f_k)|^2}{T_{coh} S_n(f_k)}$$

After performing the Hough Transform **N SFTs**, the probability that the pixel $\{a, d, f_0, f_1\}$ has a number count **n** is given by

Without Weights

Number Count

$$n = \sum_{i=1}^N n_i$$

$$p(n) = \binom{N}{n} p^n (1-p)^{N-n}$$

Signal absent

Signal present

Mean $\langle n \rangle = Nq$

$\langle n \rangle = Nh$

Variance $S^2 = Nq(1-q)$ $S^2 = Nh(1-h)$

With Weights

Number Count

$$n = \sum_{i=1}^N w_i n_i$$

$$\sum_{i=1}^N w_i = N$$

$$p(n) = \frac{1}{\sqrt{2\rho S^2}} e^{-\frac{(n-\langle n \rangle)^2}{2S^2}}$$

Signal absent

Signal present

Mean $\langle n \rangle = Nq$

$\langle n \rangle = qN + \frac{qr_{th}}{2} \sum_{i=1}^N w_i I_i$

Variance $S^2 = \sum_{i=1}^N w_i^2 q(1-q)$

$S^2 = \sum_{i=1}^N w_i^2 h_i(1-h_i)$

Frequentist upper limit

- Perform the Hough transform for a set of points in parameter space $\lambda = \{\alpha, \delta, f_o, f_i\} \in \mathbf{S}$, given the data:

$$\text{HT: } \mathbf{S} \rightarrow \mathbf{N}$$

$$\lambda \rightarrow n(\lambda)$$

- Determine the maximum number count n^*

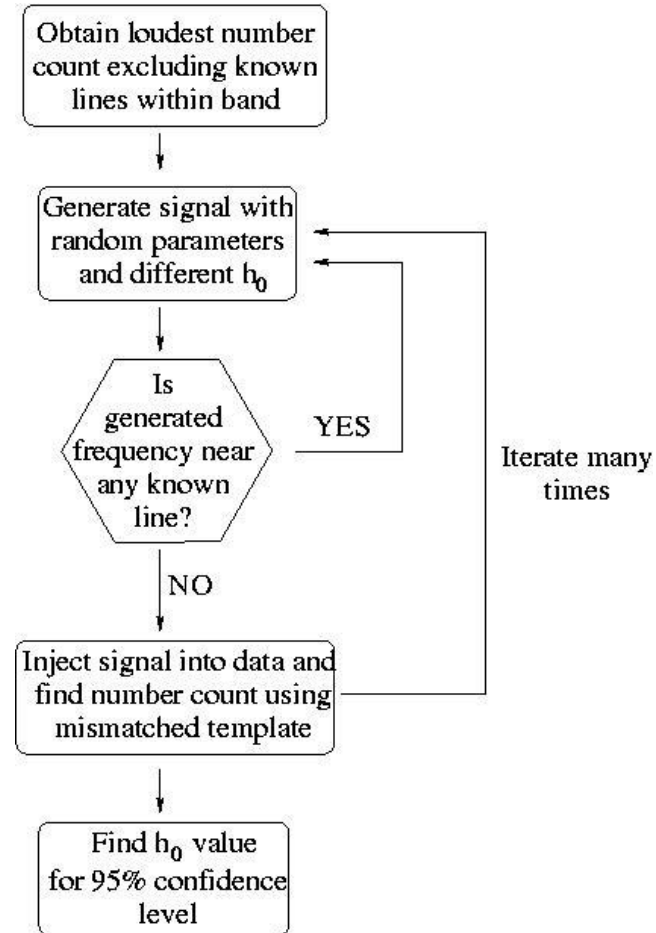
$$n^* = \max (n(\lambda)): \lambda \in \mathbf{S}$$

- Determine the probability distribution $p(n|h_o)$ for a range of h_o

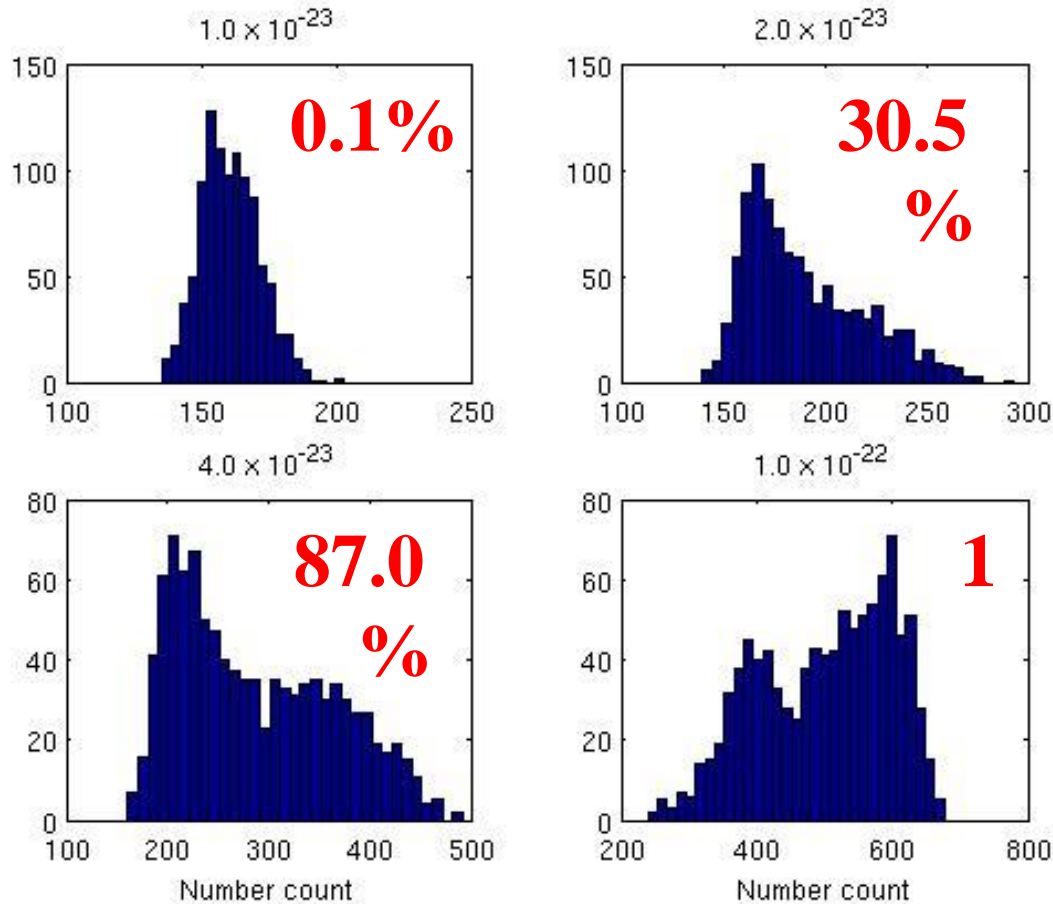
- The 95% frequentist upper limit $h_o^{95\%}$ is the value such that for repeated trials with a signal $h_o \geq h_o^{95\%}$, we would obtain $n \geq n^*$ more than 95% of the time

$$0.95 = \mathop{\text{a}}\limits_{n=n^*}^N p(n|h_o^{95\%})$$

Compute $p(n|h_o)$ via Monte Carlo signal injection, using $\lambda \in \mathbf{S}$, and $\phi_0 \in [0, 2\pi]$, $\psi \in [-\pi/4, \pi/4]$, $\cos \iota \in [-1, 1]$.



Number count distribution for signal injections



$p(n/h_0)$ ideally binomial for a target search (no weights), but:

- Amplitude modulation of the signal for different SFTs
- Different sensitivity for different sky locations
- Random mismatch between signal & templates

‘smear’ out the binomial distributions

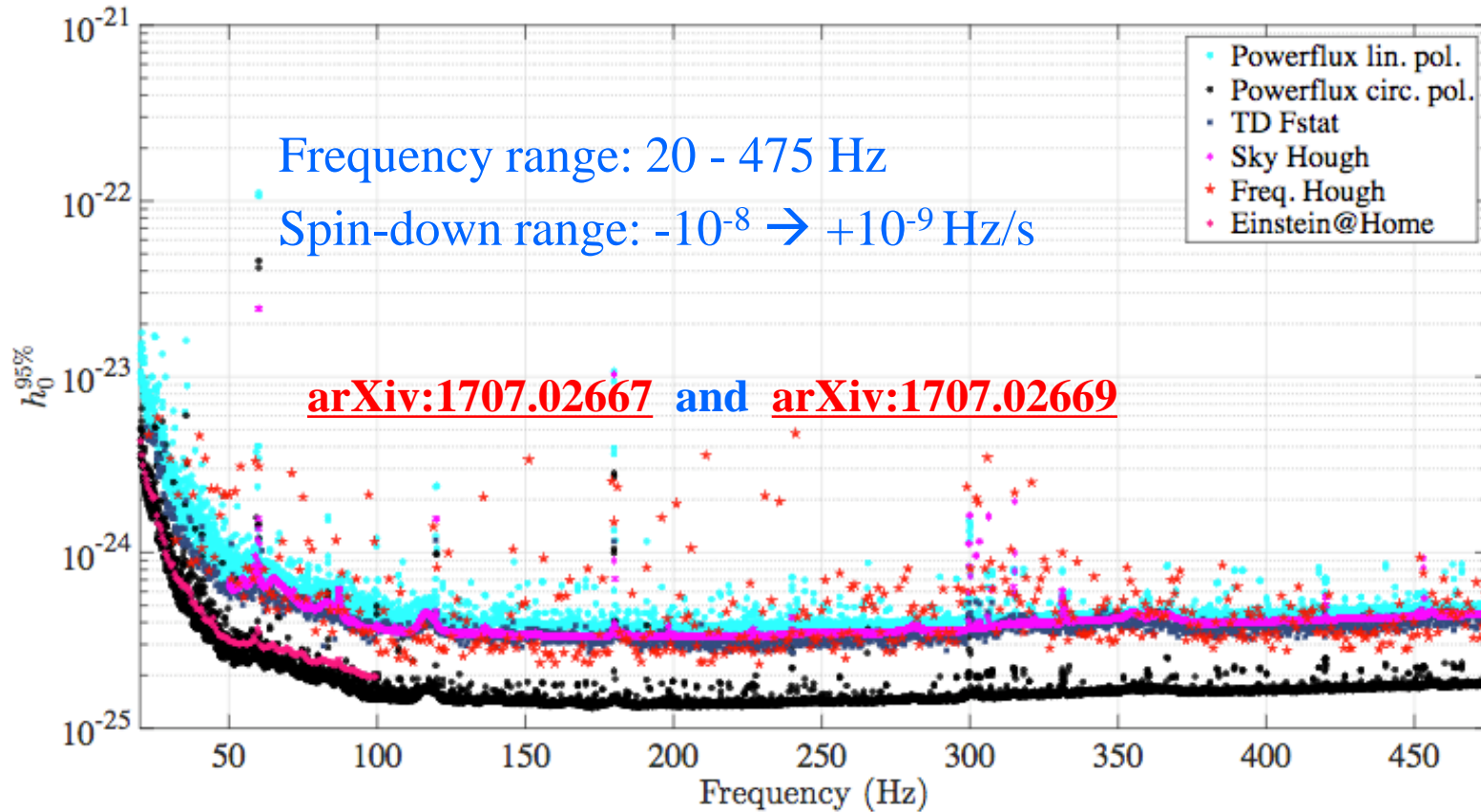
All-sky CW search in LIGO O1 [10, 475] Hz

A selection of methods:

- PowerFlux (PRD 94, 042002, 2016)
- FrequencyHough (PRD 90, 042002, 2014)
- SkyHough (CQG 31, 085014, 2014)
- Time domain **F**-statistic (CQG 31, 165014, 2014)
- Einstein@Home followup method of interesting outliers (PRD 94, 122006, 2016)

At 475 Hz we are sensitive to NSs with equatorial ellipticity $\varepsilon \simeq 8 \times 10^{-7}$ and as far away as 1 kpc,
Sensitivity several times better than LIGO S6

Highlights on O1 all-sky searches

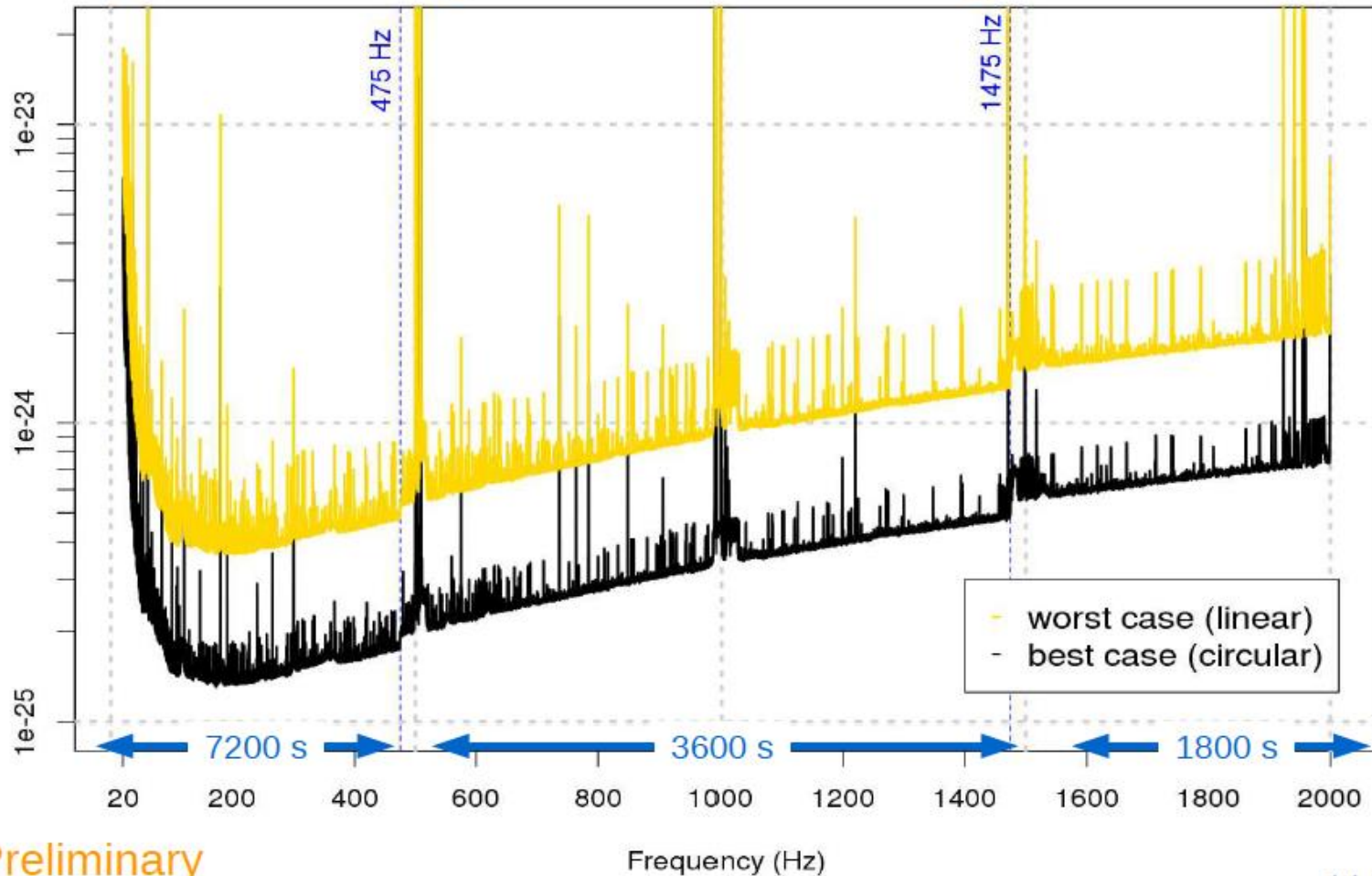


No candidate survived the follow-up

Significant improvement in the ULs with respect to past analyses ($> 3x$)

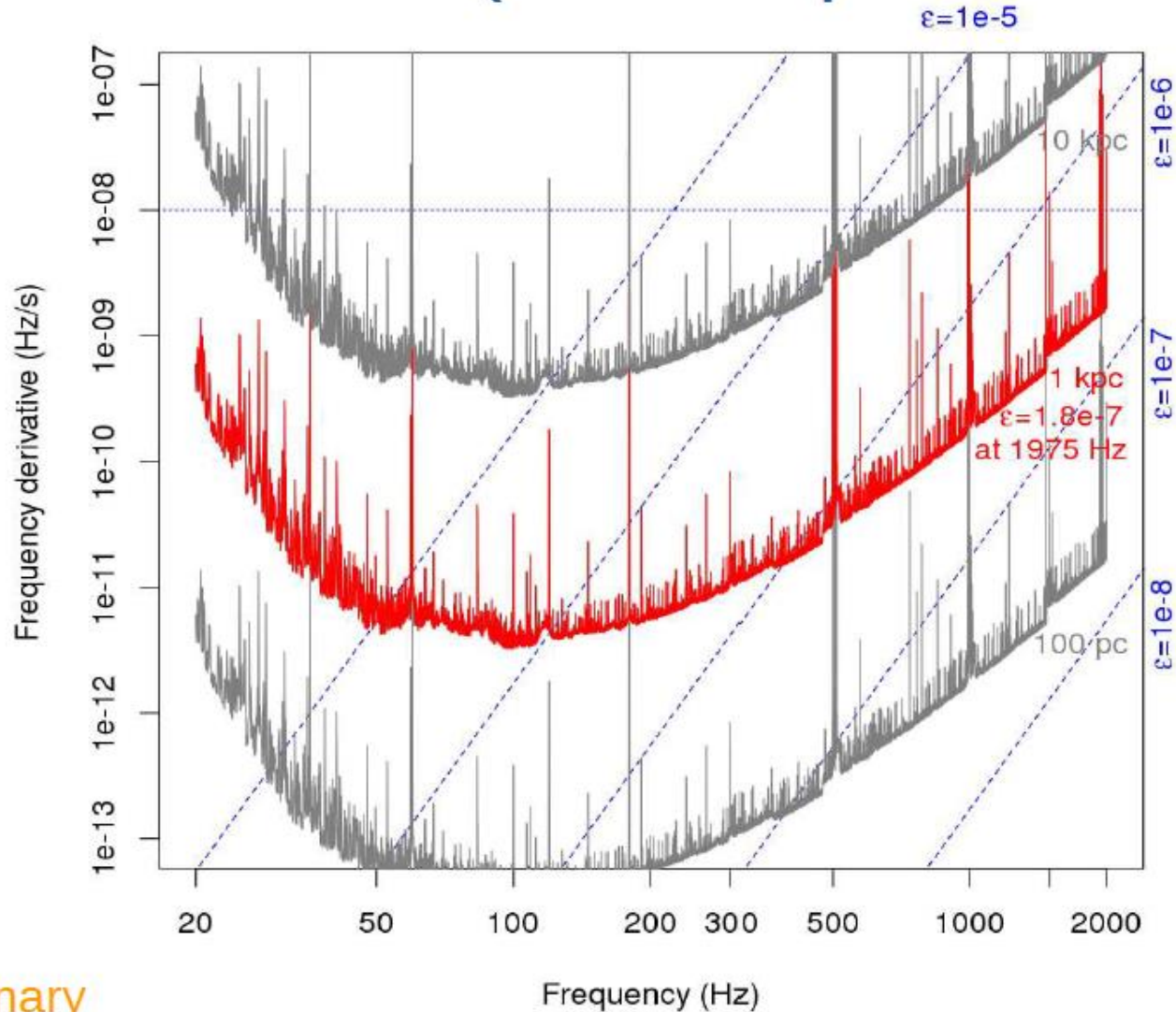
We can exclude the existence of neutron stars with $\epsilon > 10^{-5}$, spinning at a frequency larger than ~ 200 Hz, within 1 kpc from the Earth

Advanced LIGO O1 upper limits spindown range $-1e-8$ Hz/s through $1e-9$ Hz/s



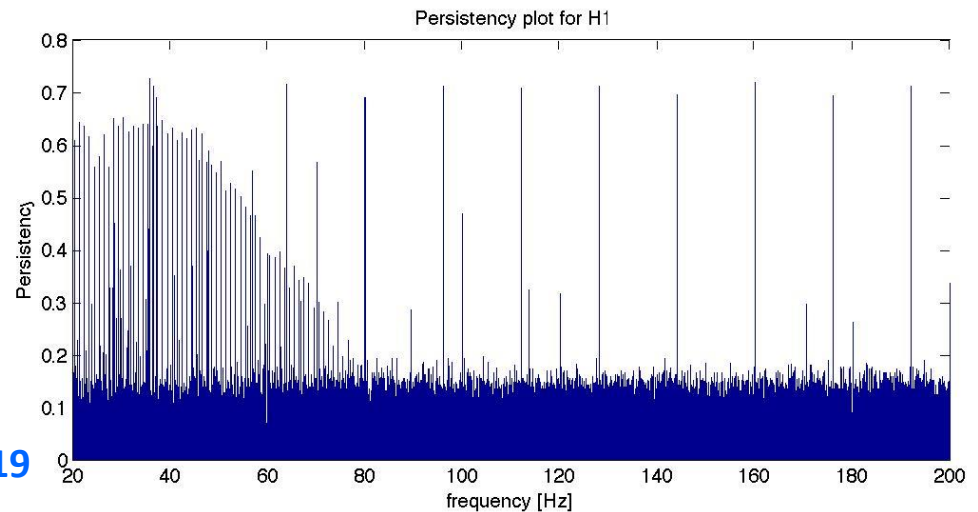
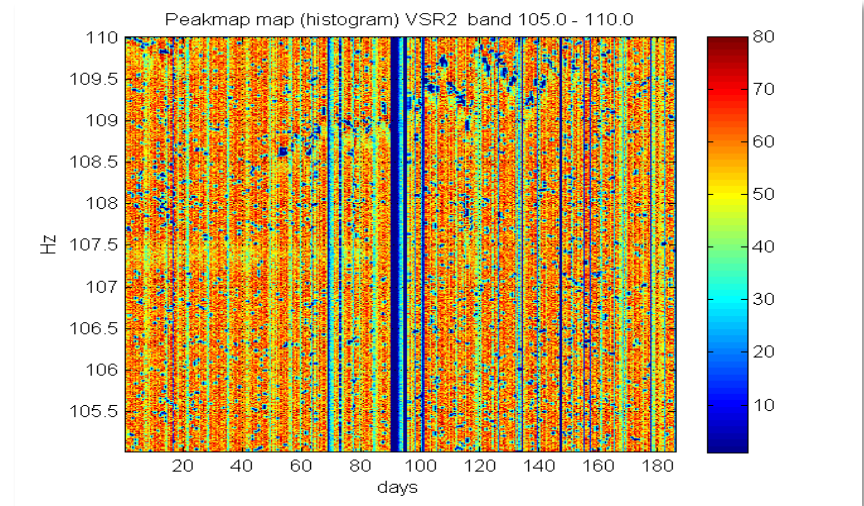
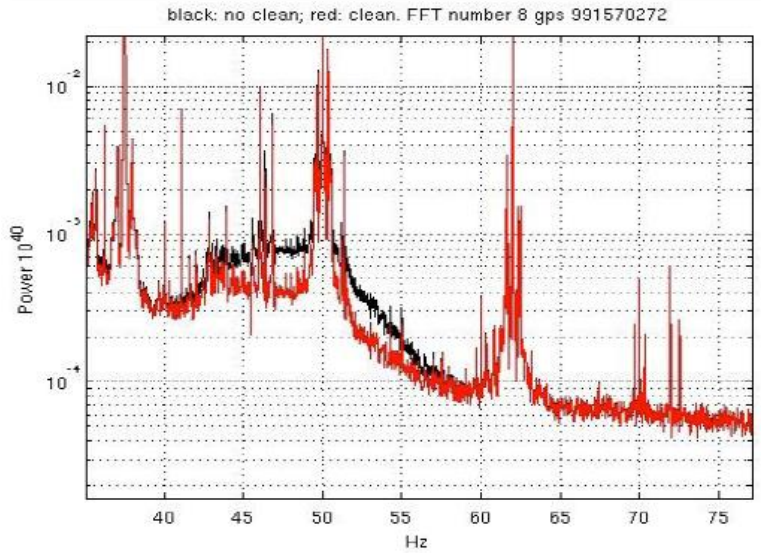
Preliminary

Search reach (circular polarization)



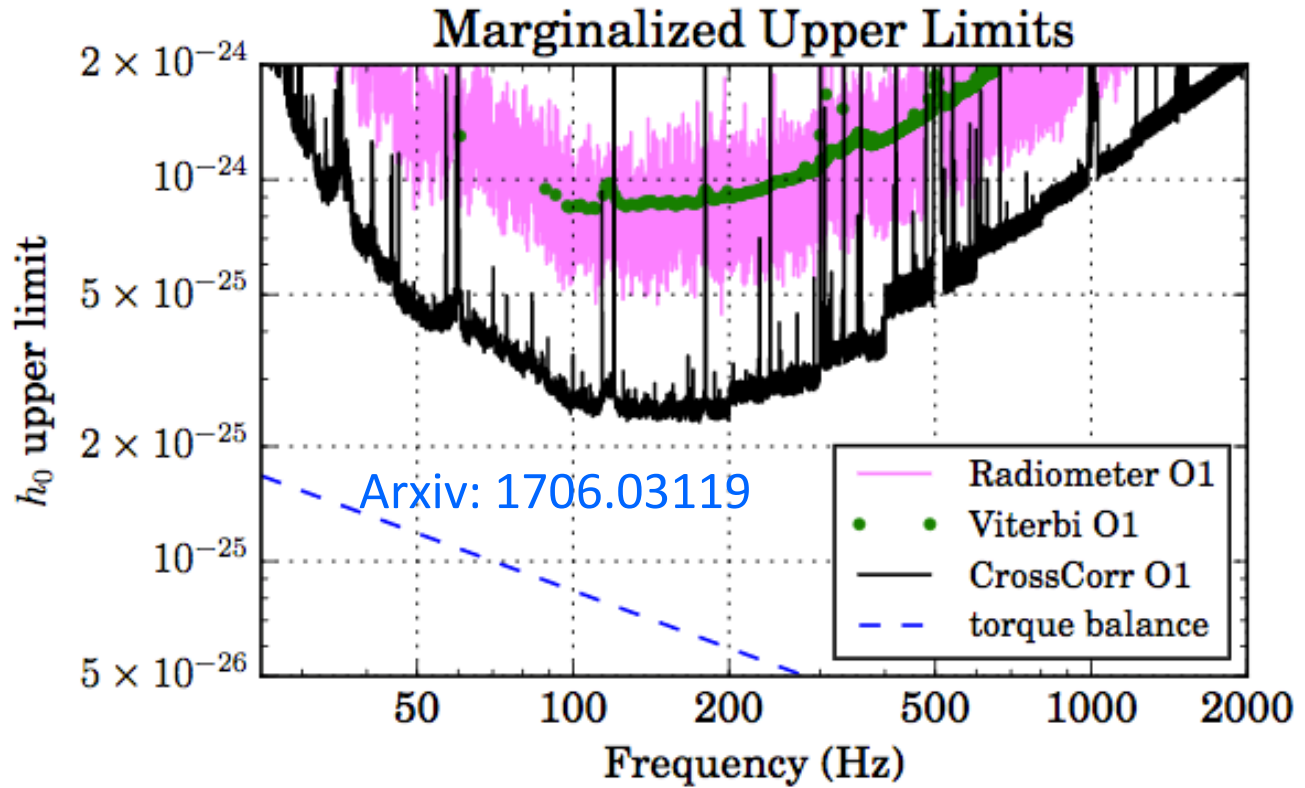
Preliminary

- Several types of disturbances affect real data. We try to identify and remove their source. Or, alternatively, they must be vetoed at the analysis level.



Highlights on O1 directed Scorpius X-1 searches

95% Upper limits
improvements of a
factor 7 over initial-
LIGO



No evidence for standard CW signal in the range 25 Hz-2kHz

About a factor of 2 above
the “torque-balance limit”

$$h_{tb} \approx 3 \cdot 10^{-27} \left(\frac{F_X}{10^{-8} \text{ erg} \cdot \text{cm}^2 \cdot \text{s}^{-1}} \right) \left(\frac{f_{rot}}{300 \text{ Hz}} \right)^{-1/2}$$

The torque balance line is an optimistic expected signal strength inferred from the X-ray flux from Sco X-1

Conclusions

- Still no CW detection so far, but several astrophysically interesting upper limits
- More results of CW searches on advanced detector data will be out in the next months.
- In the meanwhile we are developing more sensitive, more robust and faster analysis pipelines.
- A lot of physics and astrophysics can be done with CW.

Detection of CW could be the next surprise of GW astronomy!

Agradecimientos

El grupo de Relatividad y Gravitación es miembro del Instituto de Aplicaciones Computacionales de Código Comunitario (IAC3) de la UIB y del Instituto de Estudios Espaciales de Cataluña (IEEC).

Tiene el apoyo del Ministerio de Economía y Competitividad (FPA2016-76821-P, FPA2013-41042-P), la Conselleria d'Educació, Cultura i Universitats del Govern de les Illes Balears, el Fondo Social Europeo, el Fondo Europeo de Desarrollo Regional, la Red Española de Supercomputación y PRACE. Además participa en el proyecto Consolider Ingenio Multidark (CSD2009-00064) y forma parte la red consolider: Centro Nacional de Física de Partículas, Astropartículas y Nuclear (CPAN – FPA2015-69037-REDC) y de las redes de excelencia: red nacional de astropartículas (RENATA- FPA2015-68783-REDT) y red temática de ondas gravitacionales (REDONGRA – FPA2015-69815-REDT).



**Govern
de les Illes Balears**

Maximizing Λ wrt the amplitude

We can express the generic waveform $h = A h_o$, where A is the amplitude. Maximizing Λ with respect to A we get the expression:

$$\log \Lambda(s|\xi) = \frac{1}{2} \frac{(h_a|s)^2}{(h_a|h_a)}$$

Where ξ are the remaining parameters, for example the arrival time and the initial phase.

It can be seen that maximizing this last expression of Λ is equivalent to maximize the SNR according to matched filtering!

Credits: M. Maggiore- Gravitational Waves

Maximizing wrt the initial phase ϕ_0

We can express the GW signal in the form (beware that here \mathbf{s} is the signal and \mathbf{x} is the detector output and $\langle \dots \rangle$ is the scalar product):

$$\mathbf{s} = \mathbf{s}_0 \cos(\phi_0) + \mathbf{s}_1 \sin(\phi_0);$$

Then Λ has the form:

$$\frac{\langle \mathbf{s}, \mathbf{x} \rangle^2}{\langle \mathbf{s}, \mathbf{s} \rangle} = \frac{(\langle \mathbf{s}_0, \mathbf{x} \rangle + \langle \mathbf{s}_1, \mathbf{x} \rangle \tan \phi_0)^2}{\langle \mathbf{s}_0, \mathbf{s}_0 \rangle + \tan^2 \phi_0 \langle \mathbf{s}_1, \mathbf{s}_1 \rangle + 2 \tan \phi_0 \langle \mathbf{s}_0, \mathbf{s}_1 \rangle}$$

and the maximization with respect ϕ_0 gives:

$$\max_{A, \phi_0} 2 \ln \Lambda = \frac{\frac{\langle \mathbf{s}_0, \mathbf{x} \rangle^2}{\langle \mathbf{s}_0, \mathbf{s}_0 \rangle} + \frac{\langle \mathbf{s}_1, \mathbf{x} \rangle^2}{\langle \mathbf{s}_1, \mathbf{s}_1 \rangle} - 2 \frac{\langle \mathbf{s}_0, \mathbf{s}_1 \rangle \langle \mathbf{s}_0, \mathbf{x} \rangle \langle \mathbf{s}_1, \mathbf{x} \rangle}{\langle \mathbf{s}_0, \mathbf{s}_0 \rangle \langle \mathbf{s}_1, \mathbf{s}_1 \rangle}}{1 - \frac{\langle \mathbf{s}_0, \mathbf{s}_1 \rangle^2}{\langle \mathbf{s}_0, \mathbf{s}_0 \rangle \langle \mathbf{s}_1, \mathbf{s}_1 \rangle}}$$

If we use, instead of \mathbf{s}_0 and \mathbf{s}_1 , two other function \mathbf{s}_p and \mathbf{s}_q that are obtained through a rotation and are such that $\langle \mathbf{s}_p | \mathbf{s}_q \rangle = 0$, we simplify the above expression to:

$$\max_{A, \phi_0} 2 \ln \Lambda = \frac{\langle \mathbf{s}_p, \mathbf{x} \rangle^2}{\langle \mathbf{s}_p, \mathbf{s}_p \rangle} + \frac{\langle \mathbf{s}_q, \mathbf{x} \rangle^2}{\langle \mathbf{s}_q, \mathbf{s}_q \rangle}$$

Credits: A. Viceré

Windowing

- Multiplication of a signal $x(t)$ by a top-hat function is an example of *windowing*. Windowing restricts the duration of a signal to a finite range.
- The top-hat function is also called a *rectangular window* because of its obvious rectangular shape.
- *Tapered windows*, which go smoothly to zero at both the beginning and end of the window, are useful because they help suppress *leakage of power* into neighboring frequency bins.
- This leakage is basically due to the sinc-function shape of the Fourier transform of the rectangular window, which has non-negligible support at high frequencies because of the rapid turn-on and turn-off of the rectangular window in the time domain. If the frequency of a periodic signal does not lie at the one of the discrete frequencies f_k , convolution with the sinc function in the frequency domain will spread the power to neighboring frequency bins.
 - *Using a tapered window helps mitigate this problem since its smooth turn-on and turn-off give rise to a sinc-like function with much less support at high frequencies.*
 - Although there are many different tapered windows to chose from (e.g., Tukey windows, triangular windows, Welch windows, etc.), each with its own special advantages and disadvantages, a *Hann window* defined by

$$w_j := \frac{1}{2} \left[1 - \cos \left(\frac{2\pi j}{N} \right) \right], \quad j = 0, 1, \dots, N - 1 \quad (22)$$

works well for most applications.

- A matched filter (or *Weiner optimal filter*) is a frequentist detection statistic used to look for a signal with a deterministic waveform.
- We assume the detector output $x(t)$ has the form

$$x(t) = n(t) + s(t; \theta^\alpha) \quad (1)$$

where θ^α are parameters describing the deterministic signal.

- One constructs the filtered output

$$y = \int_{-\infty}^{\infty} dt x(t)K(t) = \int_{-\infty}^{\infty} df \tilde{x}(f)\tilde{K}^*(f) \quad (2)$$

where the filter function $\tilde{K}(f)$ is determined by maximising the expected signal-to-noise ratio of y .

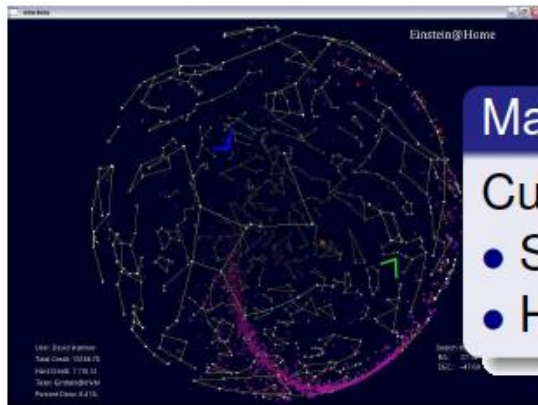
- The result of the maximisation is :

$$y(\theta^\alpha) = \int_{-\infty}^{\infty} df \frac{\tilde{x}(f)\tilde{s}^*(f; \theta^\alpha)}{P_n(f)} \quad (3)$$

where $P_n(f)$ is the detector noise PSD.

Wiener filter is the optimal detection statistic if noise is Gaussian

Grupo de Relatividad y Gravitación <http://grg.uib.es/ligo/>



Maximize available computing power

Cut parameter-space λ in small pieces $\Delta\lambda$

- Send workunits $\Delta\lambda$ to participating hosts
- Hosts return finished work and request next

- Public distributed computing project, launched Feb. 2005
- ~100,000 participants, ~ **1PFlop/s** (24x7)
- All-sky and directed searches for isolated NSs
- Workunits run ~ 6 – 12h on hosts
- Typical search runs ~ 3 – 12 months on E@H

👉 You can sign up and help! <https://einsteinathome.org>

